

1-30-2013

# Computational interior ballistics modeling

Robert Miner

Follow this and additional works at: [https://digitalrepository.unm.edu/me\\_etds](https://digitalrepository.unm.edu/me_etds)

---

## Recommended Citation

Miner, Robert. "Computational interior ballistics modeling." (2013). [https://digitalrepository.unm.edu/me\\_etds/68](https://digitalrepository.unm.edu/me_etds/68)

This Thesis is brought to you for free and open access by the Engineering ETDs at UNM Digital Repository. It has been accepted for inclusion in Mechanical Engineering ETDs by an authorized administrator of UNM Digital Repository. For more information, please contact [disc@unm.edu](mailto:disc@unm.edu).



**Computational Interior Ballistics Modeling**

**BY**

**Robert Todd Miner\***

**\*BSME, University of New Mexico, 2008**

THESIS

Submitted in Partial Fulfillment of the  
Requirements for the Degree of  
**Master of Science**

**Mechanical Engineering**

The University of New Mexico  
Albuquerque, New Mexico  
**December, 2012**

## **DEDICATION**

I would like to dedicate this paper to my parents who have always been there for me and provided me the opportunity to further my education. This would not have been possible without their love and support.

## **ACKNOWLEDGMENTS**

I would like to acknowledge my adviser Dr. Razani and my colleagues at Sandia National Laboratories. I would like to extend special thanks to my mentors Mark Anderson, Chance Hughs, and Steven Todd for making this research possible along with their expertise and support. In addition, I would also like to thank Greg Scharrer, Charles Jensen, Shawn Parks, the whole 5436 and 5437 teams for their support and guidance through my research and college years.

Special thanks to my committee members, Dr. John Russell, Dr. Arslan Razani and Dr. Steven Todd for their valuable recommendations pertaining to this study and assistance in my professional development.

# **Computational Interior Ballistics Modeling**

**Robert Todd Miner\***

**\*BSME University of New Mexico, 2008**

**M.S., Mechanical Engineering, University of New Mexico, 2012**

## **ABSTRACT**

Interior ballistics are the events in a gun system that determines the performance of any gun design. In order to efficiently design any gun system the internal ballistics should be understood to minimize energy losses and correctly define design parameters. The goal of this computational model is to develop a ballistics model to aid in gun design. A computational analysis of the dynamics events aids in the design of the gun system by providing output information such as pressure, velocity, charge burnout, and projectile distance versus time profiles. By applying the chemical and physical parameters of the propellant, gun breech geometry, projectile mass and gun barrel parameters, one can iterate through design parameters in an attempt to improve gun performance. There will be several computational models describing the main program being a lumped parameter internal ballistics analysis. The muzzle velocity of the model has been validated with empirical testing to at least one gun system and being applied to other gun systems for further validation on different designs. The validation of the muzzle velocity and breech pressure will build confidence in the model and allow for the model to be further developed into a more user friendly program.

## TABLE OF CONTENTS

DEDICATION .....	iii
ACKNOWLEDGMENTS .....	iv
ABSTRACT .....	v
CHAPTER 1 INTRODUCTION .....	1
1.0 Introduction.....	1
CHAPTER 2 INTERIOR BALLISTIC MODELING .....	3
2.0 Ballistics Problem .....	3
2.1 Pressure-Travel Curve .....	3
2.1.1 Propellant Parameters .....	5
2.1.2 Gun Parameters .....	12
2.1.3 Projectile Parameters .....	13
2.2 Numerical Techniques .....	14
2.2.1 Chemical Equilibrium Calculations .....	14
2.2.2 Closed Bomb Formulation .....	18
2.2.3 Corner's Model .....	21
2.2.4 Coppock's Model .....	23
2.2.5 IBHVG2 Lumped Parameter Model .....	36
2.2.6 XKTC Lumped Parameter Model and Codes of other Countries .....	38
2.2.7 SNL Lumped Parameter Model .....	38
CHAPTER 3 MODEL COMPARISON .....	48
3.1 Gun Models .....	48
3.2 PAN Disruptor .....	49

3.3. 0.50 Caliber Powder Gun (SNL) .....	55
3.3.1 SNL Powder Gun - .308 Winchester IMR 4350 .....	57
3.3.2 SNL Powder Gun-- .380 Winchester IMR 4064 .....	60
3.3.5 SNL Powder Gun- 0.50 BMG IMR 4350 .....	66
3.3.6 SNL Powder Gun- 0.50 BMG IMR 4064 .....	68
3.4 Thunder Range Powder Gun Results .....	70
3.5 50 mm Launcher .....	71
3.5.1- 50 mm Launcher Low Velocity Target .....	72
3.5.2-50 mm High Velocity Target .....	74
CHAPTER 4 DISCUSSION .....	76
4.1 Model Difficulties .....	76
4.2 Model Limitations .....	76
CHAPTER 5 CONCLUSIONS .....	76
5.1 Summary .....	76
5.2 Lessons Learned .....	77
5.3 Future Work .....	78
REFERENCES .....	79
APPENDIX A .....	81
<i>Propellant Formulations</i> .....	82
APPENDIX B .....	86
<i>Corners Method: Mathcad Numeric Modeling</i> .....	86
APPENDIX C .....	92
<i>Coppocks Method: Mathcad Numeric Modeling</i> .....	92

APPENDIX D .....	94
<i>Lumped Parameter Model: Mathcad Numeric Modeling</i> .....	94

## LIST OF FIGURES

Figure 1. Propellant Grain Geometries .....	6
Figure 2. Pressure vs. Grain Size .....	7
Figure 3. Pressure vs. Burn Type .....	8
Figure 4. Pressure vs. Load Density .....	8
Figure 5. Velocity Dependence vs. Ballistic Parameters .....	12
Figure 6. Chamber Pressure Dependence vs. Ballistic Parameters .....	12
Figure 7. Gun Schematic .....	13
Figure 8. Combustion Chamber Model .....	16
Figure 9. Single Perforated Grain Geometry .....	24
Figure 10. IBHVG2 GUI Interface .....	37
Figure 11. IBHVG2 Output Plot .....	38
Figure 12. Volume Fraction Diagnostic Plot .....	44
Figure 13. Pressure Diagnostic Plot .....	45
Figure 14. Projectile Velocity Diagnostic Plot .....	45
Figure 15. Burn Rate Diagnostic Plot .....	46
Figure 16. Total Volume Diagnostic plot .....	46
Figure 17. Projectile Travel Diagnostic Plot .....	47
Figure 18. Lumped Parameter Pressure, Travel, Velocity Curve .....	48
Figure 19. PAN Model Pressure .....	50
Figure 20. PAN Model Velocity .....	51
Figure 21. PAN Disruptor Model Percent Errors .....	55
Figure 22. 0.50 Cal Powder Gun Casings .....	56

Figure 23. Lumped Parameter PTV Curve .....	58
Figure 24. Pressure Curve .308 Winchester (IMR 4350) .....	58
Figure 25. Velocity Curve. 308 Winchester (IMR 4350) .....	59
Figure 26. PTV Curve .308 Winchester (IMR 4064) .....	60
Figure 27. Pressure Curve .308 Winchester (IMR 4064) .....	61
Figure 28. Velocity Curve .308 Winchester (IMR 4064) .....	61
Figure 29. PTV Curve DETS Lumped Parameter 470 Weatherby (IMR 4350) .....	62
Figure 30. Pressure Curves 470 Weatherby (IMR 4350) .....	63
Figure 31. Velocity Curve 470 Weatherby (IMR 4350).....	63
Figure 32. PTV Curve .470 Weatherby (IMR 4064) .....	64
Figure 33. Pressure Curve .470 Weatheby (IMR 4064) .....	65
Figure 34. Velocity Curve .470 Weatherby (IMR 4064).....	65
Figure 35. PTV Curve .50 BMG (IMR 4350) .....	66
Figure 36. Pressure Curve .50 BMG (IMR 4350) .....	67
Figure 37. Velocity Curve .50 BMG (IMR 4350) .....	67
Figure 38. PTV Curve .50 BMG (IMR 4064) .....	68
Figure 39. Pressure Curve .50 BMG (IMR 4064) .....	69
Figure 40. Velocity Curve .50 BMG (IMR 4064) .....	69
Figure 41. Thunder Range Powder Gun Percent Errors .....	70
Figure 42. Thunder Range Empirical Results.....	71
Figure 43. PTV Curve 50 mm (Low Velocity).....	72
Figure 44. Pressure Curve 50 mm (Low Velocity).....	73
Figure 45. Velocity Curve 50 mm (Low Velocity).....	73

Figure 46. PTV Curve 50 mm High Velocity .....	74
Figure 47. Pressure Curves 50 mm (High Velocity).....	74
Figure 48. Velocity Curves 50 mm (High Velocity) .....	75

## LIST OF TABLES

Table 1. Volume Fraction Equations .....	25
Table 2. PAN Model Input Deck .....	50
Table 3. PAN Model Output Data .....	51
Table 4. PAN Model Predictions vs Results 80 grains .....	52
Table 5. Pan Model vs Empirical Results 120 grains .....	52
Table 6. Pan Model vs Empirical Results 140 Grains .....	53
Table 7. Pan Model vs Empirical Results 240 Grains .....	53
Table 8. Pan Model vs Empirical Results 420 Grains .....	54
Table 9. Pan Model vs Empirical Results 625 Grains .....	54
Table 10. 0.308 Winchester Inputs (IMR 4350) .....	57
Table 11. Results .308 Winchester (IMR 4350) .....	59
Table 12. Results .308 Winchester (IMR 4064) .....	62
Table 13. Results .470 Weatherby (IMR 4350) .....	64
Table 14. Results .470 Weatherby (IMR 4064) .....	66
Table 15. Results .50 BMG (IMR 4350) .....	68
Table 16. Results .50 BMG (IMR 4064) .....	70
Table 17. 50 mm Low Velocity Results .....	75

**Nomenclature:**

Greek and Phonetic symbols are used in this thesis and follow the nomenclature specified unless otherwise stated.

**Greek Symbols**

$\beta$ : Burn Rate Coefficient  
 $\theta$ : Shape Function  
 $\lambda$ : Specific Force  
 $\sigma$ : Stress  
 $\gamma$ : Specific Heat Ratio  
 $\phi$ : Volume Fraction  
 $\Omega$ : Barrel Resistance /Roughness

**Phonetic Symbols**

A: Area  
 $A_s$ : Cross Sectional Area  
b: Co-Volume  
 $C_p$ : Specific Heat Constant Pressure  
 $C_T$ : Specific Heat Constant Temperature  
D: Diameter  
Ds: Launch Tube Length  
 $e_b$ : Ballistic Efficiency  
 $e_p$ : Piezometric Efficiency  
F: Force  
H: Enthalpy  
KE: Kinetic Energy  
M: Central Ballistic Parameter  
 $m_c$ : Charge Mass  
 $m_e$ : Equivalent Mass  
 $m_p$ : Projectile Mass  
n: Burn Rate Index  
P: Pressure  
 $P_a$ : Average Pressure  
 $P_B$ : Base pressure  
 $P_{bm}$ : Maximum Breech Pressure  
PE: Potential Energy  
R: Universal Gas Constant  
 $R_L$ : Lagrange Ratio  
S: Projectile Travel  
T: Temperature  
 $T_a$ : Average Temperature  
U: Internal Energy  
 $V_c$ : Chamber Volume  
 $v_{mz}$ : Muzzle Velocity  
 $V_p$ : Projectile Velocity  
W: Work  
 $x_e$ : Charge Burnout Length  
z: Form Function

## CHAPTER 1 INTRODUCTION

### *1.0 Introduction*

Interior Ballistics, the formal definition states that it is all the events inside a gun system spanning from when the firing pin strikes the primer or ignites the propellant until the projectile exits the barrel. To begin any design of a gun system the interior ballistics needs to be well understood and the actions taking place in the gun system characterized. In the past many gun designs were done by trial and error for lack of a mathematical description of the process. True mathematical description of the process did not become prevalent until the mid 18<sup>th</sup> century. One of the first works describing this process mathematically was written by Benjamin Robins. His paper “New Principles of Gunnery” was presented to the Royal Society in 1743. His paper related charge mass to velocity of given musket balls by using a ballistic pendulum that utilized the concept of momentum to calculate projectile velocity. Robins made a list of deductions from his experiments; these deductions along with his work in this area deemed him the name the “Father of Modern Gunnery”. From Robin’s initial studies came a list of scientists, engineers and academics to form what now is the base and foundation of ballistics. Some of the early pioneers include Dr. Charles Hutton a professor of mathematics at the Royal Military Academy, Chevalier D’Arcy who attempted to determine the law of pressures, Count Rumford and later Nobel and Abel who derived the equations of state for propellant gases. Through the years there has been a great deal of mathematical models developed to predict ballistic parameters i.e. muzzle velocity and chamber pressure.

Though these tools are good for rough estimates they are mostly empirically driven. The goal of this research is to gain a deeper understanding of the ballistic cycle and to understand the thermochemistry involved in this process. The sensitivities of the ballistic parameters will be studied in a more sophisticated level. This research will explore several areas of the ballistic cycle, and propellants-which will include the effects of the propellant characteristics on gun performance. The propellant parameters that will be studied will be grain geometry, and the number of active constituents of the fill pattern

and burn rates. Also included will be the different equations of state (EOS) used in the ballistic cycle and the preferred EOS for interior ballistics work. Thermophysics and Thermochemistry will be explored. There will be three different interior ballistic approaches explored. The first will be closed formed solutions that are based primarily on empirical data. The 0<sup>th</sup> order model developed by John Corner, and the 1<sup>st</sup> order model called the Coppock model will be examined. There will be chemical equilibrium calculations performed, as it will provide the maximum energy from the propellant and provide the maximum obtainable pressures and velocities obtainable by the gun system. The last approach explored will be lumped parameter models, which will be of the most interest for this research. A lumped parameter model using a Lagrange gradient will be the main focus and the code to be developed. A comparison of all these models will be compared to experimental data and to a variety of other input decks of past-published works.

The physical foundation of interior ballistics is to understand the process between converting the stored chemical potential energy of the propellant into useful kinetic energy of the projectile. To achieve optimum gun performance is to fully utilize all the potential energy the propellant contains and minimize all other energy losses such as friction, heat loss, projectile drag and recoil, among other potential losses. The way the propellant converts its potential energy to kinetic energy is by combustion and by transitioning the solid state of the propellant to a gas state that causes a pressure rise in a contained volume to do work on a projectile. The process of performing an interior ballistic computational model is to first establish all the parameters of the propellant. Thermodynamic analysis will allow you to establish most of the propellant parameters; most of this data is available from the manufacturer of the propellant. After all the propellant parameters have been obtained the next step is to define gun geometry and projectile geometry since these will be the variables that can be adjusted.

## CHAPTER 2 INTERIOR BALLISTIC MODELING

### *2.0 Ballistics Problem*

A gun system can be thought as a projectile throwing device in the most basic sense. The gun system can be broken down to two main parts the combustion chamber and the launch tube. The most basic view is the chemical energy of the solid propellant is converted to kinetic energy of the projectile. This is done by combusting the solid propellant in the combustion chamber as the hot gases are evolved from the burning surface of each grain of propellant. The chamber pressure will rise rapidly until enough pressure causes the projectile to accelerate. The projectile will travel down the barrel until it exits the system. At this point the interior ballistics problem is over and the exterior ballistics begins. The main problem is to try to use the propellant to the highest efficiency. In example is to use the least amount of propellant to get the fastest projectile velocity while minimizing the weight of the gun. The goal is to design the gun system to the appropriate barrel length by monitoring the charge burnout length and projectile acceleration. In order to monitor these parameters, interior ballistic curves have been developed that contain this information. The most useful of these curves are known as pressure-travel-velocity (PTV) curves.

### *2.1 Pressure-Travel Curve*

The main tool for interior ballistic analysis is the pressure travel velocity curve. The PTV curve allows one to overlay pressure constraints such as maximum permissible chamber pressure and gun tube pressure. The curve will allow one to see when the pressure will exceed these design constraints and let the designer decide whether to use a smaller propellant load or make the breech larger. However, most launchers have design requirements that need to be followed. The most useful part of the PTV curve is that the area underneath it is the amount of work done on the projectile by the propelling gases. The total amount of work can be characterized by equation (1.1) where  $P_B$  is the base pressure acting on the projectile,  $A_s$  is the cross sectional area of the bore and  $dS$  is the

length of the launcher. The equation is sometimes expressed as pressure volume work as shown in equation (1.2).

$$W = \int P_B A_s dS \quad (1.1)$$

$$W = \int P_B dV_c(t) \quad (1.2)$$

The kinetic energy term, equation (1.3) will reveal the projectile velocity term by using the conservation of energy where  $m_e$  is the effective mass and  $V_p$  is the projectile velocity.

$$W = \frac{1}{2} m_e V_p^2 \quad (1.3)$$

The goal of a gun design is to maximize the area under the PTV curve without exceeding the strength of materials in the gun system. The characteristic PTV curve of a gun system is most dependent on the gun geometry, propellant, burn rate and grain geometry.

Now understanding the interior ballistic problem and the tools used to solve the problem we need to develop a method of which to measure the performance of each gun design. There are two common parameters used in ballistic analysis to evaluate the merit of a gun design. One is called the piezometric efficiency ( $e_p$ ) and the other is called the ballistic efficiency ( $e_b$ ). The piezometric efficiency is found by dividing the mean pressure by the maximum breech pressure. The mean pressure is pressure exerted upon the projectile over the length of the bore that will produce the muzzle velocity of the projectile. The piezometric efficiency can be expressed as shown in equation (1.4).

$$e_p = \frac{\frac{1}{2} m_p V_p^2}{A_s S P_{BM}} \quad (1.4)$$

Where  $m_p$  is the mass of the projectile,  $V_p$  is the projectile velocity,  $A_s$  is the cross sectional area of the bore,  $S$  is the projectile travel at any time  $S=x(t)$  and  $P_{BM}$  is the maximum breech pressure. The higher the piezometric efficiency the flatter the PTV curve becomes. The ballistic efficiency can be defined as the ratio of the total work done on the projectile to the total work potential of the propellant.

The ballistic efficiency expression can be written as shown in equation (1.5).

$$e_b = \frac{\frac{1}{2} m_e V_p^2 (\gamma - 1)}{\lambda m_c} \quad (1.5)$$

Where  $m_e$  is the equivalent mass,  $\gamma$  is the specific heat ratio of the propellant,  $\lambda$  is the specific force constant and  $m_c$  is the charge mass. The ballistic efficiencies for most gun systems average around 0.33 which should be the minimum goal of most gun designs and for more advanced designs to raise this efficiency. These ballistic efficiencies along with the other design requirements being satisfied allows one to design an efficient gun system. Another ratio commonly looked at is the charge mass to projectile mass ratio where one can associate muzzle velocity and breech pressure to this parameter to have a rough idea of what to expect for both velocity and pressure.

### ***2.1.1 Propellant Parameters***

To properly model the propellant, the physical and chemical properties must be correctly established. The easiest and most apparent propellant parameter is the grain geometry. There exists a variety of different solid propellant grain geometries: sphere or ball, solid tubular, perforated tubular, or flake being the most common. These geometries play a key role in how the propellant burns. A different geometry of the same propellant will burn differently by how the size and shape vary. The burn rate type will be digressive, neutral or progressive. This burn rate type describes the amount of exposed surface area the propellant grain has as it is burned. Some propellant will reveal more surface area as it is burned making more combustible surfaces ready to burn and the pressure to remain for a longer duration but usually with a flatter curve, this is called a progressive burn type. A neutral burn type will contain a similar surface area ratio thru the burning process keeping the burn rate nearly constant. A degressive burn rate will have less and less surface area to burn as it burns resulting in a higher peak shorter duration pressure curve. The different propellant geometries are shown in Figure 1 Propellant Grain Geometries. The even more important propellant characteristic is whether the propellant is single, double or triple based. The differences between single, double or

triple based powders is how many active constituents the powder contains, i.e. single based powders use nitro-cellulose or nitro-glycerin as the active constituent. The main difference between different multibase gun propellants is how much gun bore erosion occurs. An example is that double base gun propellants produce less gas than single base gun propellants but retain a higher thermodynamic efficiency because of the production of more heat at higher flame temperatures. In effort to correct the problem of bore erosion, yet maintain the propulsive capabilities of double base powders, an explosive called nitroguanidine was added to the propellant mixture. This explosive is known as a cool burning explosive, this allows the temperatures to remain close to that of single based powders while maintaining the propulsive pressure sought after in double based powders. Figure 1 shows the more common grain geometries and their burn rate type. A wide range of propellants exists and selecting the correct powder is the first important step in gun design.

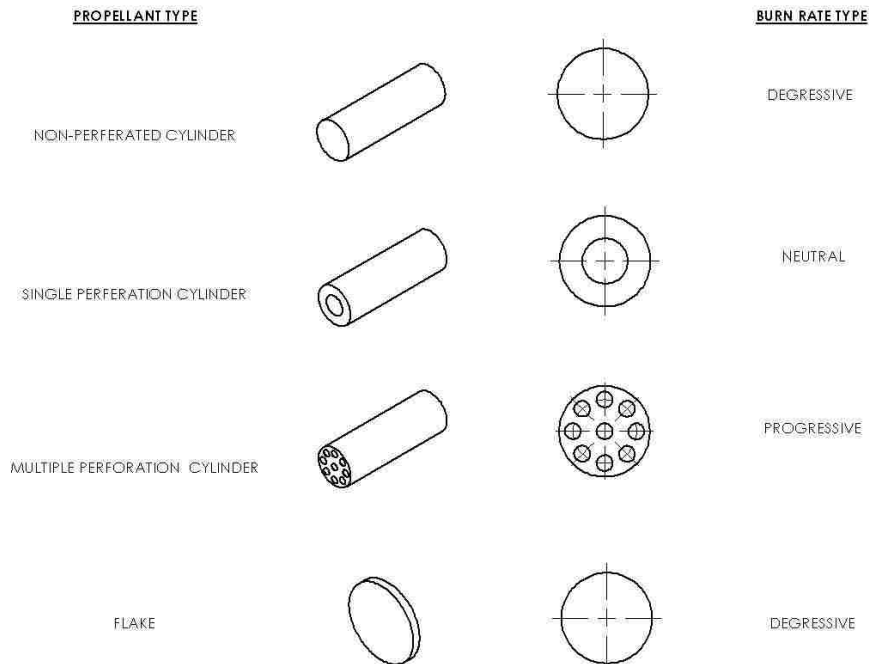


Figure 1. Propellant Grain Geometries

Figure 2 shows the effect that different types of propellant have on pressure as the projectile travels down the barrel. The smaller grain propellant will burn faster increasing

temperature, which will increase the pressure quickly. This is due to the fact that small grain propellant can burn a lot of surface area in a much smaller time interval where as the large grain propellant has a longer duration of burn which causes a lower pressure burn because the volume is consistently increasing and the large propellant will last longer with a lower overall peak pressure.

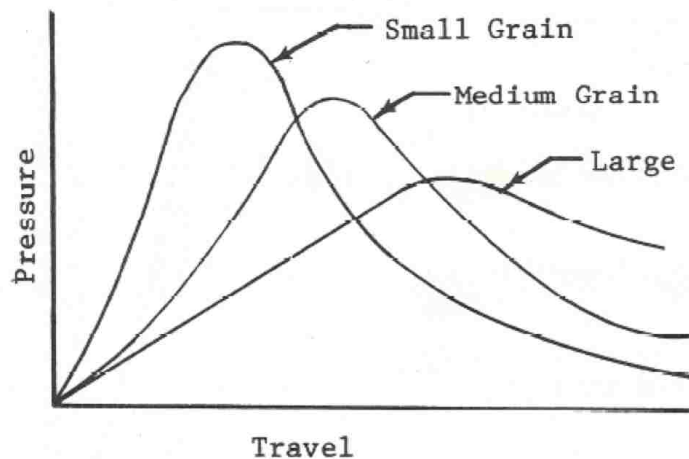


Figure 2. Pressure vs. Grain Size <sup>1</sup>

Figure 3 shows the effect of the different burn type and the corresponding typical pressure curve. It makes intuitive sense that the digressive burn rate would have a fast rise to a peak pressure and a steep decline back towards ambient pressure. This is because a lot of surface area is burned and most of the propellant consumed early in time. The neutral burn type is more consistent having a more bell shaped pressure curve because the burn will ramp up to peak pressure and return to ambient pressure on a similar downward path as the surface area of the propellant stick changes. The progressive grain propellant exposes more surface area as it is burned so it has a latent time peak pressure and lower typical peak pressure.

---

<sup>1</sup> (Krier, et al., 1979)

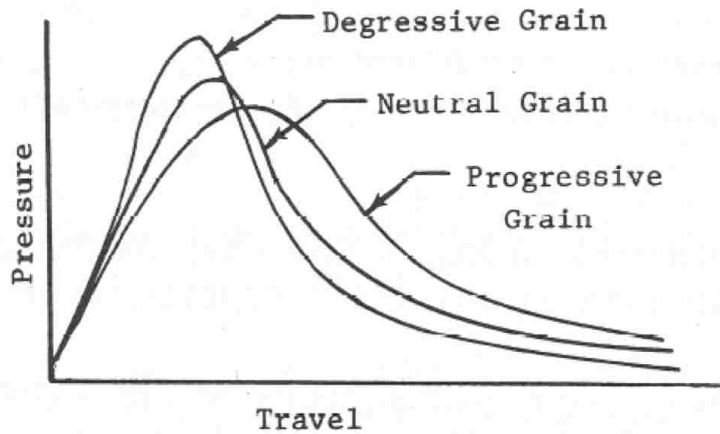


Figure 3. Pressure vs. Burn Type <sup>2</sup>

Figure 4 shows that if the combustion chamber is loaded to maximum capacity it will have a higher peak pressure and if loaded to a smaller capacity it will greatly reduce the pressure. This makes sense, as temperatures and fuel will be increased. The  $\Delta$  in the figure represents load density.

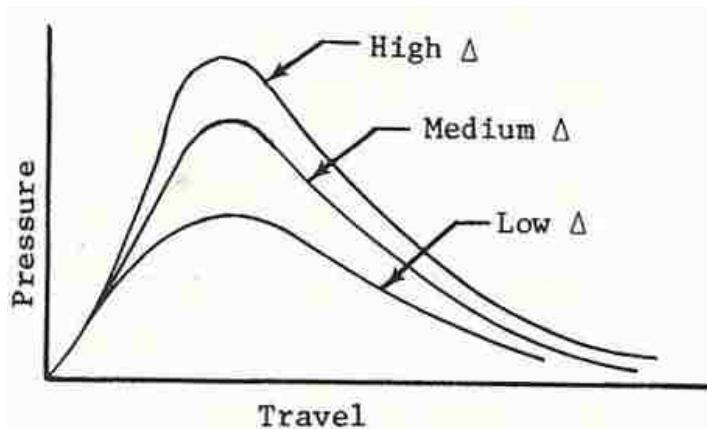


Figure 4. Pressure vs. Load Density <sup>3</sup>

Propellants are selected for specific applications primarily on the basis of their thermochemical properties and their burning rate behavior. The thermochemical properties include the flame temperature of the gases produced by the solid propellant under standard conditions. Since pressures encountered in most guns are 2000-4000 atmospheres a non ideal gas equation of state (EOS) must be used, the most common being the Nobel-Abel EOS, which includes the co-volume term  $b$ . The Nobel-Abel equation is expressed by equation(2.1). The other (EOS) commonly used in interior

<sup>2,3</sup> (Krier, Adams and Baer)

ballistic analysis is Van der Waals gas law- expressed by equation (2.2). The last EOS that can be used, but yields less accurate results and is left out of high-pressure calculations and most interior ballistic analysis, is the ideal gas law shown in equation (2.3).

$$P(V - b) = RT \quad (2.1)$$

$$P = \frac{RT}{v - b} - \frac{a}{v^2} \quad (2.2)$$

$$PV = RT \quad (2.3)$$

The first thermodynamic parameter defined is the specific heat ratio ( $\gamma$ ), this is a parameter associated with the ideal gas law. The specific heat ratio can be thought of in a few different ways as either the ratio of enthalpy to internal energy or the degrees of freedom of a molecule in the gas to rotate or translate. The specific heat ratio is the ratio of the specific heat at constant pressure ( $C_p$ ) to the specific heat at constant volume ( $C_v$ ). When an ideal gas is held at standard conditions the specific heat ratio can be held constant, but in real gases as temperatures elevate the gases can have increased vibrational and rotational states therefore increasing the specific heat held at constant volume which reduces the specific heat ratio. For the model the specific heat ratio will be treated as a constant using ideal isentropic expansion to be used in the pressure equations. The thermodynamic relations for the specific heat ratio can be expressed by equation (2.4).

$$\gamma = \frac{C_p}{C_v} \quad (2.4)$$

The thermodynamic relation for specific heat at constant pressure can be expressed by (2.5).

$$C_p = \left( \frac{\partial H}{\partial T} \right)_P \quad (2.5)$$

The thermodynamic relation for specific heat at constant volume can be expressed by (2.6).

$$C_v = \left( \frac{\partial U}{\partial T} \right)_V \quad (2.6)$$

The relation between enthalpy to internal energy is shown in equation(2.7).

$$\gamma = \frac{\left(\frac{\partial H}{\partial T}\right)_P}{\left(\frac{\partial U}{\partial T}\right)_V} = \frac{H}{U} \quad (2.7)$$

Assuming isentropic expansion, an equation for relating initial and final pressures can be developed that can be related back to the ideal gas law. These equations will be important in establishing the pressure and volume relations that will relate breech chamber volumes to corresponding pressures that will aid in the design of the chamber volume geometry.

$$P_1 V_1^\gamma = P_2 V_2^\gamma \quad (2.8)$$

$$\frac{P_1}{P_2} = \left(\frac{V_2}{V_1}\right)^\gamma = \left(\frac{T_2}{T_1}\right) \left(\frac{P_1}{P_2}\right)^\gamma \quad (2.9)$$

$$\frac{T_2}{T_1} = \left(\frac{P_2}{P_1}\right)^{\frac{\gamma-1}{\gamma}} \quad (2.10)$$

The specific force constant also referred as the impetus force is a constant that will need to be established. This constant describes how much energy per mass can be obtained by burning propellant. This parameter is important because it provides information on how much total energy is available. It assumes adiabatic conditions meaning no energy is loss to heat, which we know is not the case, but will provide a good approximation because heat loss is minimal. The specific force ( $\lambda$ ) constant can be calculated by knowing the molar mass ( $M$ ) the universal gas constant ( $\mathfrak{R}$ ) the specific gas constant ( $R$ ) and the adiabatic flame temperature ( $T_a$ ).

$$R = \frac{\mathfrak{R}}{M} \quad (2.11)$$

$$\lambda = RT_a \quad (2.12)$$

The next propellant parameter to identify is the burn rate, which is the rate that the powder burns. The manufacturer usually performs this and they are usually able to provide these values. Appendix A shows an example of a sheet obtained from the

manufacturer for propellant characteristics. If one cannot obtain the values from the manufacturer a strand burner could be used to extrapolate the burn rate or a closed bomb test could be performed. The burn rate is usually in (in/s) or (cm/s). The burn rate coefficients are used in the burn rate law to establish the burn rate of the propellant. The data obtained from closed bomb tests or strand burners are commonly fitted to de Saint Roberts equation or commonly known as the burn rate law. The burn rate can be calculated by the burn rate coefficient ( $\beta$ ), the burn rate index ( $n$ ) and the average pressure ( $P_a$ ) resulting in equation (2.13).

$$\frac{dx}{dt} = \beta P_a^n \quad (2.13)$$

The next parameter to identify is the gas co-volume ( $b$ ). This parameter describes the gas expansive volume. The reason the co-volume is so commonly used is because of its characteristic to remain approximately constant over a large range of pressures and temperatures. The co-volume depends greatly on state parameters making it an ideal parameter for thermodynamic analysis. The next parameter applies to loading information, which is the propellant load or mass. This will determine how much energy there is available to the system. The propellant load or the charge mass ( $m_c$ ) will be a tunable parameter depending on desired velocity. The solid propellant density ( $\rho_s$ ) also needs to be known to determine how much mass occupies a given volume usually the breech volume, the shell or casing. The parameters discussed above will provide most of the information needed to make a model for the propellant information. There has been work done exploring the sensitivities of these parameters on muzzle velocity and chamber pressure. This gives the interior ballistics an understanding of the importance of the ballistic parameters in effecting gun performance. The effect on muzzle velocity can be seen in Figure 5. The effect on chamber pressure is shown in Figure 6.

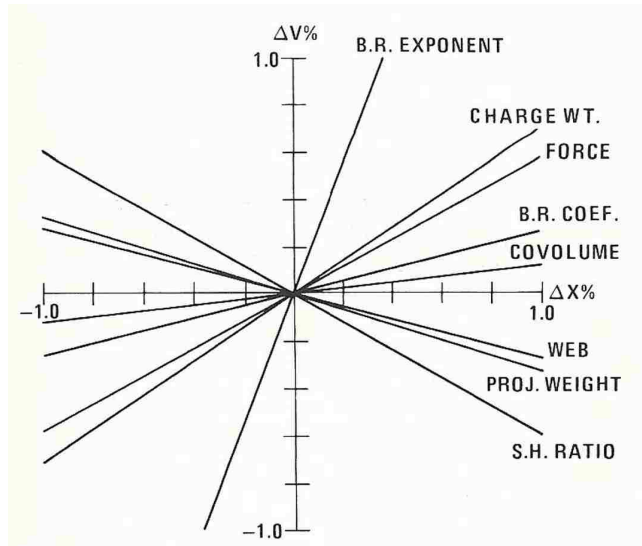


Figure 5. Velocity Dependence vs. Ballistic Parameters <sup>4</sup>

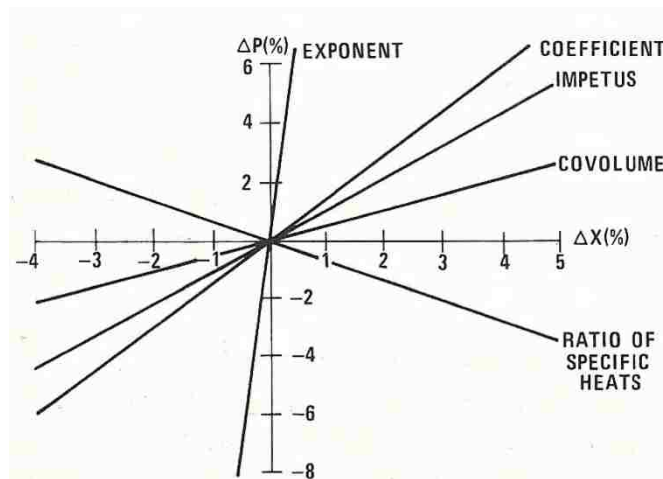


Figure 6. Chamber Pressure Dependence vs. Ballistic Parameters <sup>5</sup>

Now that the propellant parameters are understood in their basic sense and their effects in gun performance noted the gun geometry now can be explored.

### 2.1.2 Gun Parameters

There are various parts to any gun system. It is important to understand the various parts of their role in the performance and functionality in the gun system. The most basic gun components are the breech, the breechblock, the reaction chamber where the combustion process occurs, the shoulder also called the chamfer, the bore, the

<sup>4,5</sup> (Krier, et al., 1979)

muzzle, the chase and the slide cylinder. A schematic of the typical gun system is shown in Figure 7.

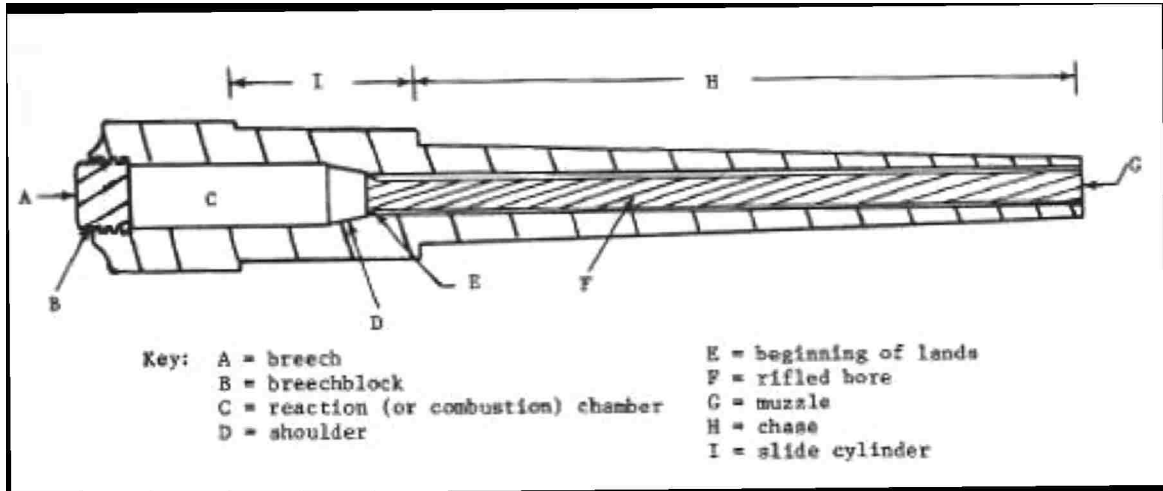


Figure 7. Gun Schematic <sup>6</sup>

The gun geometry is usually fixed by design constraints. The parameters usually tuned in gun design are the reaction chamber diameter and length, the bore diameter and length, the shoulder and whether the gun is rifled or a smooth bore. The reaction chamber volume is the most crucial parameter because it determines the overall confinement or propellant load available and where the pressure driving the projectile is developed.

### 2.1.3 Projectile Parameters

The last parameter that can be explored is the projectile design. The projectile design could be a subject of research all on its own. However, the most important parameters and how it effects the interior ballistic calculations will be explored. The most important projectile parameter is the projectile diameter and the mass of the projectile. There are many ways to design a projectile with each having its own unique capability. In example many heavy weighted projectiles use a sabot system especially in hyper velocity launchers. The lighter materials may be used with larger diameter projectiles to still achieve the high surface area on the back to allow more pressure while being able to lighten the overall projectile mass. The sabot also allows for multiple projectiles to be

<sup>6</sup> (Krier, et al., 1979)

used in the same bore gun. The projectile design is also important in barrels that are rifled, the material being used and the amount of rifling will all dictate the projectile design. The code being developed at Sandia will only take smooth bored gun barrels into consideration, however one could model rifling by increasing the bore friction parameter in the code to model a rifled barreled gun.

## ***2.2 Numerical Techniques***

There exists a variety of numerical techniques to try to describe the interior ballistic process; those being chemical equilibrium, closed bomb formulations, zero order analytical methods and lumped parameter methods. All methods will be explored to compare the accuracy and usefulness of all models. By exploring all the different models available we will be able to compare the developed lumped parameter model to existing models and also to empirical data to test for accuracy and usability.

### ***2.2.1 Chemical Equilibrium Calculations***

In order to perform a chemical equilibrium calculation one should have a baseline understanding of thermophysics and thermochemistry. Thermophysics can be thought of as the quantification of changes in a substance's energy state caused in the physical changes of the material. Thermochemistry is then the quantification of changes in a substances energy state caused by the chemical composition of the material's molecules. Combustion is the natural outgrowth of thermophysics and thermochemistry because combustion is the quantification of energy associated with fuel-oxidizer reactions. In order to perform the analysis one needs to think of energy in two forms - potential and kinetic energy. The gun launch physics can be thought of as a balance of energy between kinetic and potential. To start to formulate a thermodynamic description of the problem we look to the conservation of energy and thermodynamic equations. One of the first equations considers work, internal energy and enthalpy. It is usually written in the differential form but can also appear without the differential as seen in equations (2.14) and (2.15).

$$dH = dU + pdV \tag{2.14}$$

$$H = U + pV \quad (2.15)$$

When a substance changes form chemically or physically energy is either absorbed or released. The method used to quantify these energy changes is through heats of formation, which is the same as an enthalpy change. To quantify whether products are being released or absorbed we look at the equation for heat reaction (2.16). If the heat of reaction is a negative number, heat is liberated by the reaction. If the heat of reaction  $\Delta H_r^\circ$  is positive then heat is absorbed.

$$\Delta H_r^\circ = \sum_{\text{Products}} \Delta H_f^\circ - \sum_{\text{Reactants}} \Delta H_f^\circ \quad (2.16)$$

The heat of combustion  $\Delta H_c^\circ$  is obtained when propellant is burned in a closed volume. Equation (2.16) is modified to reflect a combustion heat reaction.

$$\Delta H_c^\circ = \sum_{\text{Products}} \Delta H_f^\circ - \sum_{\text{Reactants}} \Delta H_f^\circ \quad (2.17)$$

This concept will come into play when the first law of thermodynamics is considered. The first equation to establish is an energy representation for the system that will account for all the energy available. We can define energy for any system as (2.18).

$$E = U + KE + PE \quad (2.18)$$

(E) is the total energy comprised of the internal energy (U), kinetic energy (KE) and the potential energy (PE). The Lagrangian approach relates the energy to the thermodynamic process where the material is of a fixed mass. The first law of thermodynamics states that the energy added to the system plus the work performed on or by the system equals the change in the energy state of the material. The  $i$  stands for the initial state and the  $f$  for some final state. The first law of thermodynamics can be expressed by

$$Q_{i-f} + W_{i-f} = \Delta E_{i-f} \quad (2.19)$$

Replace E with the energy defined for the system as (2.18) so the equation becomes (2.20) where  $u$  is the internal energy.

$$Q_{i-f} + W_{i-f} = m \left( \left( u_f + \frac{1}{2} V_f^2 \right) - \left( u_i + \frac{1}{2} V_i^2 \right) \right) \quad (2.20)$$

The internal energy can be replaced with the equation for enthalpy so the equation becomes (2.21) where  $V$  is the velocity.

$$Q_{i-f} + W_{i-f} = m \left( \left( h_f - pv_f + \frac{1}{2} V_f^2 \right) - \left( h_i - pv_i + \frac{1}{2} V_i^2 \right) \right) \quad (2.21)$$

The first law of thermodynamics in its rate form is written as the equation (2.21).

$$\frac{dQ}{dt} + \frac{dW}{dt} = \frac{dm}{dt}_{out} \left( u_{out} + \frac{1}{2} V_{out}^2 + p_{out} v_{out} \right) - \frac{dm}{dt}_{in} \left( u_{in} + \frac{1}{2} V_{in}^2 + p_{in} v_{in} \right) \quad (2.22)$$

This equation becomes important because it will allow a solution for the work being done on the projectile and finally the muzzle energy after removing the projectile velocity. The concept of a fixed control volume (CV) can model the combustion chamber of the launcher. The model of the combustion chamber along with equation governing the thermodynamics can be seen in Figure 8 and equation (2.23) respectively.

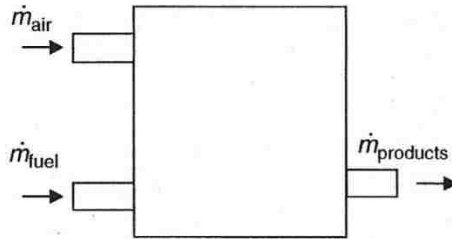


Figure 8. Combustion Chamber Model <sup>7</sup>

$$\frac{dQ}{dt} + \frac{dW}{dt} = \frac{dm}{dt}_{products} \left( h_{products} + \frac{1}{2} V_{products}^2 \right) - \frac{dm}{dt}_{air} \left( h_{air} + \frac{1}{2} V_{air}^2 \right) - \frac{dm}{dt}_{fuel} \left( h_{fuel} + \frac{1}{2} V_{fuel}^2 \right) \quad (2.23)$$

Through chemical reaction equation there must be a balance in order to determine the energy converted. . Knowledge of the species of the air and fuel in order to perform an equilibrium balance is necessary. Assume a convention presented in many thermodynamic textbooks. Air will be modeled as being a mixture of N<sub>2</sub> and O<sub>2</sub> with oxygen being 21 percent and nitrogen being 79 percent. In order to figure out how many moles of oxygen exists to nitrogen one divides nitrogen by oxygen.

$$\frac{.79 \left[ \frac{\text{Moles N}_2}{\text{Mole air}} \right]}{.21 \left[ \frac{\text{Moles O}_2}{\text{Mole air}} \right]} = 3.76 \left[ \frac{\text{Moles N}_2}{\text{Mole O}_2} \right] \quad (2.24)$$

<sup>7</sup> (Carlucci & Jacobson, 2008)

The air is relatively simple however the species for propellant are numerous and have multiple species. The composition can be obtained from most manufacturers; an example of one of the propellants used in this study can be seen in Appendix A under propellant characteristics. The composition of this particular propellant contained nitrocellulose which is the energetic function, nitroglycerine which is an energetic making double base propellant, diphenylamine which is a stabilizer, potassium nitrate which is used as a flash suppressant, carbon black which is an opacifier deterrent which can be used as a burn rate modifier, graphite which is used as a static reduction agent and residual water and solvents which make up less than 1 percent. The combustion gas composition products can be calculated by a code such as BLAKE, CHEETAH, CEA or NASA Lewis to find the equilibrium composition. Chemical equilibrium assumes a complete reaction. Chemical equilibrium is reached when the rate of the forward reaction equals the rate of the reverse reaction. In interior ballistics this will determine the maximum theoretical energy available to do work on the projectile because it assumes that propellant has been completely reacted with the oxidizer. The enthalpy of the reaction products is what needs to be calculated in order to determine the muzzle velocity. A sample calculation is shown in general variables the dummy variables can be replaced with the constituents of the propellant being explored. This calculation shows the maximum feasible muzzle velocity from the mass load of the propellant. The process for finding the muzzle velocity is to first determine the reaction products of the reactants, which will be air and the solid propellant. A general form for this type of calculation is seen in equation (2.25) where  $\alpha$  is the number of moles of reactant species A and  $\beta$  is the number of moles for reactant species B,  $\sigma$  is the number of moles for product species S and  $\tau$  is the number of moles for product species T.



The forward reaction rate or the reactants rate can be expressed by (2.26)

$$\text{Forward Reaction Rate} = k_+ A^\alpha B^\beta \quad (2.26)$$

The reverse reaction rate or the product rate can be expressed by (2.27)

$$\text{Reverse Reaction Rate} = k_- S^\sigma T^\tau \quad (2.27)$$

The equilibrium constant K is defined as the ratio of forward and reverse reaction rates.

$$K = \frac{k_+}{k_-} = \frac{S^\sigma T^\tau}{A^\alpha B^\beta} \quad (2.28)$$

This type of balanced equation is an example of a stoichiometrically balanced equation using a molar basis. There are times when a particular propellant or fuels is burned that either too much air is used which results in an over oxidized state or too little air is used which results in a under oxidized state.

### **2.2.2 Closed Bomb Formulation**

The closed bomb formulation is a useful way to determine propellant parameters and though mostly an academic exercise it is useful in understanding the characteristics of the combustion process. The most useful parameter to solve for is the propellant burn out time which is the calculation shown here. The propellant mass is handled in mass fraction terms with the web fraction being the crucial parameter. The amount of propellant remaining is determined by (2.29). The web fraction ( $f$ ) is going to be used to determine the amount of unburned propellant where ( $D$ ) is the original diameter of the propellant grain and ( $d$ ) is the diameter of the propellant at any given point in time. When the propellant is completely consumed  $d=0$  and therefore  $f = 0$  and the propellant has been completely burned and evolved into gas.

$$d(t) = fD \quad (2.29)$$

The volume of the propellant that has evolved into gas develops a parameter that tracks the fraction of propellant burnt  $\phi$ . This will be called the propellant fraction function (PFF) and is a propellant geometry driven relation. The PFF for a single perforated grain can be expressed as

$$\phi(t) = 1 - f(t) \quad (2.30)$$

For most general shapes of propellant the PFF can be expressed by a quadratic function of web fraction through use of a shape function  $\theta$ . The relationship between web fraction and time is shown in equations (2.31) and (2.32). The time when all the propellant has evolved into gas is the burnout time ( $t_b$ ).

$$f(0) = 1 \quad (2.31)$$

$$f(t_b) = 0 \quad (2.32)$$

$$f = \frac{d(t)}{D} \quad (2.33)$$

The relationship for most shapes can be expressed by the quadratic function shown in equation (2.34) where  $(\theta)$  is the shape function which is different for every grain geometry,  $\theta=0$  is for a single perforated grain and  $\theta=1$  for cylindrical grains.

$$\phi(t) = [1 - f(t)][1 + \theta f(t)] \quad (2.34)$$

A relationship between the propellant burning and the pressure must be established. The burn rate law is related to the time rate of change of the web. Two different burn rate laws are commonly used in interior ballistic analysis and are provided in equation (2.35) and (2.36). The symbol  $\beta$  represents the burn rate coefficient and  $\alpha$  represents the burn rate index.

$$D \frac{df}{dt} = -\beta P_B(t)^\alpha \quad (2.35)$$

$$D \frac{df}{dt} = -\beta (P_B(t) - P_1) \quad (2.36)$$

To choose an equation of state and for the closed bomb formulation analysis here is based on the ideal gas equation of state. From this equation of state develops a propellant gas mass to propellant charge mass that can relate back to the quadratic function developing a new equation (2.37)

$$\phi(t) = \frac{m_g(t)}{m_c} \quad (2.37)$$

Resolving the burn rate law for pressure obtains a relation for pressure as a function of the burn rate coefficient ( $\beta$ ), the rate of change of the web and the initial web. The resulting pressure equation is shown in

$$P_B(t) = \frac{D}{\beta} \frac{df}{dt} \quad (2.38)$$

It is more convenient to represent the pressure in terms of the fraction of propellant burnt.

$$f(t) = \sqrt{1 - \phi(t)} \quad (2.39)$$

Differentiating this equation with respect to time, the expression allows this equation to be plugged back into the pressure equation. Then by relating the pressure equation back to an equation of state allows for solving parameters of interest.

$$\frac{df}{dt} = \frac{-1}{2\sqrt{1-\phi(t)}} \frac{d\phi}{dt} \quad (2.40)$$

$$P_B(t) = \frac{D}{2\beta\sqrt{1-\phi(t)}} \frac{d\phi}{dt} \quad (2.41)$$

$$P_B(t)V = m_g(t)RT(t) \quad (2.42)$$

Introduction of the propellant force ( $\lambda$ ) is required to relate the temperature in the equation of state. The propellant force is the amount of energy released under adiabatic conditions. It is the most energy that can be obtained by burning propellant. The specific force can be expressed by equation where (R) is the specific gas constant and ( $T_a$ ) is the adiabatic flame temperature.

$$\lambda = RT_a \quad (2.43)$$

$$P_B(t)V = \lambda m_g(t) \quad (2.44)$$

$$\frac{\lambda m_g(t)}{V} = \frac{D}{2\beta\sqrt{1-\phi(t)}} \frac{d\phi}{dt} \quad (2.45)$$

$$\frac{\lambda m_c \phi(t)}{V} = \frac{D}{2\beta\sqrt{1-\phi(t)}} \frac{d\phi}{dt} \quad (2.46)$$

$$\frac{1}{\phi(t)\sqrt{1-\phi(t)}} \frac{d\phi}{dt} = \frac{2\beta\lambda m_c}{DV} \quad (2.47)$$

Equation (2.47) could be used to solve for a variety of unknown variables and can be integrated to solve for the charge burn out time. The closed bomb test is also useful in determining the burn rate coefficient of propellant because one could set up an apparatus where the (V) and (P) could be controlled and (T) measured and ( $\beta$ ) calculated with equation (2.47).

### 2.2.3 Corner's Model

Corner's model is a popular closed form solution used in interior ballistic analysis. It has been developed through empirical data and has been proven to be a useful tool for providing maximum values in an interior ballistic analysis such as pressure at charge burn out, the maximum breech pressure and the muzzle velocity. Since the pressure is the main concern in breech and barrel design it can provide aid in a gun design. It can be used as an initial start off point to discover a range of operation. Some of the benefits of this solution is that it uses a variety of dimensionless ballistic parameters.

The input parameters needed are the projectile diameter, the charge mass, the solid propellant density, the bulk propellant density, the burn rate coefficient, the gas co-volume, the specific heat, the propellant force, the chamber volume, the adiabatic flame temperature, the specific gas constant, the barrel length and diameter.

The first ballistic parameter described in corners method is the central ballistic parameter. This dimensionless parameter is used to reduce cumbersome calculation and is a function of the gun, the charge and the projectile. The central ballistic parameter is derived through the conservation of energy, momentum and continuity equations. The equation for the central ballistic parameter (M) is shown in equation (2.48). where  $A_p$  is the area, D is the web fraction,  $m_c$  is the charge mass,  $m_p$  is the projectile mass,  $\lambda$  is the specific force and  $\beta$  is the burn rate coefficient.

$$M = \frac{A_p^2 D^2}{m_p m_c \lambda \beta^2} \left[ \frac{\left(1 + \frac{m_c}{3m_p}\right)}{\left(1 + \frac{m_c}{2m_p}\right)^2} \right] \quad (2.48)$$

The mass fraction of the propellant is the next parameter to be established it is a function of the central ballistic parameter (M) and the shape function ( $\theta$ ). The shape function is determined from the propellant geometry. The mass fraction  $f_m$  is shown in equation (2.49).

$$f_m = \frac{M + \theta - 1}{M + 2\theta} \quad (2.49)$$

The Lagrange Ratio ( $R_L$ ) is used in the breech pressure equation and the last dimensionless parameter (Q).

$$R_L = \frac{\left(1 + \frac{m_c}{2m_p}\right)}{\left(1 + \frac{m_c}{3m_p}\right)} \quad (2.50)$$

The dimensionless parameter (Q) is a function of the gun geometry, the Lagrange Ratio ( $R_L$ ) and the propellant specific force.

$$Q = \frac{\lambda m_c R_L}{V_i} \quad (2.51)$$

The volume fraction of the propellant is a function of the central ballistic parameter and the shape function and is shown in equation (2.52) where  $\phi < 0$ .

$$\phi = \frac{(M + \theta)(1 + \theta)^2}{(M + 2\theta)^2} \quad (2.52)$$

The maximum breech pressure will be a function of the two dimensionless parameters Q and M and is shown in equation (2.53).

$$P_{b,\max} = Q(1 - f_m)e^{-M(1-f_m)} \quad (2.53)$$

The other pressure measurements that can provide useful design information to the interior ballistics is the pressure at the charge burn out time. It can help the designer to determine how long the barrel or breech needs to be in order to be efficient.

$$P_c = Qe^{-M} \quad (2.54)$$

The charge burnout length, and the velocity at charge burnout may be other parameters of interest. The charge burnout length is shown in the following equation.

$$x_c = L_c e^M - L_c \quad (2.55)$$

The  $\Phi$  value needs to be calculated which is a function of the specific heat ratio and charge burn out length.

$$\Phi = \frac{2}{1 - \gamma} \left[ \left( \frac{L_B + L_c}{x_c + L_c} \right) - 1 \right] \quad (2.56)$$

The velocity equations include the charge burnout velocity  $v_{xc}$ , the average velocity  $v_m$  and the muzzle velocity  $v_{mz}$ . They are shown in equations(2.57), (2.58) and (2.59) respectively.

$$v_{xc} = \frac{A_p D}{\beta \left( m_p + \frac{m_c}{2} \right)} \quad (2.57)$$

$$v_m = \frac{A_p D(1 - f_m)}{\beta m_p \left( 1 + \frac{m_c}{2m_p} \right)} \quad (2.58)$$

$$v_{mz} = \sqrt{\frac{m_c \lambda (M + \Phi)}{m_p + \frac{m_c}{3}}} \quad (2.59)$$

Corner's method is a good initial analysis and a relative simple analysis that can be completed by hand or with a math program such as Maple ®, Mathcad ®, Mathematica ® or Matlab ® to list a few. Closed form solutions are convenient because they give you a basis of what parameters are important and how they can affect the overall performance of the launcher.

#### ***2.2.4 Coppock's Model***

Coppock's model is another type of closed form solution. Again this type of solution is an analytical solution and is useful in testing the convergence and accuracy of a numeric model. It provides a good starting point for understanding a numerical solution and like chemical equilibrium provides a check against a solution obtained through numerical techniques. Coppock's model will be covered in more detail than Corner's model because it proves to be the more accurate model for muzzle velocity. The equations used in Coppock's models are based on some general assumptions. The first assumption is that the powder mass burn rate is proportional to the chamber pressure and the surface area of the powder. The surface area of the powder is computed as it burns. The powder burns at the breech pressure. The increase in volume behind the projectile with projectile travel is adjusted appropriately. The pressure gradient between the breech and projectile base is computed and assumed to be constant on the charge weight and the

projectile weight ratio. The model assumes a few correction factors for the powder energy content, the gas heat capacity and use of the ideal gas instead of a more sophisticated EOS. The model attempts to approximate mechanical losses of energy such as friction and recoil by raising the projectile mass by a few percent. Heat loss to the barrel is estimated by the Thornhill method.

The burn rate of the propellant is handled very similar to Corner's method. The form function for the grain shape is handled slightly different however. The mass of the gas produced will be equal to the mass of powder that has burned which would be proportional to the volume of the powder grain that has burned. Coppock's model uses a volume fraction of the powder burned which will also be similar to the way the lumped parameter models will handle the propellant. Coppock calls the form function in terms of a parameter called ( $z$ ) which can be established for various grain geometries with equation (2.60).

$$z = \frac{V_o - V(t)}{V_o} \quad (2.60)$$

To illustrate this we choose a single perforated grain geometry with a wall thickness ( $W$ ), radius ( $R$ ) and length ( $L$ ) the geometry would reflect Figure 9.

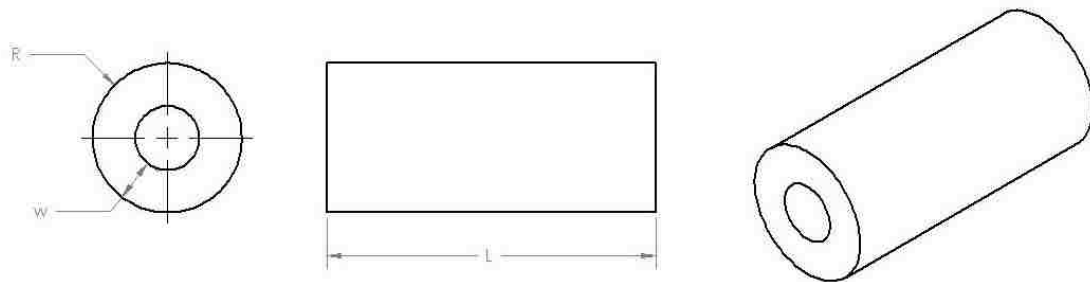


Figure 9. Single Perforated Grain Geometry

The initial volume of this grain can be described by (2.61), where  $D$  is the perforation diameter.

$$V_o = 2\pi RDL \quad (2.61)$$

At time equal ( $t$ ) the wall thickness term would reflect equation (2.62) and the length ( $L$ ) would reflect equation (2.63).

$$D - (1 - f)D = fD \quad (2.62)$$

$$L = (1 - f)D \quad (2.63)$$

The volume at time equal (t) would then be a function of (f) which would result equation (2.64)

$$V(t) = 2\pi Rfd [L - (1 - f)D] \quad (2.64)$$

Substituting (2.61) and (2.64) the initial volume and the volume at time (t) into equation (2.60) an equation for the volume fraction (z) is developed

$$z = \frac{2\pi RDL - 2\pi Rfd [L - (1 - f)D]}{2\pi RDL} \quad (2.65)$$

Simplifying this expression

$$z = (1 - f) \left( 1 + f \frac{D}{L} \right) \quad (2.66)$$

This expression allows one to develop a general expression based on a shape function called ( $\theta$ ) which will represent certain grain geometry. The general form equation is represented by equation (2.67)

$$z = (1 - f)(1 + \theta f) \quad (2.67)$$

An example of the different grain geometries is shown in

Type	f	$\theta$	Z
Solid Cylinder	1	1	$(1 - f)(1 + f)$
Flake / Disk	0	$\frac{2D}{L}$	$(1 - f) \left( 1 + \frac{2Df}{L} \right)$
Ball	0	1	$(1 - f)^3$
Single Perforated Cylinder	0	$\frac{D}{L}$	$(1 - f) \left( 1 + \frac{Df}{L} \right)$

Table 1. Volume Fraction Equations

The form factor used is determined by the burn characteristics of the powder. If it is a neutral burning powder the form factor would be zero, a digressive powder would be a 1 for the form factor, and a progressive powder will be a -1 for the form factor.

To start to form a solution all the equations regarding the physics and thermochemistry must be recognized and then appropriately related. The first equation will be the equation of motion for the projectile. Newton's second law will be used to correlate the breech pressure to the velocity of the projectile.

$$F = m_p a \quad (2.68)$$

The projectile mass ( $m_p$ ) can be substituted and the acceleration term can be replaced with the time derivative of velocity

$$a = \frac{dv}{dt} \quad (2.69)$$

The force term can be substituted with base pressure multiplied by the projectile base area.

$$F = P_b(x)A \quad (2.70)$$

Replacing all the terms in the equation of motion the equation becomes

$$P_b(x)A = m_p \frac{dv}{dt} \quad (2.71)$$

The next equation to be established is the equation state of the gas. As stated before most interior ballistic analysis uses the Nobe-Able equation of state. This equation of state is used because the ideal gas law yields to be accurate at higher pressures experienced in gun chambers. The co-volume term can be thought as a term of correction for this breakdown.

$$P(v-b) = RT \quad (2.72)$$

The impetus force is a function of the specific gas constant

$$F = \lambda = RT_o \quad (2.73)$$

One of the initial assumptions was that the process is carried out under adiabatic expansion. An adiabatic expansion process implies that the heat cannot be transferred across a boundary- instead all the energy is given to the gas and results in the gas gaining or losing heat according to the heat capacity of the gas. The energy that is absorbed by the gas written in differential form is shown in equation (2.74) where ( $n$ ) is the number of moles, ( $C_v$ ) is the specific heat and ( $dT$ ) is the differential of temperature.

$$dE = nC_v dT \quad (2.74)$$

Since the work is equal to force multiplied by the distance we can make the relation that the pressure multiplied the volume is the amount of work performed.

$$-PdV = nC_v dT \quad (2.75)$$

If we substitute the ideal gas law into equation (2.75) we get equation separating the variables

$$\frac{-nRT}{V} dV = nC_v dT \quad (2.76)$$

$$C_v \frac{dT}{T} = -R \frac{dV}{V} \quad (2.77)$$

From thermodynamics a specific gas constant is the heat capacity at constant pressure minus the heat capacity at constant volume. Substituting this relation in for (R) equation is generated.

$$C_p - C_v = R$$

$$\frac{C_p}{C_v} - \frac{C_v}{C_v} = \frac{R}{C_v}$$

$$\gamma = \frac{C_p}{C_v}$$

specific heat ratio  $\gamma$  is used to create a relation between the specific gas constant and the specific heat at constant volume that can be substituted into the adiabatic expansion equation.

$$(\gamma - 1) = \frac{R}{C_v}$$

$$\frac{dT}{T} = -(\gamma - 1) \frac{dV}{V} \quad (2.78)$$

The adiabatic expansion equation can be expanded by integrating between the initial state and the final state 1 and 2.

$$\ln\left(\frac{T_2}{T_1}\right) = -(\gamma - 1) \ln\left(\frac{V_2}{V_1}\right) \quad (2.79)$$

$$\frac{T_2}{T_1} = \left(\frac{V_1}{V_2}\right)^{\gamma - 1} \quad (2.80)$$

$$P_1 V_1^\gamma = P_2 V_2^\gamma \quad (2.81)$$

The conservation of energy becomes important, as energy must be conserved through the internal ballistics process. The work done by the gas goes into heating the barrel and

doing pressure-volume expansion work accelerates the projectile. The work done by the gas is equated in terms of the heat capacity, temperature difference, pressure volume work and heat loss. The energy equation for the interior ballistics process is shown in equation (2.82) where ( $T_o$ ) is the initial temperature and ( $E_h$ ) is the energy loss to heat.

$$\frac{m_c z}{m_w} C_v (T_o - T) = A \int P dx + E_h \quad (2.82)$$

The temperature can be replaced with equation of state and moved to the right hand side.

$$\frac{m_c z}{m_w} C_v T_o = m_c z C_v \frac{P(V-b)}{R} + A \int P dx + E_h \quad (2.83)$$

The specific heat ( $C_v$ ) can be substituted with terms of the specific gas constant and the specific heat ratio.

$$\frac{m_c z}{m_w} \frac{RT_o}{(\gamma-1)} = \frac{m_c z P(V-b)}{(\gamma-1)} + A \int P dx + E_h \quad (2.84)$$

The  $RT_o$  term can be replaced with the impetus force of the propellant resulting in equation (2.85).

$$\frac{\lambda m_c z}{(\gamma-1)} = \frac{P m_c z (V-b)}{(\gamma-1)} + A \int P dx + E_h \quad (2.85)$$

Equation (2.86) is the total volume occupied by the gas that is equal to the chamber volume minus the volume of the solid propellant plus the volume of the bore behind the projectile.

$$m_c z V = V_c + Ax - \frac{m_c (1-z)}{\rho} \quad (2.86)$$

Substituting equation (2.86) into the energy equation gives a final expression for the energy.

$$\frac{\lambda m_c z}{(\gamma-1)} = \frac{P}{(\gamma-1)} \left( V_c + Ax - \frac{m_c}{\rho} - \frac{m_c z (b-1)}{\rho} \right) + A \int P dx + E_h \quad (2.87)$$

The energy equation of (2.87) can be further simplified but it is helpful to understand the pressure gradient in the ballistics process. The pressure gradient is known as the Lagrange pressure gradient. There are two pressures to be considered the pressure from the equation of state of the gases and the base shot pressure. There will be a pressure

gradient from the breech of the launcher to the base of the projectile due to the inertia of the propellant gases. Lagrange was able to solve this problem by considering a volume element at position  $\sigma$  where  $\sigma$  is a fraction of the distance from the breech to the projectile base. If  $(V)$  is the volume at any moment between breech and the shot base then  $\sigma V$  will be the volume behind the cross section at  $(\sigma)$ . A volume element at  $\sigma$  will have mass of  $\rho V d\sigma$ . The velocity of the element will be  $\sigma v$  the momentum of the volume element is  $\sigma v \rho V d\sigma$ . The time derivative of the momentum gives the inertial force, which is equal to the force from the pressure on the section. This results in the following equation.

$$\sigma \frac{d(\rho V v)}{dt} = -A \frac{dP}{d\sigma} \quad (2.88)$$

Integrating both sides of the equation and substituting the equation of motion (2.91) derived earlier establishes equation (2.93).

$$A \int_{\sigma=P}^{\sigma=P_s} \frac{dP}{d\sigma} = \int \frac{d(\rho V v)}{dt} \sigma d\sigma \quad (2.89)$$

$$A(P - P_s) = \int \frac{d(\rho V v)}{dt} \sigma d\sigma \quad (2.90)$$

$$AP_s = m_p \frac{dv}{dt} \quad (2.91)$$

$$\frac{P - P_s}{P_s} = \int \frac{d(\rho V v)}{dv} \frac{\sigma}{m_p} d\sigma \quad (2.92)$$

By integrating the right hand side in terms of  $\sigma$  the equation becomes

$$\frac{P - P_s}{P_s} = \frac{m_c}{2m_p} \frac{d(zv)}{dv} (1 - \sigma^2) \quad (2.93)$$

If equation (2.93) is solved for breech pressure ( $P_b$ ) where  $\sigma=0$  and combined with the original equation the equation becomes

$$P - P_s = (1 - \sigma^2) (P_b - P_s) \quad (2.94)$$

The average pressure can be expressed as equation (2.95) if it is solved using the expression for P developed earlier in (2.88) then the average pressure becomes equation (2.96).

$$P_m = \int_{\sigma=0}^{\sigma=1} P d\sigma \quad (2.95)$$

$$P_m = \frac{1}{3}(2P_b + P_s) \quad (2.96)$$

Equation (2.96) can be resolved in terms of any of the pressures resulting in equation (2.98)

$$\frac{P_b}{P_s} = \left(1 - \frac{m_c}{2m_p}\right) \quad (2.97)$$

$$P_s = \frac{P_b}{\left(1 + \frac{m_c}{2m_p}\right)} = \frac{P_m}{\left(1 + \frac{m_c}{3m_p}\right)} \quad (2.98)$$

The kinetic energy of the propellant gases can be done by the same process integrating over  $\sigma$  since the same process is performed the results will only be presented.

$$KE = \int_{\sigma=0}^{\sigma=1} \frac{1}{2} \rho V \sigma^2 v^2 d\sigma \quad (2.99)$$

$$\rho V = m_c z \quad (2.100)$$

$$KE = \frac{1}{6} m_c z v^2 \quad (2.101)$$

Coppocks model assumes that 5% of the energy of the projectile goes into friction and recoil of the launcher system. This energy is accounted for by increasing the projectile mass by 5%. The energy for the mechanical portion, which was left in the integral form in equation (2.87), can now be replaced with the kinetic energy terms. The integral equation will become equation (2.102)

$$A \int P dx = \frac{1}{2} (1.05 m_p) v^2 + \frac{1}{6} m_c v^2 \quad (2.102)$$

To make the calculation less cumbersome we can make just one kinetic energy term by using a dummy variable ( $\alpha$ ) for his derivation.

$$\alpha = 1.05m_p + \frac{1}{3}m_c \quad (2.103)$$

$$KE = \frac{1}{2}\alpha v^2 \quad (2.104)$$

We can treat the kinetic energy of the heat loss to the barrel in a similar way by assigning a fraction of the kinetic energy term as ( $\chi$ )

$$E_h = \frac{1}{2}\chi\alpha v^2 \quad (2.105)$$

To reduce calculation we generate a term called the effective gamma that is used to keep the analytical solution manageable

$$(\gamma_{eff} - 1) = (1 + \chi)(\gamma - 1) \quad (2.106)$$

$$\chi = \frac{E_h}{E_s} \quad (2.107)$$

$$E_s = \frac{1}{2}\alpha v^2 \quad (2.108)$$

The only problem with this term is that the final projectile muzzle velocity needs to be known to solve the equation. The solution is achieved by iterating the calculation several times until convergence is achieved. The heat loss to the barrel is calculated through an empirical equation that is a function of the powder charge, temperature and bore dimensions. The Thornhill formulation was based on many test firings combined with theoretical calculation for the total heat loss to the barrel.

$$E_h = \frac{10.13Hd_b V_{tot}}{A_b} \quad (2.109)$$

$$H = .0127\Omega T \sqrt{d_b} \quad (2.110)$$

$$T = \frac{(T_o - T_{amb})}{1.7 + .38\sqrt{d_b} \left( \frac{d_b^2}{m_c} \right)^{.86}} \quad (2.111)$$

$$E_h = \frac{397d_b^{\left(\frac{3}{2}\right)} V_{tot}}{A_b T \Omega} \quad (2.112)$$

Now that all the equations have been developed a Coppock solution can be performed. To summarize there are four basic equations driving the interior ballistic process-first the powder burn rate equation, second the powder form function that relates the mass of gas produced to the linear function of the powder grain that has burned, third the equation of motion for the projectile and lastly the conservation of energy equation which must be balanced including all components of energy. Now that all the equations are accounted a Coppock solution can be carried out. The parameters that need to be supplied are shown in the input parameter list. The output equations are shown as functions of the input parameters and other output equations as they are solved. Mathcad an engineering calculation software was used for the analytical solution and an example problem is provided in Appendix C for the Coppock model. The first equation is the ratio of breech pressure (2.113)

$$R_{ba} = \frac{1 + \frac{m_c}{2w_1}}{1 + \frac{m_c}{2w_1}} \quad (2.113)$$

The Thornhill heat loss equation (2.114)

$$E_h = \frac{.397\Omega d^{\frac{3}{2}} \frac{L_b + l_{ec}}{in} (T_o - T_{amb})}{1.7 + .38\sqrt{d} \left( \frac{d^2}{\frac{m_c}{lb}} \right)^{.86}} \quad (2.114)$$

### Input Parameters

$d_p$  : Diameter of the Bore

A : Area of the Bore

$m_c$  : Charge Mass

$m_p$  : Projectile Mass

$w_1$  : Adjusted Projectile Mass

$\rho$  : Solid Propellant Density

D: Web

$L_p$  : Powder Tube Length

$\lambda$ : Impetus Force

$T_a$  : Adiabatic Flame Temperature

$L_B$  : Barrel Length

$\beta$ : Burn Rate of Propellant

$V_c$  : Chamber Volume

$\Omega$  : Hydronamic Barrel Rougness (1.25-1.4)

$b$ : Co-volume

$v_{est}$  : Estimated Muzzle Velocity

The output equations are shown and explained for clarification through the example in the appendix C. The kinetic energy of the shot and gas is shown in equation (2.115).

$$E_{sg} = \frac{1}{2} \left( w_1 + \frac{m_c}{3} \right) v_{est}^2 \quad (2.115)$$

The fraction of shot and gas energy lost as heat is used to evaluate the effective gamma.

$$\chi = \frac{E_h}{E_{sg}} \quad (2.116)$$

$$\gamma_1 = (1 + \chi)(\gamma - 1) + 1 \quad (2.117)$$

The effective gamma  $\gamma_1$  will be used in the peak pressure equation and the (F<sub>1</sub> equation.

The Coppock solution like Corner's method also uses the central ballistic parameter equation (2.118) to (2.121)

$$M = \frac{A^2 D^2}{m_c \lambda \beta^2 \left( w_1 + \frac{m_c}{3} \right) R_{ba}^2} \quad (2.118)$$

$$\theta_1 = \theta + \frac{1}{2}(\gamma_1 - 1)M \quad (2.119)$$

$$Z_b = 1 - \frac{1}{2}(\gamma_1 - 1)M \quad (2.120)$$

$$\tau = \frac{\theta}{M} \quad (2.121)$$

There must be a dimensionless covolume correction used in the pressure equations and the expansion ratio equation.

$$\eta = \left( b - \frac{1}{\delta} \right) \frac{m_c}{Al_c} \quad (2.122)$$

$$F_{1ex} = \frac{\gamma_1(e + \gamma_1 - 2) + (3\gamma_1 + 1)\tau + 2\tau^2}{\left( \frac{1}{2}(\gamma_1 + 1) + \tau \right)(\gamma_1 + 2\tau)} \quad (2.123)$$

The peak pressure equation is shown in equation (2.124).

$$P_1 = \frac{\lambda m_c R_{ba}}{Al_c} \left( \frac{((e + \gamma_1 - 2)M + 4\theta)}{(1 + \theta)^2} - \eta F_{1ex} \right)^{-1} \quad (2.124)$$

The Coppock solution has a conditional statement that allows the user to know if the peak pressure occurs before or after the propellant is all burnt.

$$\text{if } \gamma_1 M \geq (1 - \theta) \left( 1 + \left( b - \frac{1}{\delta} \right) \frac{P_1}{\lambda R_{ba}} \right) \text{ then Peak Pressure occurs before all burnt}$$

The Coppock solution gives the distance at which all the propellant is consumed. It is done by calculating three different ballistic coefficients and plugging them into equation (2.128).

$$A_b = l_c(1 - \eta) \quad (2.125)$$

$$B_b = l_c \left( \frac{1 + \theta}{Z_b} \right)^{\frac{M}{\theta_1}} \left( 1 - \frac{\gamma_1 \eta M (1 + \theta)^2}{(M + \theta_1)(M + 2\theta_1)} \right) \quad (2.126)$$

$$C_b = \eta l_c Z_b \left( \frac{(\gamma_1 - \theta)M - 2\theta^2}{(M + \theta_1)(M + 2\theta_1)} \right) \quad (2.127)$$

$$x_b = B_b + C_b - A_b \quad (2.128)$$

Coppocks Model also provides a solution for the fraction of propellant burnt at the maximum pressure.

$$k = \frac{Al_c \eta P_1}{\lambda m_c R_{ba}} \quad (2.129)$$

Since only a fraction of the propellant is consumed, a new effective gamma  $\gamma_p$  must be established.

$$\gamma_p = \frac{\gamma_1}{1+k} \quad (2.130)$$

$$\xi = \gamma_p - \gamma_1 + 1 \quad (2.131)$$

The fraction burned at peak pressure represented by equation (2.132).

$$f_m = 1 - \left( \frac{1+\theta}{\xi M + 2\theta_1} \right) \quad (2.132)$$

The volume fraction represented by equation (2.133)

$$Z_m = \frac{(1+\theta)(\xi M + \theta_1)}{\xi M + 2\theta_1} \quad (2.133)$$

The mass fraction represented by equation (2.134)

$$\phi_m = (1 - f_m)(1 + \theta f_m) \quad (2.134)$$

The distance at maximum pressure is found in similar manner as before solving for the ballistic coefficients with the new found values for the propellant information.

$$A_m = l_c (1 - \eta \phi_m) \quad (2.135)$$

$$B_m = l_c (eM + 4\theta_1) \left( 1 - \frac{\gamma_1 \eta M (1+\theta)^2}{(M + \theta_1)(M + 2\theta_1)} \right) \quad (2.136)$$

$$C_m = \frac{\eta l_c (1+\theta)^2 (\gamma_1 M (\xi M + 2\theta_1) - 2\theta (M + \theta_1))}{(M + \theta_1)(M + 2\theta_1)} \quad (2.137)$$

$$E_m = \frac{(\xi M + 2\theta_1)^2}{(\xi M + \theta_1)} \quad (2.138)$$

These ballistic coefficients can be plugged into equation to establish the distance of the maximum pressure and the fraction of propellant burnt at this location.

$$x_m = \frac{B_m}{E_m} + \frac{C_m}{E_m} - A_m \quad (2.139)$$

The maximum pressure then can be written as equation (2.140)

$$P_m = \frac{m_c \lambda R_{ba} (1 + \theta)^2 (\xi M + \theta_1)}{A (\xi M + 2\theta_1)^2 (x_m + l_c (1 - \eta \phi_m))} \quad (2.140)$$

The last equation to be established is the muzzle velocity. The first formula the muzzle velocity requires the expansion ratio for the all burnt powder equation (2.141)

$$r = \frac{L_b + l_c (1 - \eta)}{x_b + l_c (1 - \eta)} \quad (2.141)$$

$$\Phi = \frac{2(1 - r^{1-\gamma_1})}{(\gamma_1 - 1)} \quad (2.142)$$

$$v_{me} = \sqrt{\frac{\lambda m_c (M + Z_b \Phi)}{\left(w_1 + \frac{m_c}{3}\right)}} \quad (2.143)$$

The Coppock solution is a useful analytical solution. This could be programmed into a graphing calculator or easily implemented into a mathematical package or even performed by hand.

### **2.2.5 IBHVG2 Lumped Parameter Model**

The IBHVG2 Model was developed by the Army Research Laboratory at the Aberdeen Proving Grounds in Maryland. The IBHVG2 model is a lumped parameter model that is an advancement of the Baer-Frankle model. The model was originally written in the Fortran programming language. A Matlab compiled version from Dr. Amer Hammed from Cranfield University of the UK at the annual Aeroballistic Range Association (ARA) meeting in Baltimore was obtained for this study. The IBHVG2 model has been the mostly widely used interior ballistic model in research laboratories in the United States. The IBHVG2 model has been proven to be a reliable tool in the use of launcher design and has proven to be one of the most accurate lumped parameter models. The object of this study is not to establish the accuracy of the IBHVG2 model but to compare the lumped parameter code developed to other accepted lumped parameter ballistic

models. For the validation of the IBHVG2 model refer to references. A source code for the IBHVG2 could not be obtained so it is treated as a black box type software with an input deck and output deck. The main reason for the development of this lumped parameter ballistic code given in this study is to gain a deeper understanding of what is driving the lumped parameter model. From the literature the IBHVG2 model uses the assumption of uniform and simultaneous ignition of the entire propellant charge, combustion assumed to take place in a well-mixed reactor. The burn rate is determined by the instantaneous space mean chamber pressure. There is an assumed longitudinal pressure gradient superimposed on the solution at each instant in time to appropriately reduce the pressure on the base of the projectile.

The input screen for the Matlab® graphical user interface is shown in Figure 10 the numbers shown are the default numbers that can be edited to any desired value. The output deck is shown in Figure 11 it can display pressure versus time, velocity versus time, heat versus time, propellant burnt versus time or any of those parameters versus distance it also gives a summary option and an output deck in a text file. The output deck will be used in comparison of my own lumped parameter ballistic model.

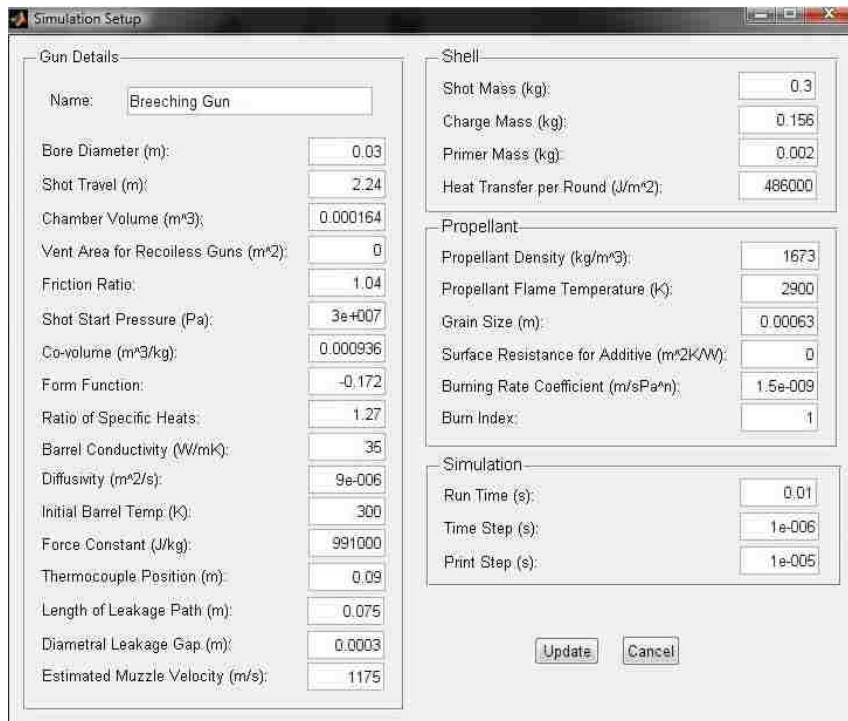


Figure 10. IBHVG2 GUI Interface

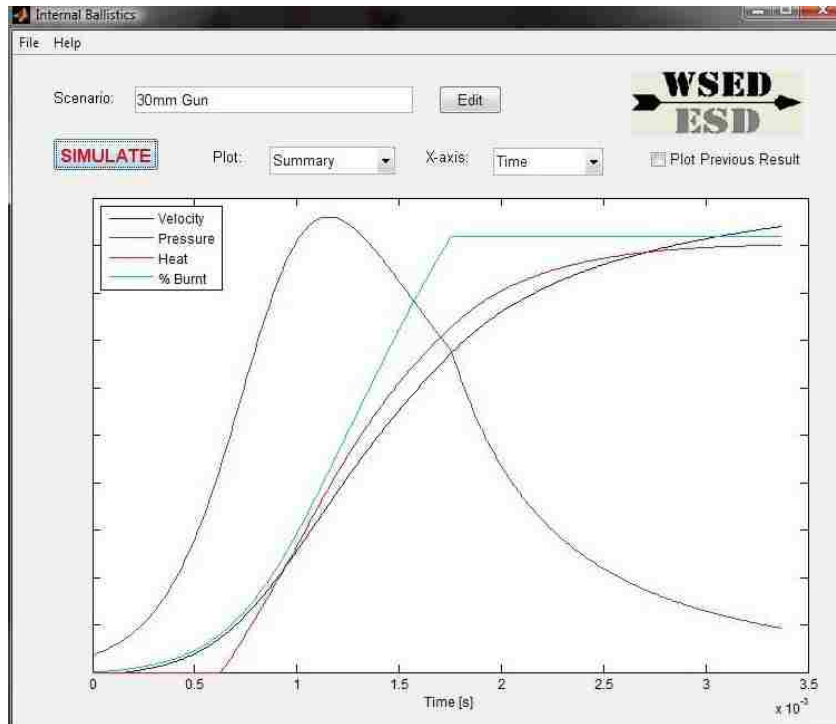


Figure 11. IBHVG2 Output Plot

### ***2.2.6 XKTC Lumped Parameter Model and Codes of other Countries***

An additional model was used in the lumped parameter ballistic model comparison called the XKTC program. This is the only other code developed in the United States. It is a 1D Lagrangian code developed in C++ language and also in a Fortran developed version. The file runs as an executable form much in the same way the IBHVG2 model runs with input decks. The input is run through the command prompt on the PC. The software again is a black box program where there is an input and output with no real knowledge of the internal workings. Other ballistic codes that could not be obtained due to financial or availability reasons are the CTA1 model of the UK, Mobidic-NG 1D and Mobidic-NG 2D of France.

### ***2.2.7 SNL Lumped Parameter Model***

The SNL lumped parameter model is based on the Lagrangian frame of reference tracking finite volume elements through the ballistic cycle. The derivation of the model comes from using the conservation laws along with Newtonian mechanics and writing out the equations of motion of the projectile. The potential energy of the propellant will

be converted to the kinetic energy of the projectile. Since the derivation of these equations was presented earlier only a summary of the essential equations used and the resulting equations will be presented only. There are four principal underlying equations the conservation of energy equation (2.156), the conservation of momentum equation (2.157), the conservation of mass equation (2.159) and finally the equation of motion (2.160). The entire model can be found in Appendix D with the script fully commented for further explanation. There will be seven ordinary differential equations with seven variables to be solved simultaneously-the conservation laws and burn rate laws will be used in these equations. The mass fraction is handled slightly different than the analytical models therefore the derivations of these equations are shown below. The first derivation is shown for spherical grain geometry. The volume fraction form is shown in equation (2.144).

$$Z(t) = \frac{V_i - V(t)}{V_i} = 1 - \frac{V(t)}{V_i} \quad (2.144)$$

The volume for a sphere is a function of the grain radius ( $R_g$ ) and shown in equation (2.145). The initial volume for a sphere grain is shown.

$$V_i = \frac{4}{3} \pi R_g^3 \quad (2.145)$$

The volume of the grain at any given time is a function of the initial grain radius and the burn rate law indicating the change in grain radius as a function of time and pressure.

$$V(t) = \frac{4}{3} \pi (R_g - X(t))^3 \quad (2.146)$$

$$X(t) = \beta P_a(t)^n \quad (2.147)$$

$$Z(t) = 1 - \frac{(R_g - X(t))^3}{(R_g)^3} \quad (2.148)$$

The differential form rate of change of the mass fraction is described in equation (2.149). The differential form is used so we can use an ODE solver and also because of the Lagrangian frame of reference tracking volume elements in time.

$$\frac{d}{dt} Z(t) = \frac{d}{dt} \left[ 1 - \frac{(R_g - X(t))^3}{(R_g)^3} \right] = \frac{\left( 3 \frac{d}{dt} X(t) \right) (R_g - X(t))^2}{(R_g)^3} \quad (2.149)$$

Other grain geometries can be handled in a similar manner this can be done for virtually any grain geometry. For cylindrical grain geometry the mass fraction equation is expressed by equation (2.150).

$$Z(t) = 1 - \frac{V(t)}{V_i} = 1 - \frac{(R_g - X(t))^2 (L_g - 2X(t))}{R_g^2 L_g} \quad (2.150)$$

The initial volume for a cylindrical geometry is shown in equation (2.151)

$$V_i = \pi R_g^2 L_g \quad (2.151)$$

therefore

$$V(t) = \pi (R_g - X(t))^2 (L_g - 2X(t)) \quad (2.152)$$

$$\frac{d}{dt} Z(t) = \frac{d}{dt} \left[ 1 - \frac{(R_g - X(t))^2 (L_g - 2X(t))}{R_g^2 L_g} \right] \quad (2.153)$$

$$\frac{d}{dt} Z(t) = \frac{2 \frac{d}{dt} X(t) (R_g - X(t))^2}{R_g^2 L_g} + \frac{2 \frac{d}{dt} X(t) (R_g - X(t)) (L_g - 2X(t))}{R_g^2 L_g} \quad (2.154)$$

The lumped parameter allows one to choose the propellant type applying the correct form for the volume fraction.

The conservation of energy principle can be expressed, as the net change in the total energy of the system during a process is equal to the difference between the total energy entering and the total energy leaving the system and can be expressed by equation (2.155).

$$\Delta E_{system} = E_{in} - E_{out} \quad (2.155)$$

Energy can be transferred to or from a system in three forms heat (Q), work (W) and mass flow ( $E_{mass}$ ). Heat transfer to a system increases the energy of the molecules and thus the internal energy of the system and heat transfer from a system decreases it since the energy transferred out as heat comes from the energy of the molecules of the system.

$$\Delta E_{system} = (Q_{in} - Q_{out}) + (W_{in} - W_{out}) + (E_{mass,in} - E_{mass,out}) \quad (2.156)$$

The conservation of momentum for the combustion gases needs to be accounted for and can be represented by equation (2.157).

$$\sum F = \frac{dp}{dt} = m \frac{dv}{dt} + v \frac{dm}{dt} = 0 \quad (2.157)$$

The conservation of mass plays a role in the phase change of the solid propellant to gas form the mass of the propellant must be conserved.

$$m_f - m_i = 0 \quad (2.158)$$

$$(\rho VA)_f - (\rho VA)_i = 0 \quad (2.159)$$

The equation of motion comes from Newtonian mechanics and newtons second law it follows that the sum of can be used to calculate the projectile velocity  $v_p$ .

$$\sum F = m \frac{d^2x}{dt} = m\ddot{x} = ma \quad (2.160)$$

The seven differential equations that need to be solved are shown in equations (2.161) to(2.166). The first term in the differential series is the rate change of the projectile or the velocity equation (2.161).

$$\frac{d}{dt} S_p(t) = V_p(t) \quad (2.161)$$

The projectile acceleration or the rate of change of velocity is a function of the base pressures the projectile mass and the bore area equation (2.162). If one wants to correct for friction in the barrel one can use equation (2.163) as a substitute it needs to only be selected in the program and a frictional force input chosen.

$$\frac{d}{dt} V_p(t) = \frac{A_s P_b(t)}{W_s} \quad (2.162)$$

$$\frac{d}{dt} V_p(t) = \frac{A_s P_b(t)}{W_s} - \frac{F_r}{W_s} \quad (2.163)$$

The burn rate law for the propellant is a function of pressure, the burn rate coefficient and the burn rate index equation (2.164).

$$\frac{d}{dt} X(t) = B P_a(t)^n \quad (2.164)$$

The volume fraction equation, which is dependent on the grain geometry equation, is given in (2.165) the right circular cylinder.

$$\frac{d}{dt}Z(t) = \frac{2 \frac{d}{dt}X(t)(R_g - X(t))^2}{R_g^2 L_g} + \frac{2 \frac{d}{dt}X(t)(R_g - X(t))(L_g - 2X(t))}{R_g^2 L_g} \quad (2.165)$$

The total volume of the system tracked as the propellant is burned and the projectile is accelerated down the barrel can be written as

$$\frac{d}{dt}V_T(t) = A_s V_p(t) + \frac{C_m}{\rho_s} \frac{d}{dt}Z(t) - C_m \eta \frac{d}{dt}Z(t) \quad (2.166)$$

The average gas pressure with heat loss accounted for is a rather complex equation which tracks rate change of pressure.

$$\frac{d}{dt}P_a(t) = \frac{\lambda C_m \frac{d}{dt}Z(t) - \frac{1}{6}(\gamma-1)(1+\beta)C_m \frac{d}{dt}Z(t)V_p(t)^2 - (\gamma-1)(1+\beta)\left(W_s + \frac{1}{3}C_m Z(t)\right)V_p(t) \frac{d}{dt}V_p(t)}{V_T(t)} \quad (2.167)$$

$$\dots - \frac{\lambda C_m Z(t) - \frac{1}{2}(\gamma-1)(1+\beta)\left(W_s + \frac{1}{3}C_m Z(t)\right)V_p(t)^2 \frac{d}{dt}V_T(t)}{V_T(t)^2}$$

The last equation to be solved is the base pressure acting on the projectile equation

$$\frac{d}{dt}P_b(t) = \frac{d}{dt}P_a(t) \left(1 + \frac{1}{2} \frac{\gamma-1}{\delta_c} \frac{V_p(t)^2}{g_a \lambda}\right)^{-\frac{\gamma}{\gamma-1}} \quad (2.168)$$

$$-P_a(t) \frac{\left(1 + \frac{1}{2} \frac{\gamma-1}{\delta_c} \frac{V_p(t)^2}{g_a \lambda}\right)^{-\frac{\gamma}{\gamma-1}}}{\delta_c} \frac{V_p(t)}{g_a \lambda} \frac{\frac{d}{dt}V_p(t)}{\left(1 + \frac{1}{2} \frac{\gamma-1}{\delta_c} \frac{V_p(t)^2}{g_a \lambda}\right)}$$

The seven differential equations must be solved simultaneously. A Runge Kutta matrix ODE solver is used together with the seven initial conditions that must be established along with a desired time step. The time step must be chosen appropriately to ensure that there are no numerical instabilities. The matrix ODE solver equation (2.169) along with the seven initial conditions is shown for clarification.

$$\begin{pmatrix} Z \\ P_a \\ P_b \\ V_T \\ X \\ V_p \\ S_p \end{pmatrix} = \text{odesolve} \left( \begin{pmatrix} Z \\ P_a \\ P_b \\ V_T \\ X \\ V_p \\ S_p \end{pmatrix} = t, .001 \right) \quad (2.169)$$

$$\begin{aligned} S_p(0) &= 0 \\ V_p(0) &= 0 \\ X(0) &= 0 \\ Z(0) &= 0 \\ V_T(0) &= V_{co} - \frac{C_m}{\rho_s} \\ P_a(0) &= P_{ambient} \\ P_b(0) &= P_{ambient} \end{aligned} \quad (2.170)$$

In order to stop the iteration process two “while loops” are employed. The first is to find the time when the projectile exits the barrel and to stop the calculation and the second loop is to find the maximum pressure. Mathcad is again employed for this calculation and the while loop syntax is displayed in equations (2.171) and (2.172).

$$T_{end} = \begin{array}{l} j \leftarrow 0 \\ tol \leftarrow 0.00000001 \\ \text{while } S_p(j) \leq L_b \\ \quad j \leftarrow j + tol \\ \quad j \end{array} \quad (2.171)$$

$$P_{\max} = \begin{cases} j \leftarrow 0 \\ tol \leftarrow 0.00000001 \\ \text{while } P_a(j+tol) \geq P_a(j) \\ \quad j \leftarrow j+tol \\ \quad P_a(j) \end{cases} \quad (2.172)$$

There are six diagnostic plots available to the user for variable tracking. These serve as a check to see if the variables act according to the expected behavior. The units can be either metric or english depending on preference. The first diagnostic plot is the volume fraction that should start at 0 and continue on until a value of 1 at which the propellant is completely consumed. Figure 12 shows this diagnostic plot. The second diagnostic plot (Figure 13) is the average pressure, which should rise as the propellant is burning, and the combustion gases are building in the reactor, Then the projectile begins to move and the pressure will decrease as the volume increases and the projectile accelerates down the barrel.

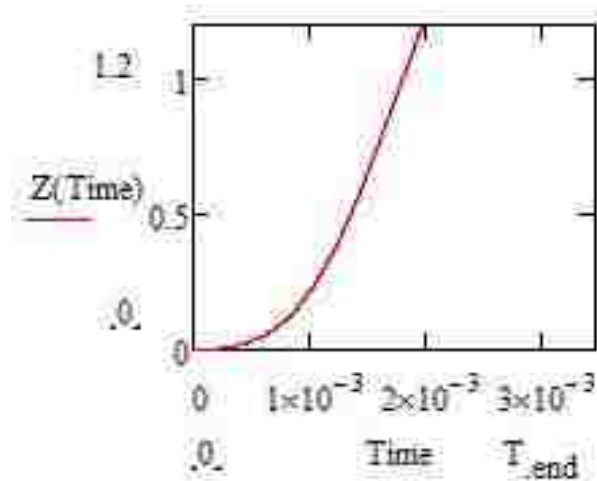


Figure 12. Volume Fraction Diagnostic Plot

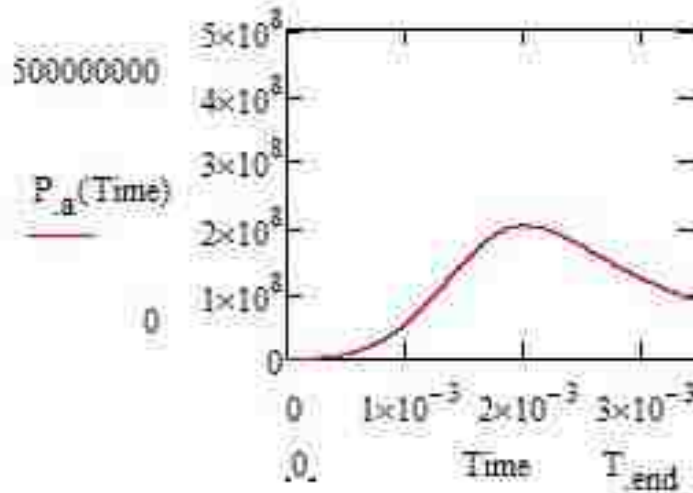


Figure 13. Pressure Diagnostic Plot

The third diagnostic plot (Figure 14) is the projectile velocity which should start at 0 and increase as the pressure increases having a positive velocity gradient until the projectile is no longer being accelerated and have a velocity gradient closer to zero which is good for an efficient gun design because it means that the barrel is the correct length. If the velocity gradient becomes negative the projectile is slowing down in the barrel or the charge mass is not high enough to accelerate the projectile for the length of the barrel so the charge mass must either increase to accelerate the projectile for a longer duration or the barrel shortened if the breech pressure is becoming unsafe for proper operation.

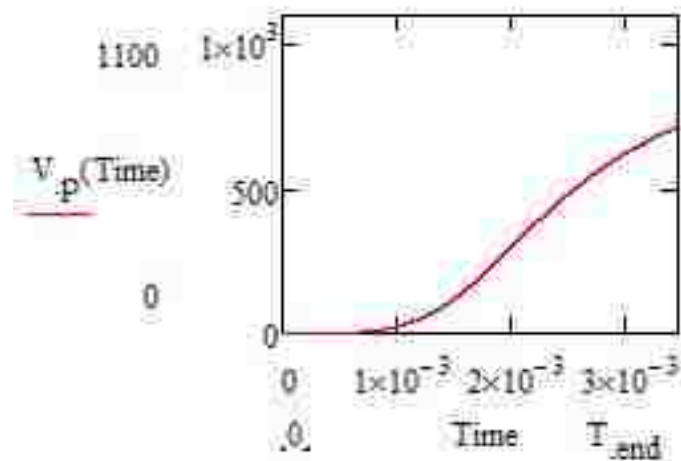


Figure 14. Projectile Velocity Diagnostic Plot

The fourth diagnostic plot (Figure 15) is the propellant burn history, which shows how the propellant is burning through the ballistic cycle. This should start at 0 and increase as the pressure increases and flattens as the pressure decreases and charge mass is consumed.

The fifth diagnostic plot is the total volume, which should start at the reactor volume and increase as the projectile travels down the barrel.

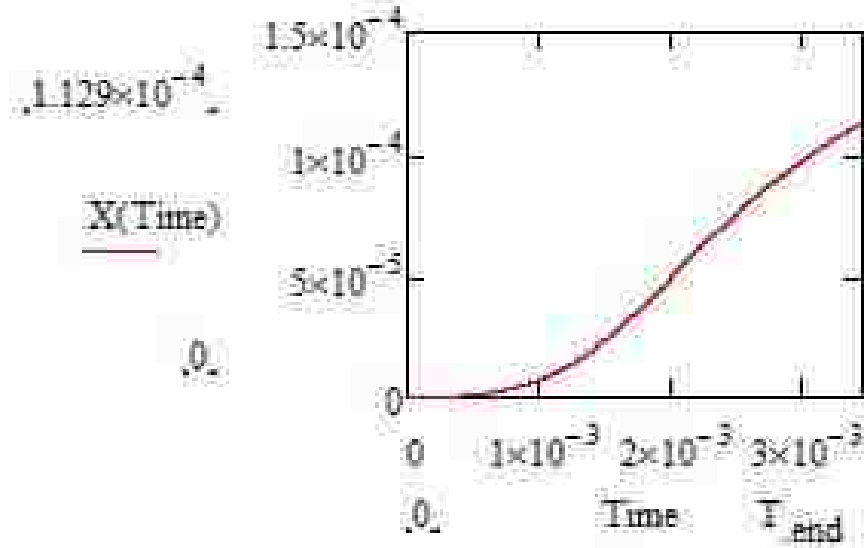


Figure 15. Burn Rate Diagnostic Plot

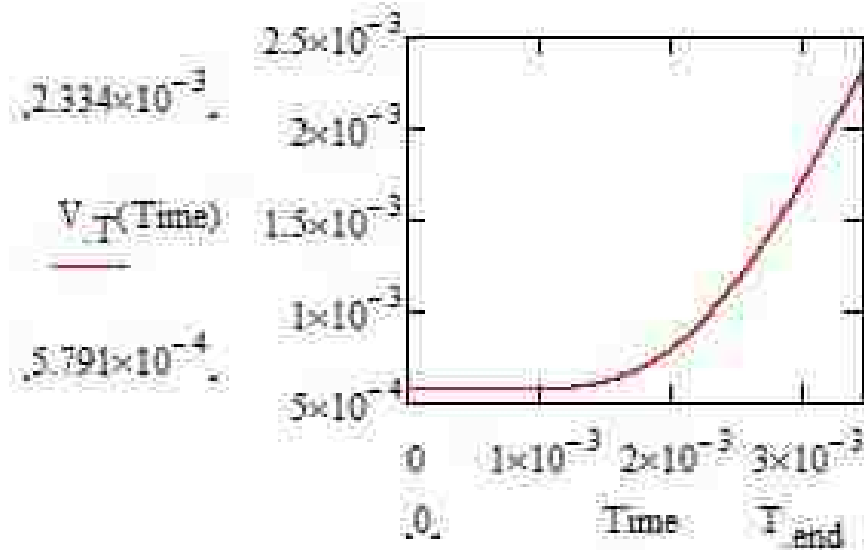


Figure 16. Total Volume Diagnostic plot

The final diagnostic plot (Figure 17) available is the projectile travel that tracks the projectile as it moves down the barrel. This plot should start at 0 and finish at the length of the barrel.

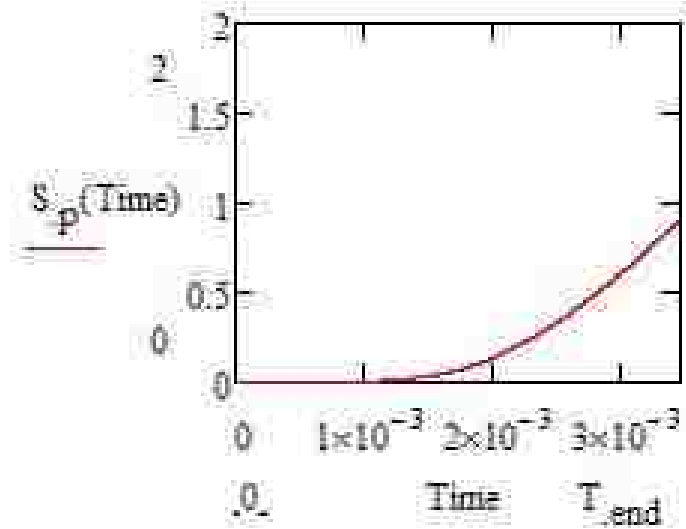


Figure 17. Projectile Travel Diagnostic Plot

The final result of the program is the pressure travel curve with the projectile travel, projectile velocity and pressure overlaid on the same plot. The left vertical axis being the pressure in kpsi and travel in inches and the right vertical axis representing the projectile velocity in feet per second the maximum pressure, the muzzle velocity and the end time for the ballistic cycle are also displayed below the plot for quick reference.

The program can also output a data file to be pulled into another program such as Excel ® or Matlab ® for further analysis or comparison of other models which is the process performed for this study. The analytical solutions along with the lumped parameter models will be compared in this way. The data file can also be used in a finite element package for analyzing the gun design. The tool used for this study was the LS-DYNA finite element package. An illustration of this study will be shown in subsequent chapters. It illustrates how interior ballistics results directly relate back to launcher design.

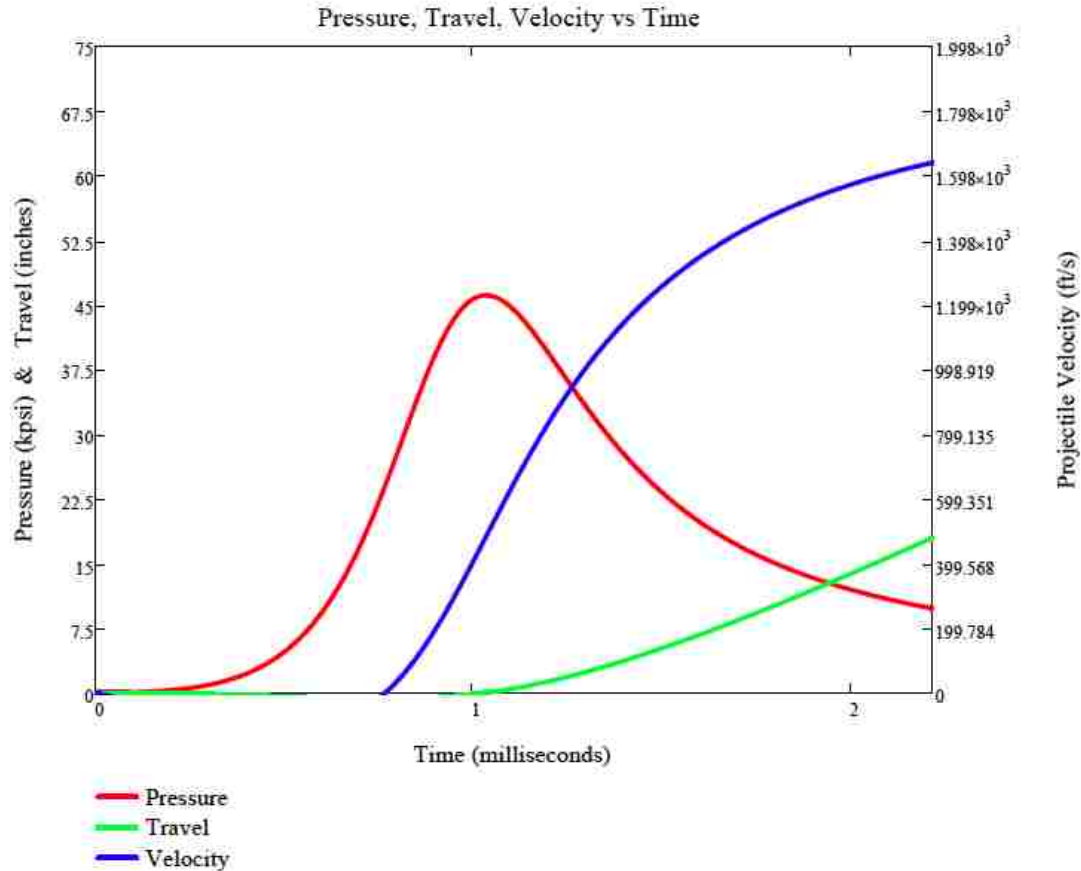


Figure 18. Lumped Parameter Pressure, Travel, Velocity Curve

### CHAPTER 3 MODEL COMPARISON

#### 3.1 Gun Models

This section of the study will be to compare all the models described in the previous sections. The comparison will be done with a few different methods. The first method will be to compare the same input deck for all the different models. A chemical equilibrium calculation will be performed to determine the maximum performance level, then a closed bomb calculation performed, the two different analytical closed form solutions performed and lastly the three lumped parameter models compared. The output variables of comparison will be the maximum pressure, the muzzle velocity along with the piezometric and ballistic efficiencies. The models will be later compared to empirical results obtained from experimentation of three launcher systems-a small caliber short barrel PAN disrupter, a small .50 caliber powder gun and a 50 mm powder gun. The

input deck for the PAN, the .50 caliber and the 50 mm powder gun are shown in tables respectively. The output results are tabularized and also graphically represent the lumped and analytical models plotted on the same plot. The analytical models' values are shown as constants because they are not a function of time. They are done this way only for maximum value comparisons and not to be confused as the actual ballistic curves.

### ***3.2 PAN Disruptor***

The PAN Disruptor is a precision aim tool originally developed at Sandia National Laboratories used to disable conventional handmade type bombs remotely. The PAN can be deployed by mounting it to a stand or by robot deployment. This tool has become the primary tool used by bomb squads and EOD (Explosive Ordnance Disposal) teams to render safe IED (Improvised Explosive Devices) and other HMEs (Home Made Explosives). The PAN has been manufactured in a variety of lengths and sizes and a wide variety are used for specific application. The PAN was chosen to study because of the large availability of data and the close relation to the gun types of interest. It provides a good way to characterize the models with reliable data. The study for this paper was to analyze the 18-inch barrel, 3.5 inch 12 gauge chamber and the bore precision drilled to .730 inch. The loadings for the PAN can range anywhere from 30 grains to 625 grains again depending on application. The velocity can be tailored anywhere from 230 feet per second to 2,840 feet per second depending on the mass of projectile and propellant load. A 420 grain load has been shown for the purpose of showing how the process works by taking the input parameters performing the different analysis techniques and producing the PTV curves for the different grain loadings. A table for the different grain loadings and the respected velocities and the results for all the analysis techniques will give an average accuracy to the empirical velocity data available. Pressure curves for these loadings for the PAN disruptors do not exist only as maximum pressures recorded in the combustion chamber.

Term	Data (Metric)	Data (English)
<b>Bore Diameter</b>	18.52 (mm)	.729 (in)
<b>Barrel Length</b>	457.2 (mm)	18 (in)
<b>Projectile Mass</b>	.044(kg)	.098 (lb)
<b>Propellant Mass</b>	.0012(kg)	.06(lb)
<b>Propellant Type</b>	Cylindrical	Cylindrical
<b>Propellant Length</b>	.152 (mm)	.006 (in)
<b>Propellant Diameter</b>	1.575 (mm)	.062 (in)
<b>Adiabatic Flame Temperature T</b>	3379 (K)	3379 (K)
<b>Impetus F</b>	1100000 (N)	368000 (ft-lb/lb)
<b>Specific Heat Ratio</b>	1.222	1.222
<b>Density</b>	.61 (gm/cc)	.022 (lb/cuin)
<b>Covolume</b>	.890 (cc/gm)	24.635 (cuin/lb)
<b>Chamber Volume</b>	983200 (cumm)	1.461 (cuin)

Table 2. PAN Model Input Deck

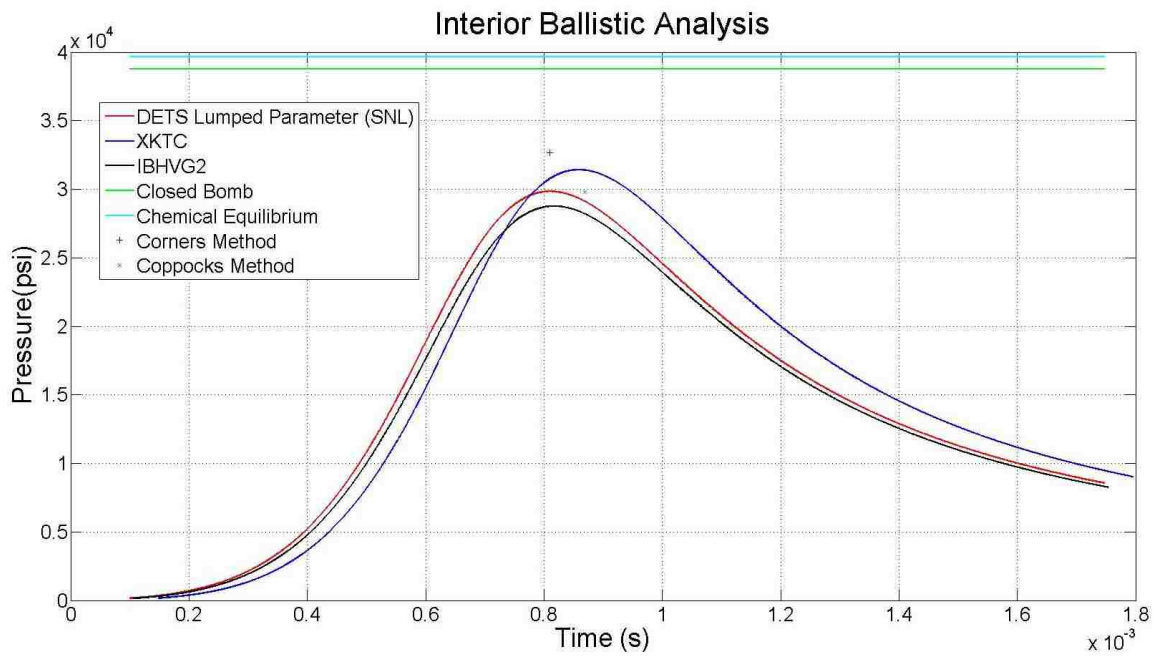


Figure 19. PAN Model Pressure

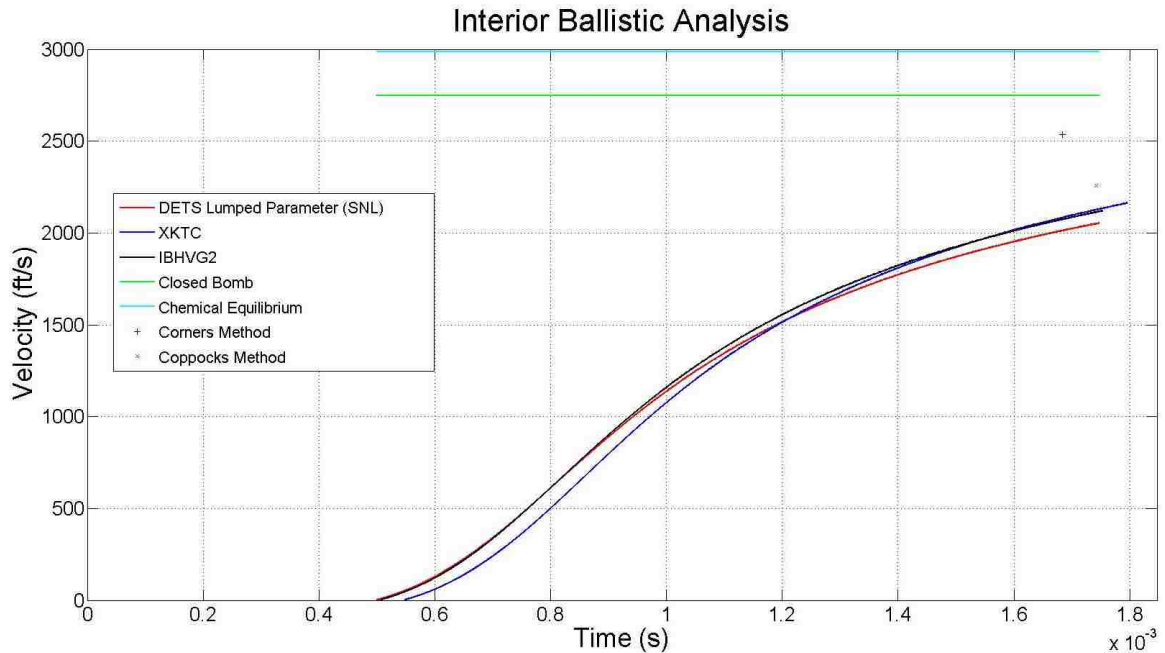


Figure 20. PAN Model Velocity

Model	OUTPUT PARAMETERS				$e_p$ (Piezometric Efficiency)	$e_b$ (Ballistic Efficiency)	Velocity Ratio	% Error
	Max Breech Pressure (MPa)	Max Breech Pressure (psi)	Muzzle Velocity (m/s)	Muzzle Velocity (ft/s)				
Chemical Equilibrium	273.55	39675.32	910.25	2986.54	0.54132	30.074	1.26	26.0
Closed Bomb	267.28	38765.43	837.30	2747.18	0.46877	25.447	1.16	15.9
Corners Method	225.38	32687.94	772.71	2535.26	0.47347	21.672	1.07	7.0
Coppocks Model	205.33	29780.56	688.25	2258.14	0.41229	17.193	0.95	4.7
Lumped Parameter	205.75	29841.00	689.48	2262.17	0.41293	17.255	0.95	4.5
IBHVG2	198.33	28765.43	646.28	2120.43	0.37637	15.160	0.89	10.5
XKTC	216.65	31422.57	659.08	2162.43	0.35832	15.767	0.91	8.8
Emperical Results	210.19	30486.00	722.34	2370.00				

Table 3. PAN Model Output Data

The curves generated for all the different calculation methods along with the analytical answers show the percent error for the actual tested velocity published for the PAN disrupter. The lumped parameter had the best result followed by the two analytical models followed by the XKTC model and IBHVG2 model. The following tables for

different propellant loads show all the derived values generated from the plots.

Propellant Mass 80 Grains								
Model	Max Breech Pressure (MPa)	Max Breech Pressure (psi)	Muzzle Velocity (m/s)	Muzzle Velocity (ft/s)	$e_p$ (Piezometric Efficiency)	$e_b$ (Ballistic Efficiency)	Velocity Ratio	% Error
Chemical Equilibrium	127.23	18452.61	275.62	904.32	0.10671	0.662	1.45	44.9
Closed Bomb	120.95	17542.12	238.72	783.23	0.08420	0.496	1.26	25.5
Corners Method	104.69	15184.26	211.59	694.23	0.07643	0.390	1.11	11.3
Coppocks Model	102.13	14812.34	208.24	683.25	0.07589	0.378	1.09	9.5
Lumped Parameter	83.47	12105.63	185.35	608.12	0.07356	0.299	0.97	2.5
IBHVG2	81.45	11813.12	174.87	573.74	0.06710	0.266	0.92	8.1
XKTC	72.91	10575.42	155.47	510.10	0.05924	0.211	0.82	18.3
Emperical Results	86.05	12481.00	190.19	624.00				

Table 4. PAN Model Predictions vs Results 80 grains

The lumped parameter models seemed to be more consistently accurate. The lumped parameter model had a percent error in velocity of 2.5 percent and the IBHVG2 model had a percent error in velocity of 8.1 percent. The chemical equilibrium calculation has the worst velocity percent error at 44.9 percent. This is due to the fact that the chemical equilibrium calculation does not take into account any losses by the gun such as friction, heat, leaking etc. The reason the chemical equilibrium calculation does not yield good results is because of the assumption of absolute conversion of the reactants into products consuming all available fuel and oxygen have been exhausted and converting all available stored chemical energy or potential energy into kinetic energy to the projectile. The quick analytical methods provide fairly accurate results with Corners method having a velocity percent error of 11.3 percent and Coppocks model being about 9.5 percent.

Propellant Mass 120 Grains								
Model	Max Breech Pressure (MPa)	Max Breech Pressure (psi)	Muzzle Velocity (m/s)	Muzzle Velocity (ft/s)	$e_p$ (Piezometric Efficiency)	$e_b$ (Ballistic Efficiency)	Velocity Ratio	% Error
Chemical Equilibrium	176.65	25621.16	341.66	1121.00	0.11810	0.654	1.35	34.9
Closed Bomb	154.83	22456.12	329.26	1080.30	0.12514	0.607	1.30	30.0
Corners Method	140.14	20325.12	268.91	882.30	0.09222	0.405	1.06	6.2
Coppocks Model	133.84	19412.35	267.06	876.23	0.09523	0.399	1.05	5.4
Lumped Parameter	123.80	17956.23	245.78	806.42	0.08721	0.338	0.97	3.0
IBHVG2	120.13	17423.56	227.16	745.32	0.07677	0.289	0.90	10.3
XKTC	104.40	15142.13	190.49	625.00	0.06212	0.203	0.75	24.8
Emperical Results	125.11	18146.00	253.28	831.00				

Table 5. Pan Model vs Empirical Results 120 grains

The results for 120 grains are seen above. The results for this charge mass show a similar trend in the models behavior to predict velocity. There are some improvements in the analytical models capability to predict velocity and tend to over predict the pressure. The closed bomb and chemical equilibrium results agreed with the previous analysis.

Propellant Mass 140 Grains								
Model	Max Breech Pressure (MPa)	Max Breech Pressure (psi)	Muzzle Velocity (m/s)	Muzzle Velocity (ft/s)	$e_p$ (Piezometric Efficiency)	$e_b$ (Ballistic Efficiency)	Velocity Ratio	% Error
Chemical Equilibrium	273.55	39675.32	447.50	1468.24	0.13083	0.890	1.33	32.8
Closed Bomb	267.28	38765.43	410.02	1345.26	0.11241	0.747	1.22	21.7
Corners Method	225.38	32687.94	303.15	994.62	0.07287	0.408	0.90	10.0
Coppocks Model	205.33	29780.56	363.08	1191.25	0.11474	0.586	1.08	7.7
Lumped Parameter	138.29	20057.12	329.22	1080.16	0.14007	0.482	0.98	2.3
IBHVG2	133.93	19424.23	278.20	912.76	0.10328	0.344	0.83	17.4
XKTC	127.04	18426.12	256.72	842.31	0.09271	0.293	0.76	23.8
Emperical Results	139.04	20165.41	336.97	1105.61				

Table 6. Pan Model vs Empirical Results 140 Grains

The results for the 140 grain case were consistent also with the previous models. The chemical equilibrium and the closed bomb solutions had the highest percent error and of course the highest ballistic efficiency. The lumped parameter model developed had only a 2.3 percent error. The IBHVG2 model had a percent error of 17.4 and the XKTC model a percent error of 23.8.

Propellant Mass 240 Grains								
Model	Max Breech Pressure (MPa)	Max Breech Pressure (psi)	Muzzle Velocity (m/s)	Muzzle Velocity (ft/s)	$e_p$ (Piezometric Efficiency)	$e_b$ (Ballistic Efficiency)	Velocity Ratio	% Error
Chemical Equilibrium	294.07	42651.23	586.85	1925.46	0.20930	0.964	1.16	15.8
Closed Bomb	272.04	39456.21	562.52	1845.62	0.20788	0.886	1.11	11.0
Corners Method	238.29	34561.26	524.64	1721.35	0.20643	0.770	1.04	3.5
Coppocks Model	221.69	32153.51	555.12	1821.35	0.24842	0.863	1.10	9.5
Lumped Parameter	160.07	23215.61	483.28	1585.64	0.26077	0.654	0.95	4.7
IBHVG2	140.05	20312.56	443.83	1456.21	0.25137	0.551	0.88	12.4
XKTC	132.49	19216.61	379.56	1245.32	0.19432	0.403	0.75	25.1
Emperical Results	167.69	24321.16	506.86	1663.00				

Table 7. Pan Model vs Empirical Results 240 Grains

The results for a grain load of 240 are shown in Table 7. The results are still consistent with previous analysis and the zero order method provided the best results and corners method provided the best results and agreed better with the published empirical results.

Propellant Mass 420 Grains								
Model	Max Breech Pressure (MPa)	Max Breech Pressure (psi)	Muzzle Velocity (m/s)	Muzzle Velocity (ft/s)	$e_p$ (Piezometric Efficiency)	$e_b$ (Ballistic Efficiency)	Velocity Ratio	% Error
Chemical Equilibrium	273.55	39675.32	910.25	2986.54	0.54132	1.325	1.26	26.0
Closed Bomb	267.28	38765.43	837.30	2747.18	0.46877	1.121	1.16	15.9
Corners Method	225.38	32687.94	772.71	2535.26	0.47347	0.955	1.07	7.0
Coppocks Model	205.33	29780.56	688.25	2258.14	0.41229	0.757	0.95	4.7
Lumped Parameter	205.75	29841.00	689.48	2262.17	0.41293	0.760	0.95	4.5
IBHVG2	198.33	28765.43	646.28	2120.43	0.37637	0.668	0.89	10.5
XKTC	192.22	27878.65	659.08	2162.43	0.40387	0.695	0.91	8.8
Emperical Results	210.19	30486.00	722.34	2370.00				

Table 8. Pan Model vs Empirical Results 420 Grains

The 420 grain load showed that the lumped parameter model was in the best agreement with the empirical results. The lumped parameter model has the best standard deviation from the previous analysis and continues to have a more consistent prediction for the published values.

Propellant Mass 625 Grains								
Model	Max Breech Pressure (MPa)	Max Breech Pressure (psi)	Muzzle Velocity (m/s)	Muzzle Velocity (ft/s)	$e_p$ (Piezometric Efficiency)	$e_b$ (Ballistic Efficiency)	Velocity Ratio	% Error
Chemical Equilibrium	273.55	39675.32	952.65	3125.63	0.59291	0.975	1.10	10.1
Closed Bomb	267.28	38765.43	928.26	3045.62	0.57616	0.926	1.07	7.2
Corners Method	225.38	32687.94	815.49	2675.62	0.52735	0.715	0.94	5.8
Coppocks Model	205.33	29780.56	826.75	2712.56	0.59492	0.734	0.96	4.5
Lumped Parameter	233.56	33875.62	818.54	2685.62	0.51267	0.720	0.95	5.4
IBHVG2	224.37	32542.15	800.78	2627.36	0.51077	0.689	0.93	7.5
XKTC	210.46	30524.62	772.42	2534.32	0.50665	0.641	0.89	10.8
Emperical Results	238.65	34613.00	865.59	2840.00				

Table 9. Pan Model vs Empirical Results 625 Grains

The lumped parameter model had a percent error of 4.4 for the velocity prediction and predicted the velocity better than the other lumped parameter models. Coppock's model was accurate in predicting the velocity with a percent error of 5.5. The zero order models and lumped parameter models predict more accurate than the closed bomb and chemical equilibrium analysis models. The lumped parameter model was the best in predicting velocity over all other models explored. Recording all the percent errors for the different

powder mass loadings for the pan disruptor results in a favorable result in that the lumped parameter model was able to predict the results with higher consistency and lower percent error. The surprise was that the IBHVG2 model and XKTC models had a higher percent error than expected and that the zero order models actually predicted the velocity better. The only downside of this study is that actual pressure ballistic curves were unobtainable and only maximum breech pressures were recorded. Breech pressures were not directly compared for the percent error of the model. The velocity variable was used for the analysis. The downside of zero order models is they only give a maximum obtainable breech pressure and not a time or distance related pressure curve. This does not allow for a refined Finite Element Analysis (FEA) to be performed and must be done in a static versus dynamic environment that is totally different because of the rate of loading and failure mechanisms not being captured with a static study.

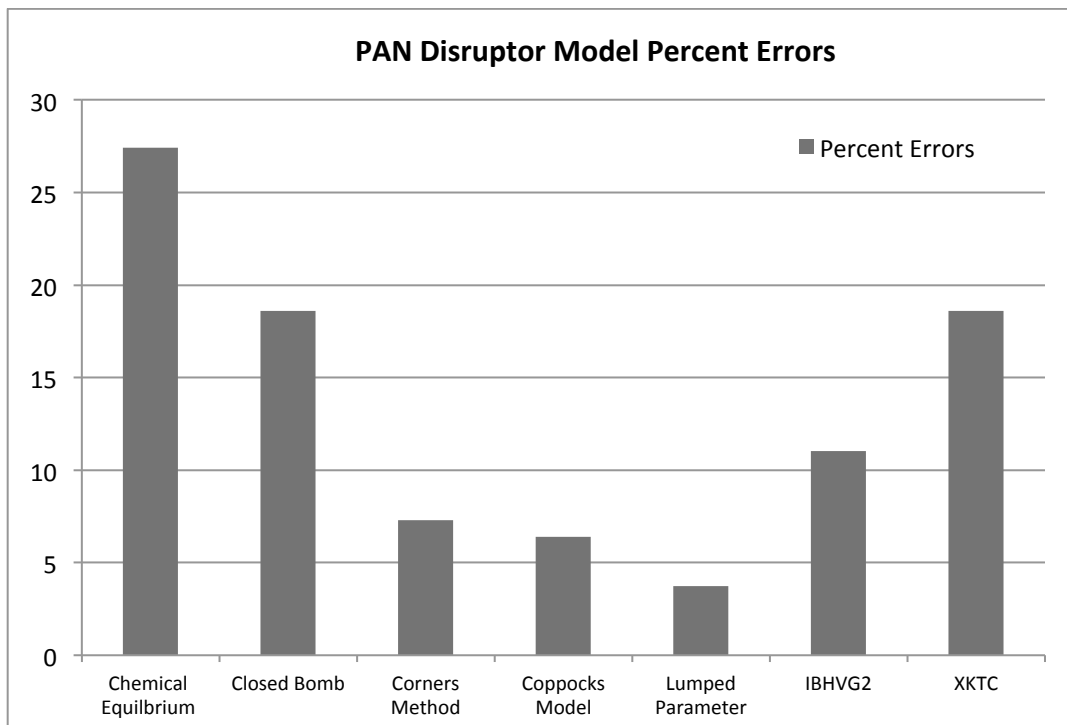


Figure 21. PAN Disruptor Model Percent Errors

### 3.3. 0.50 Caliber Powder Gun (SNL)

The 0.50 caliber powder gun being used for the internal ballistic programs model comparison is a gun used at Sandia for material models. There have been numerous shots performed with this gun system with a variety of propellants with different composition

and burn rate. Two powders were chosen for the study IMR 4064 and IMR 4350 with a projectile commonly shot in the gun. The model will be tested with three different powder cartridges a .308 Winchester, .460 Weatherby and a .50 BMG (Figure 22. 0.50 Cal Powder Gun Casings), which allows to test for three different breech volumes and three different powder loads. The projectile is a consistent 241grain projectile made from brass and will be referred to as the BPB. There are over 250 shots recorded with this barrel with different velocity ranges, powder load weights and cartridge volumes. A plot for each different cartridge is represented picking a commonly shot propellant load for that cartridge and have looked at the burn rate change by selecting a different powder to analyze with all the different methods. This analyst tests the lumped parameter code for accuracy for different case volumes and a different caliber gun with a longer barrel.

The first model to be analyzed is the .308 Winchester. A table of all the input parameters and a plot of all the different methods compiled on the same plot are illustrated.



Figure 22. 0.50 Cal Powder Gun Casings

Figure 22 shows the different cases to be studied. The cases can be partially filled or fully filled for desired velocities but the shots pulled for this study were all loaded to full capacity of the cartridge to have a consistent control for the experimental runs modeled.

The 0.308 Winchester is the smallest cartridge and lowest velocity and then followed by the 0.470 Weatherby cartridge, which will be the intermediate velocity and then followed by the 0.50 BMG cartridge. These are the only three cartridges studied, as they are the only cartridges our breech is designed to hold and the only three cartridges fired on the SNL Thunder Range powder gun.

### 3.3.1 SNL Powder Gun - .308 Winchester IMR 4350

<b>.308 Winchester (IMR 4350)</b>		
<b>Term</b>	<b>Data (Metric)</b>	<b>Data (English)</b>
<b>Bore Diameter</b>	12.7 (mm)	.50 (in)
<b>Barrel Length</b>	1828.8 (mm)	72 (in)
<b>Projectile Mass</b>	15.6619 (gm)	241.70 (grain)
<b>Propellant Mass</b>	2.23 (gram)	34.4 (grain)
<b>Propellant Type</b>	Cylinder	Cylinder
<b>Propellant Length</b>	2.00 (mm)	0.079 (in)
<b>Propellant Diameter</b>	.965 (mm)	0.038 (in)
<b>Adiabatic Flame temperature</b>	3248 (K)	3248 (K)
<b>Impetus F</b>	1122000 (N)	368000 (ft-lb/lb)
<b>Specific Heat Ratio</b>	1.22	1.22
<b>Density</b>	0.664 (gm/cc)	.024 (lb/cuin)
<b>Covolume</b>	.890 (cc/gm)	24.635 (cuin/lb)
<b>Chamber Volume</b>	4097 (cumm)	.25 (cuin)

Table 10. 0.308 Winchester Inputs (IMR 4350)

Table 10. 0.308 Winchester Inputs (IMR 4350) shows the input deck for the 0.308 Winchester using IMR 4350 propellant. This table will be omitted for the later series because the only change is in the chamber volume and the propellant characteristics

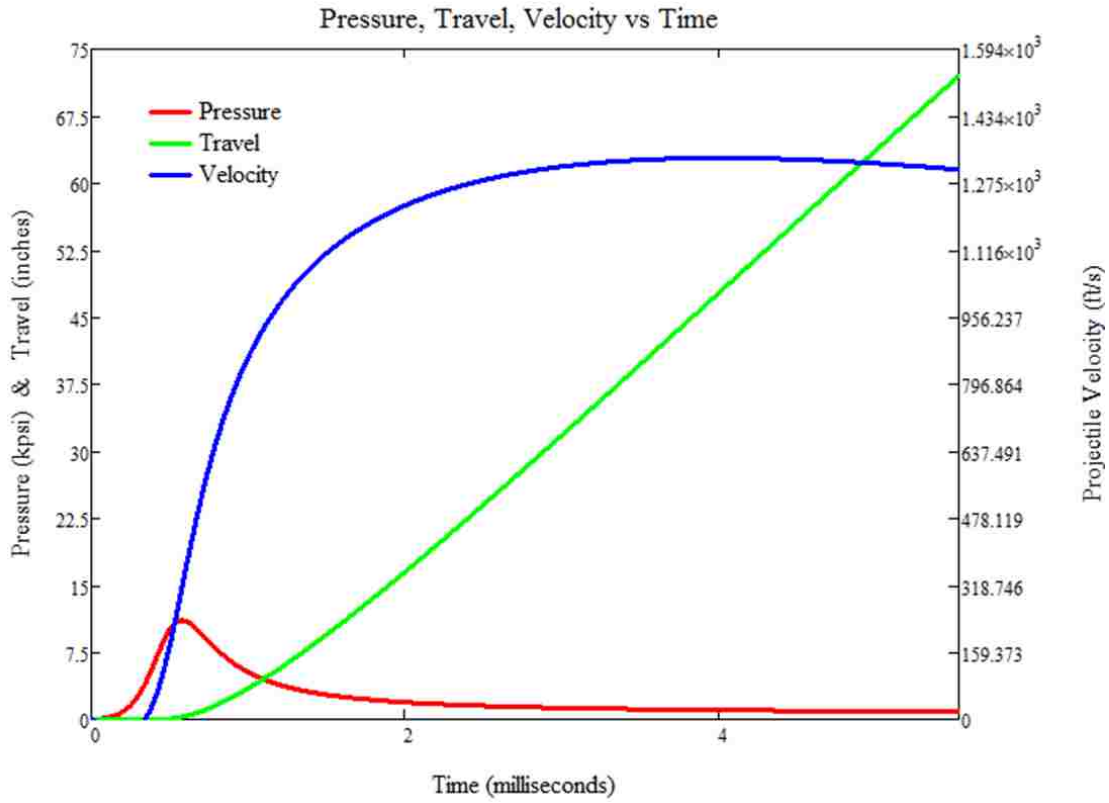


Figure 23. Lumped Parameter PTV Curve

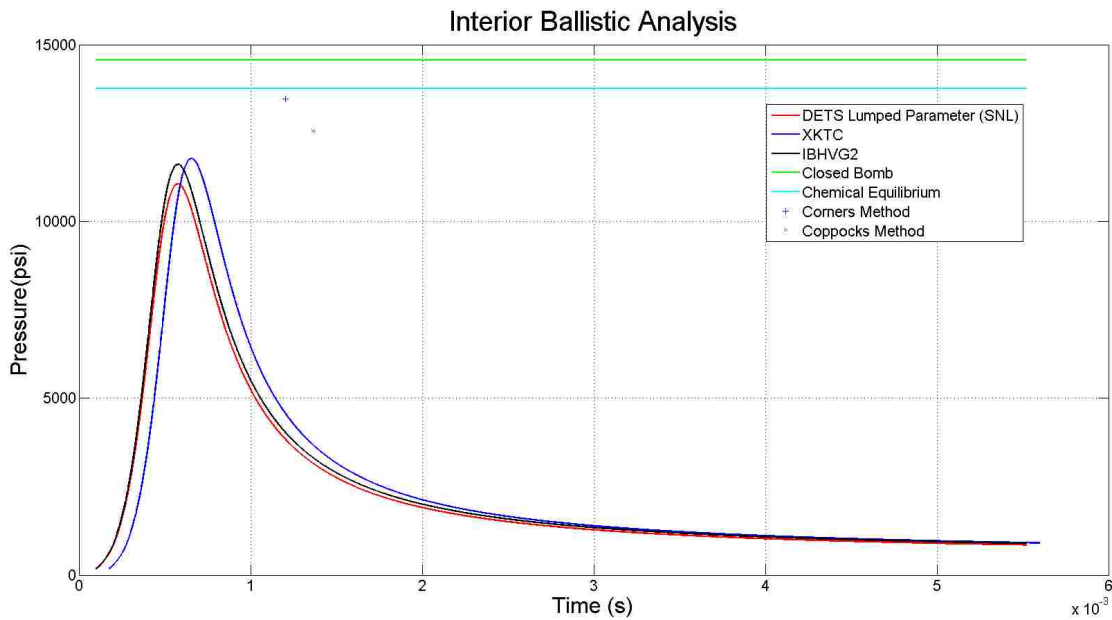


Figure 24. Pressure Curve .308 Winchester (IMR 4350)

For the .308 Winchester IMR 4350 shot and the resulting data is pulled into a Matlab program along with all the other methods to be compared. The data requires a shift in time to align at the same time zero for the plots to overlay. Again the plots seem to agree well with each other in that all have very similar pressure curves.

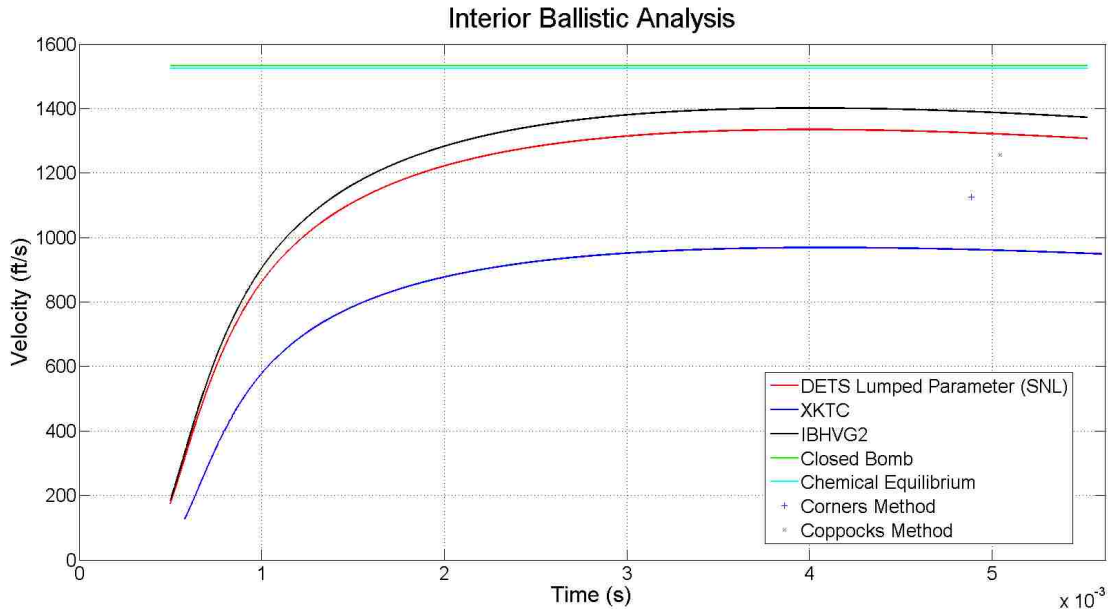


Figure 25. Velocity Curve. 308 Winchester (IMR 4350)

Model	Max Breech Pressure (MPa)	Max Breech Pressure (psi)	Muzzle Velocity (m/s)	Muzzle Velocity (ft/s)	$e_p$ (Piezometric Efficiency)	$e_b$ (Ballistic Efficiency)	Velocity Ratio	% Error
Chemical Equilibrium	100.40	14562.00	577.87	1896.00	0.07587	0.120	1.45	44.7
Closed Bomb	94.87	13760.00	464.80	1525.00	0.05194	0.078	1.16	16.4
Corners Method	92.79	13458.00	342.88	1125.00	0.02890	0.042	0.86	14.1
Coppocks Model	86.61	12562.00	382.81	1256.00	0.03859	0.053	0.96	4.1
Lumped Parameter	76.26	11060.83	398.35	1307.00	0.04746	0.057	1.00	0.2
IBHVG2	80.07	11613.87	427.12	1401.39	0.05197	0.066	1.07	7.0
XKTC	81.22	11779.78	295.26	968.74	0.02448	0.031	0.74	26.1
Emperical Results	76.28	11064.00	399.29	1310.00				

Table 11. Results .308 Winchester (IMR 4350)

### 3.3.2 SNL Powder Gun-- .380 Winchester IMR 4064

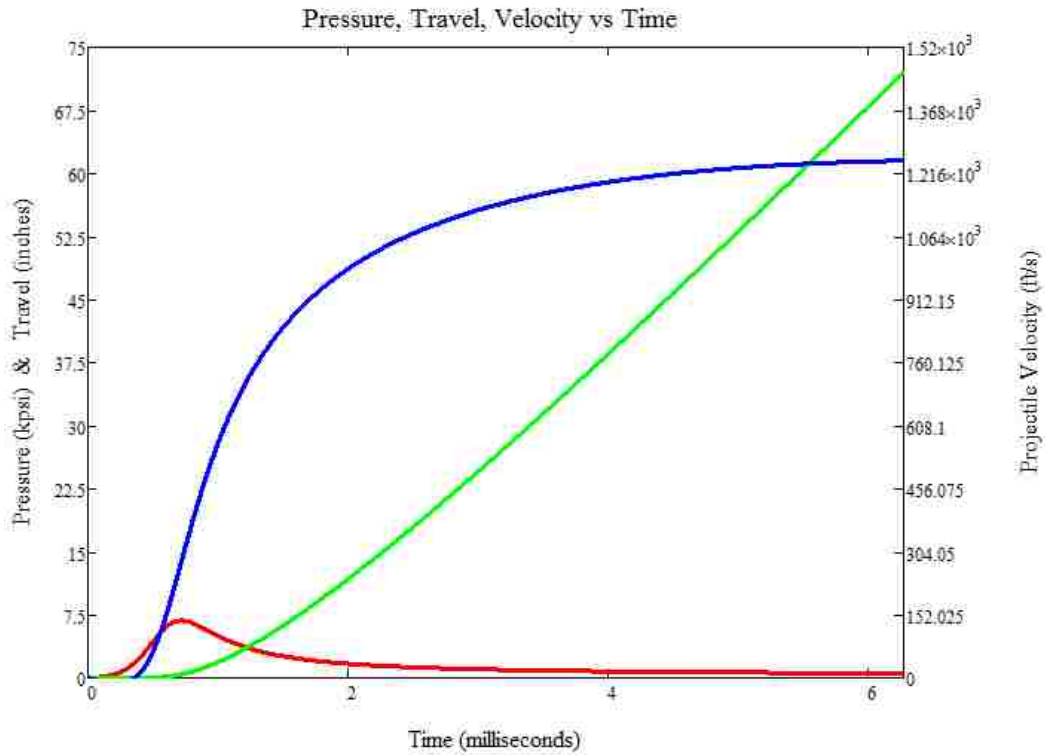


Figure 26. PTV Curve .308 Winchester (IMR 4064)

The results of a different powder burn rate are as expected and the PTV curve shown in Figure 26 captures the subtle changes that occur when changing the burn rate characteristics.

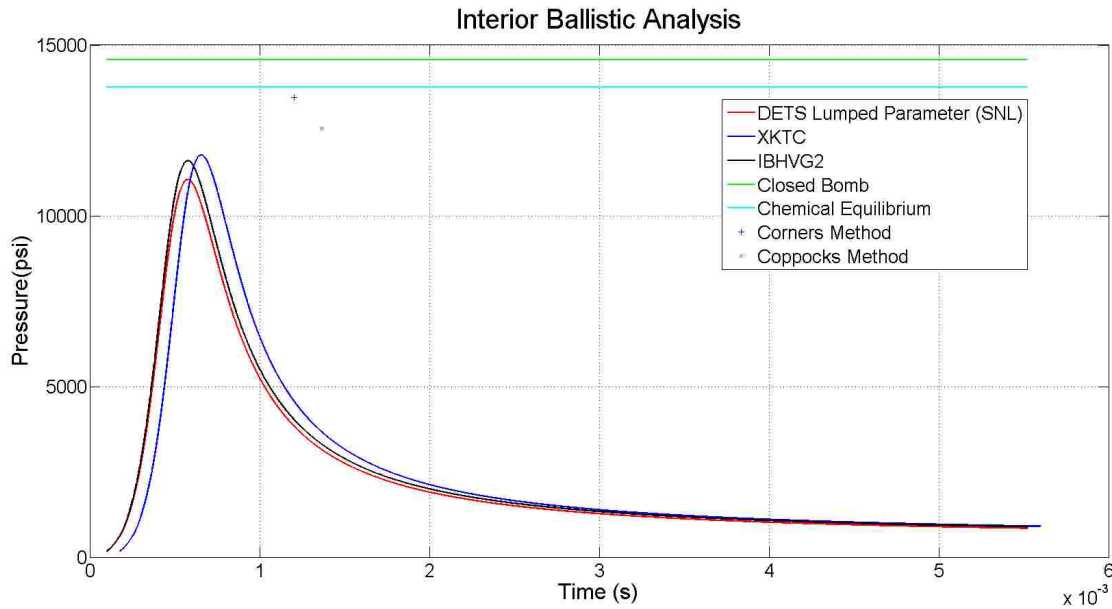


Figure 27. Pressure Curve .308 Winchester (IMR 4064)

The pressure curve is different with a slight change in the peak pressure and time response making the curve longer. The result is a slower velocity, which is depicted by Figure 28.

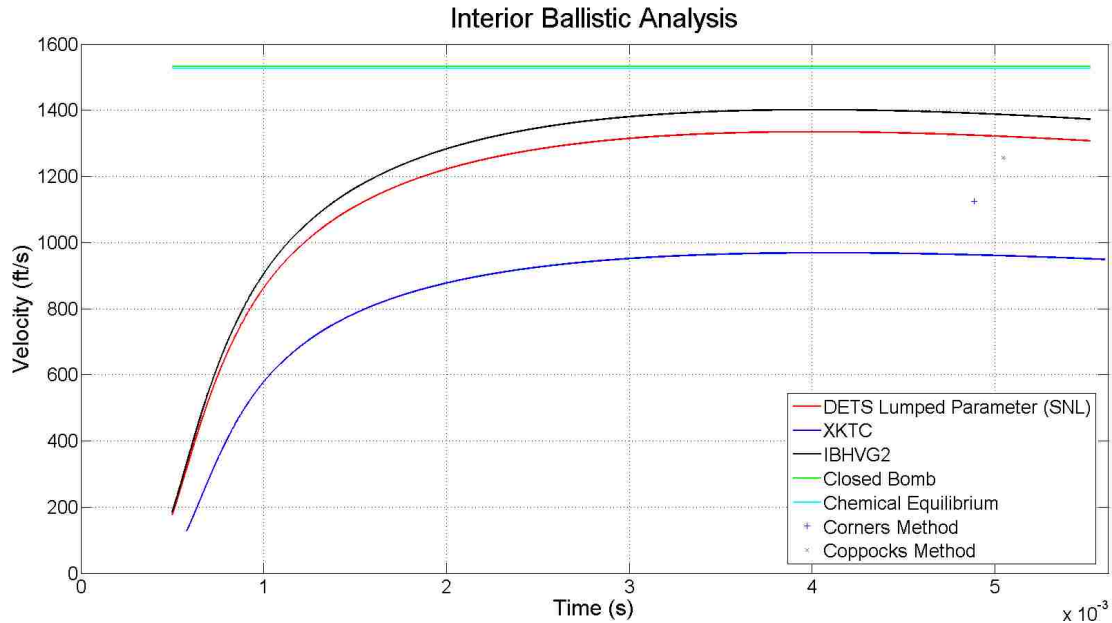


Figure 28. Velocity Curve .308 Winchester (IMR 4064)

Model	OUTPUT PARAMETERS				$e_p$ (Piezometric Efficiency)	$e_b$ (Ballistic Efficiency)	Velocity Ratio	% Error
	Max Breech Pressure (MPa)	Max Breech Pressure (psi)	Muzzle Velocity (m/s)	Muzzle Velocity (ft/s)				
Chemical Equilibrium	100.40	14562.00	577.87	1896.00	0.07587	0.120	1.45	44.7
Closed Bomb	94.87	13760.00	464.80	1525.00	0.05194	0.078	1.16	16.4
Corners Method	92.79	13458.00	342.88	1125.00	0.02890	0.042	0.86	14.1
Coppocks Model	86.61	12562.00	382.81	1256.00	0.03859	0.053	0.96	4.1
Lumped Parameter	76.26	11060.83	398.35	1307.00	0.04746	0.057	1.00	0.2
IBHVG2	80.07	11613.87	427.12	1401.39	0.05197	0.066	1.07	7.0
XKTC	81.22	11779.78	295.26	968.74	0.02448	0.031	0.74	26.1
Empirical Results	76.28	11064.00	399.29	1310.00				

Table 12. Results .308 Winchester (IMR 4064)

The compiled results are shown in Table 12 and it follows the hypothesis that the chemical equilibrium calculations and closed bomb calculations predict higher with a larger percent error in the velocity prediction and that the lumped parameter model predicts the best with a .2 percent error. This table shows that the lumped parameter model is still consistent in velocity predictions with a change in burn rate.

### 3.3.3 SNL Powder Gun- 0.470 Weatherby IMR 3450

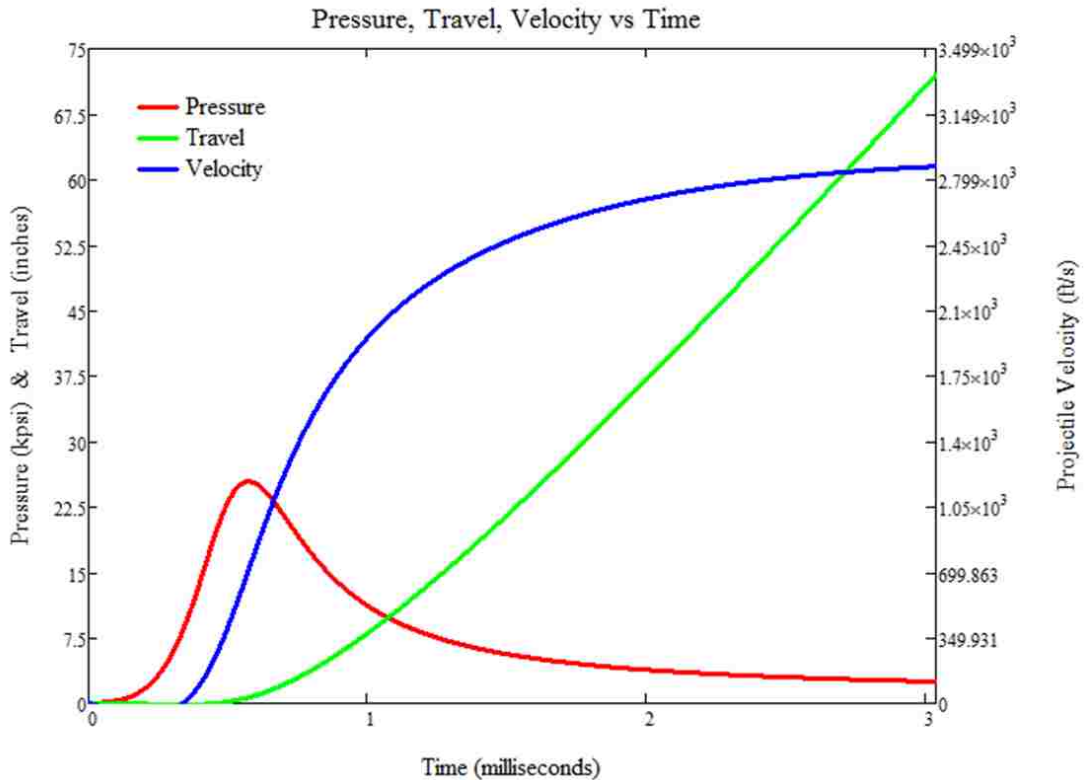


Figure 29. PTV Curve DETS Lumped Parameter 470 Weatherby (IMR 4350)

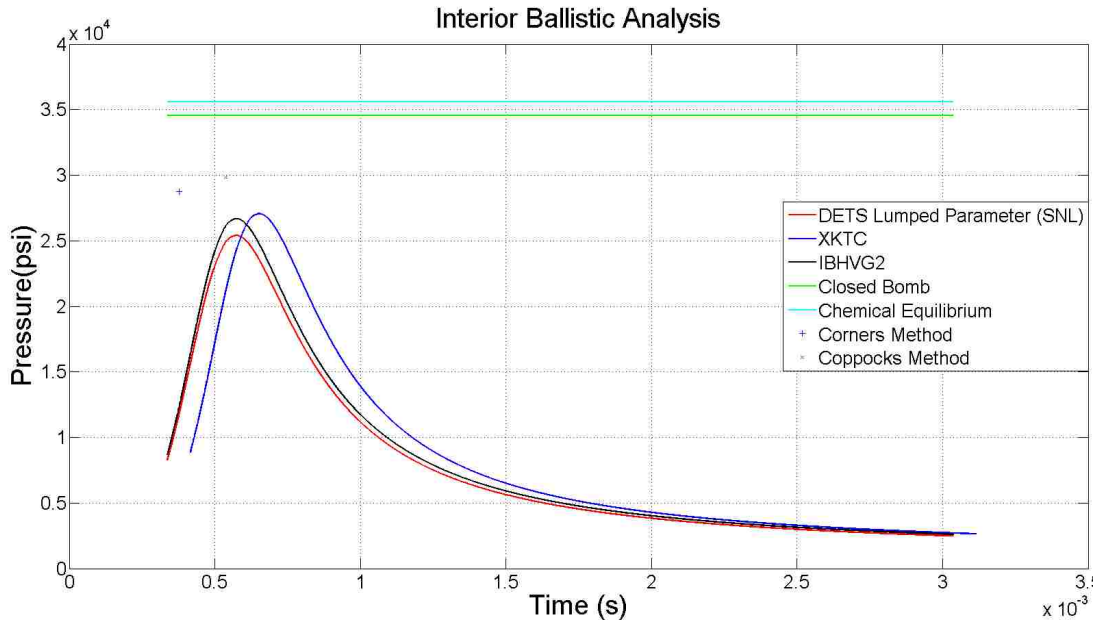


Figure 30. Pressure Curves 470 Weatherby (IMR 4350)

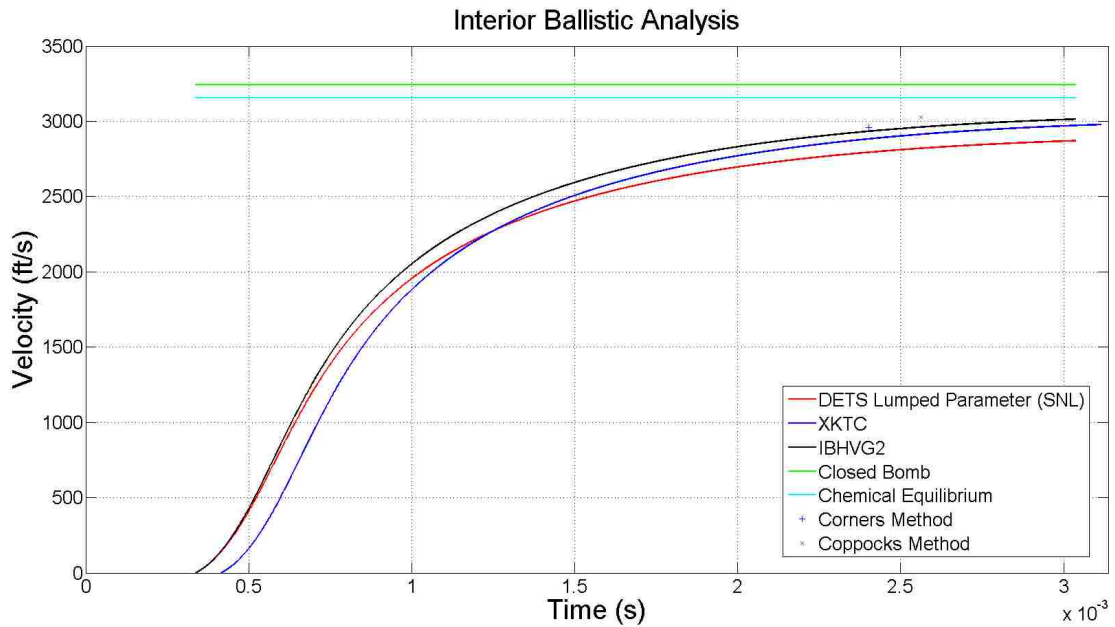


Figure 31. Velocity Curve 470 Weatherby (IMR 4350)

Model	OUTPUT PARAMETERS				$e_p$ (Piezometric Efficiency)	$e_b$ (Ballistic Efficiency)	Velocity Ratio	% Error
	Max Breech Pressure (MPa)	Max Breech Pressure (psi)	Muzzle Velocity (m/s)	Muzzle Velocity (ft/s)				
Chemical Equilibrium	245.45	35600.00	987.50	3240.00	0.09063	0.350	1.23	22.6
Closed Bomb	238.01	34520.00	962.21	3157.00	0.08873	0.333	1.19	19.4
Corners Method	198.19	28745.00	901.25	2957.00	0.09349	0.292	1.12	11.9
Coppocks Model	205.84	29854.00	921.98	3025.00	0.09420	0.305	1.14	14.5
Lumped Parameter	175.19	25408.75	874.83	2870.31	0.09965	0.275	1.09	8.6
IBHVG2	183.95	26679.18	918.57	3013.82	0.10463	0.303	1.14	14.0
XKTC	186.57	27060.32	907.65	2978.00	0.10072	0.296	1.13	12.7
Emperical Results	217.18	31500.00	259.08	2643.00				

Table 13. Results .470 Weatherby (IMR 4350)

The pressure curves and velocity curves are still consistent for the lumped parameter model and is successful in handling a chamber volume adjustment with no errors or problems running and is a able to converge on the solution and is able to still predict within less than ten percent of the empirical velocity.

### 3.3.4 SNL Powder Gun-0.470 Weatherby IMR 4064

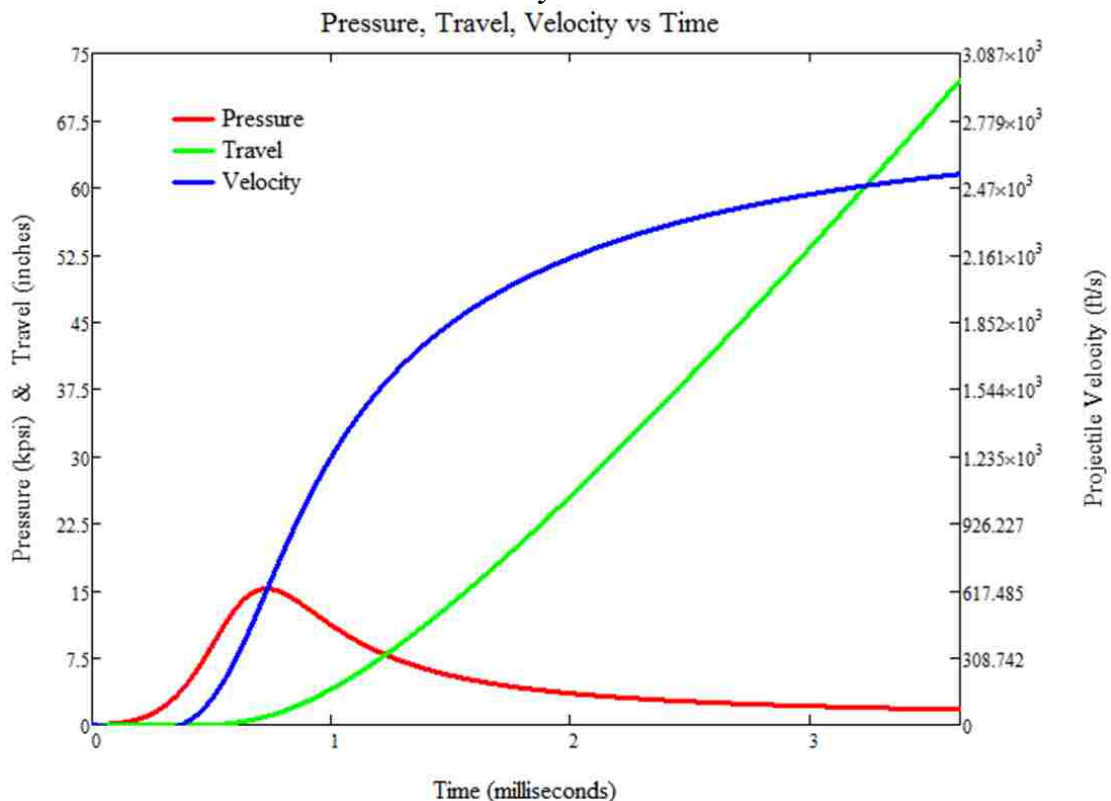


Figure 32. PTV Curve .470 Weatherby (IMR 4064)

The PTV curve for the .470 Weatherby using the IMR 4064 powder is shown in Figure 32 the PTV curve shows that the velocity curve is starting to flatten out and the velocity

is no longer increasing and the acceleration is nearly zero and if one looks at the powder burn plot then one sees that near the end of the muzzle the powder is almost completely burnt which is good it shows the barrel length is sufficient for the charge being used.

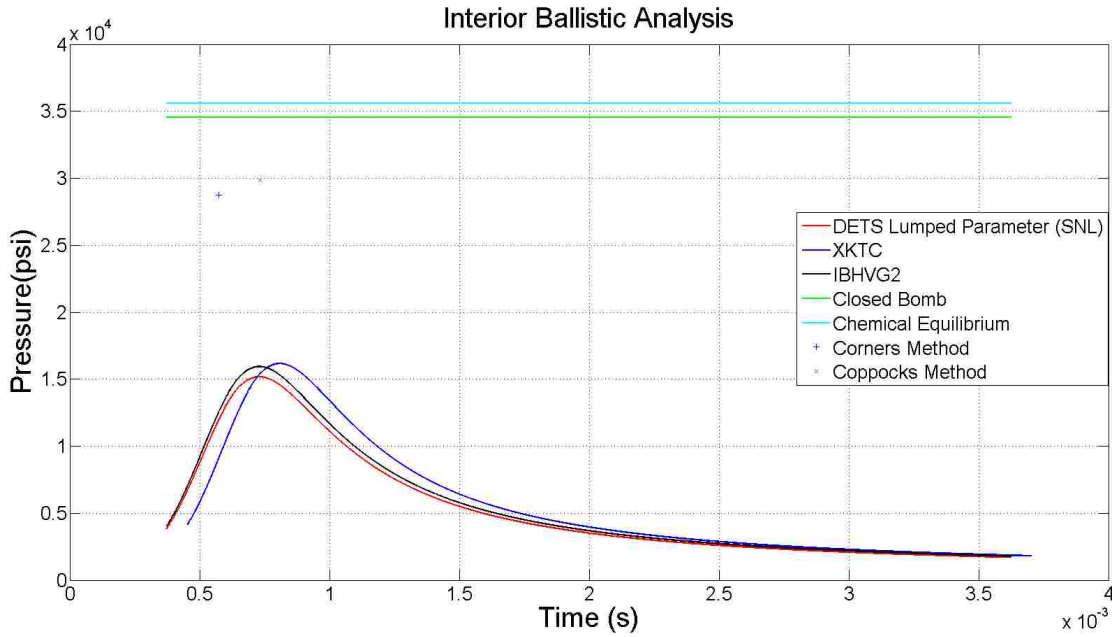


Figure 33. Pressure Curve .470 Weatherby (IMR 4064)

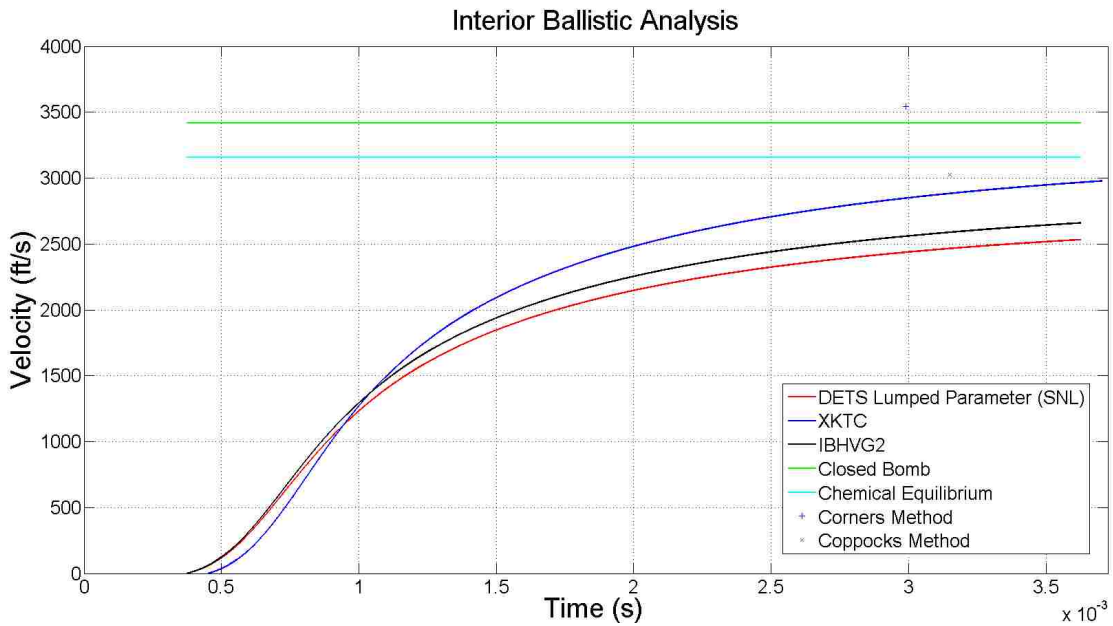


Figure 34. Velocity Curve .470 Weatherby (IMR 4064)

Model	OUTPUT PARAMETERS				$e_p$ (Piezometric Efficiency)	$e_b$ (Ballistic Efficiency)	Velocity Ratio	% Error
	Max Breech Pressure (MPa)	Max Breech Pressure (psi)	Muzzle Velocity (m/s)	Muzzle Velocity (ft/s)				
Chemical Equilibrium	245.45	35600.00	1042.41	3420.16	0.10098	0.390	1.30	29.9
Closed Bomb	238.01	34520.00	962.21	3157.00	0.08873	0.333	1.20	19.9
Corners Method	198.19	28745.00	1079.55	3542.00	0.13414	0.419	1.35	34.6
Coppocks Model	205.84	29854.00	921.98	3025.00	0.09420	0.305	1.15	14.9
Lumped Parameter	104.68	15182.43	771.86	2532.46	0.12982	0.214	0.96	3.8
IBHVG2	109.91	15941.55	810.45	2659.08	0.13631	0.236	1.01	1.0
XKTC	111.48	16169.29	907.65	2978.00	0.16856	0.296	1.13	13.1
Emperical Results	148.24	21500.00	259.08	2632.00				

Table 14. Results .470 Weatherby (IMR 4064)

### 3.3.5 SNL Powder Gun- 0.50 BMG IMR 4350

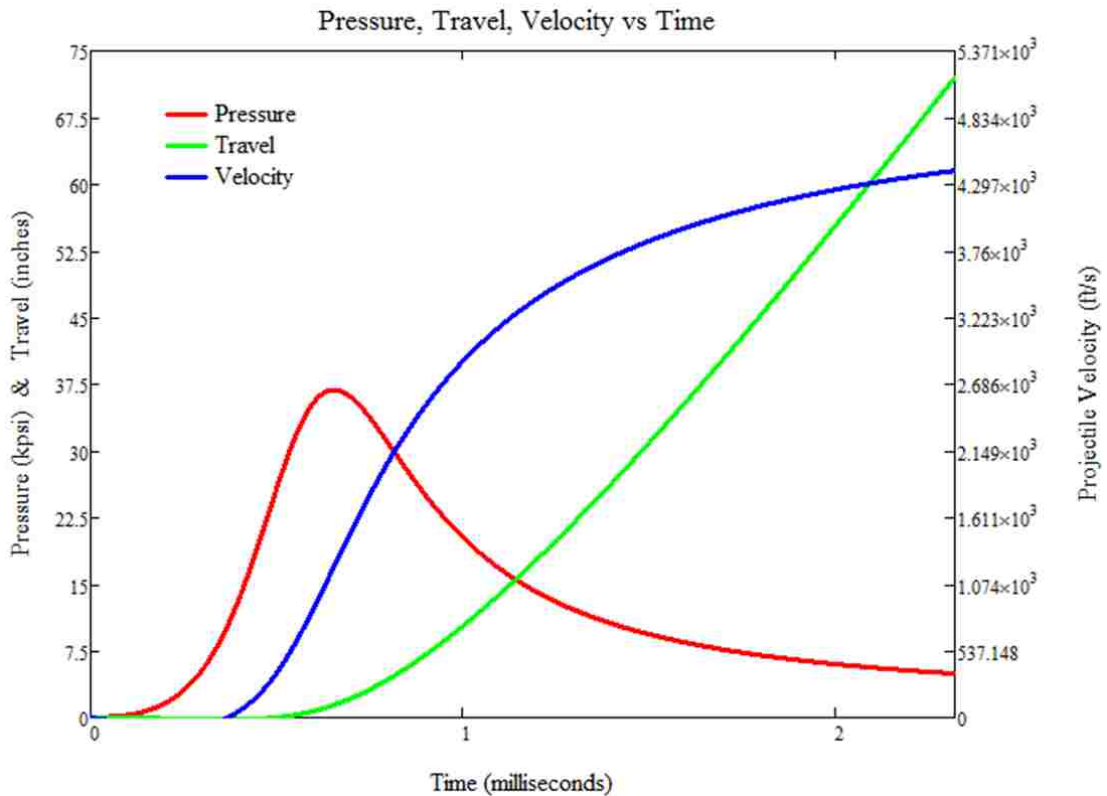


Figure 35. PTV Curve .50 BMG (IMR 4350)

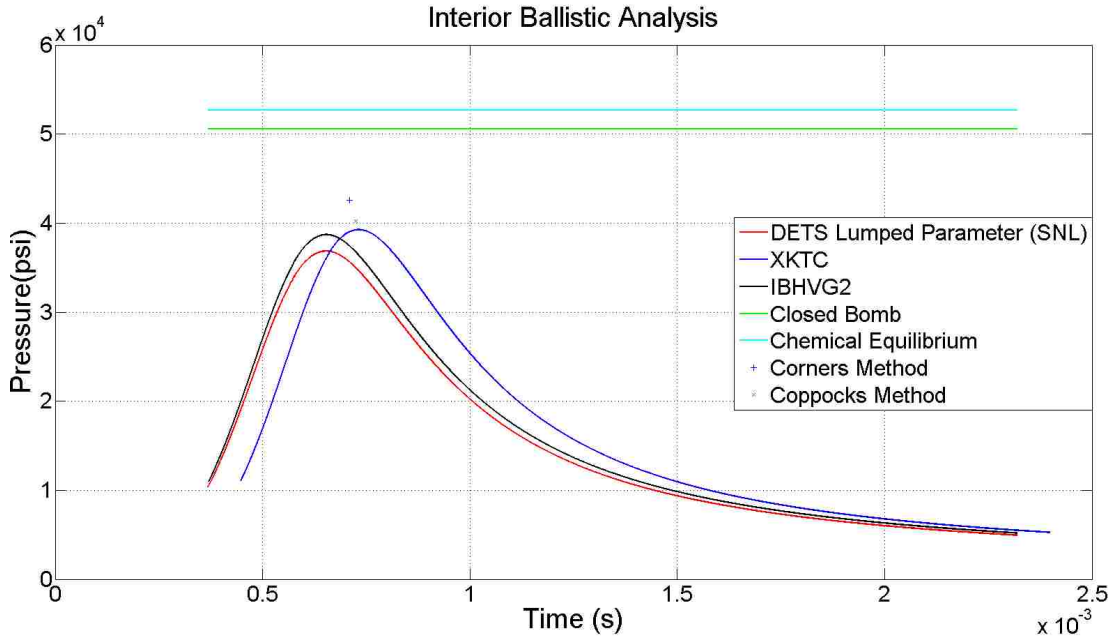


Figure 36. Pressure Curve .50 BMG (IMR 4350)

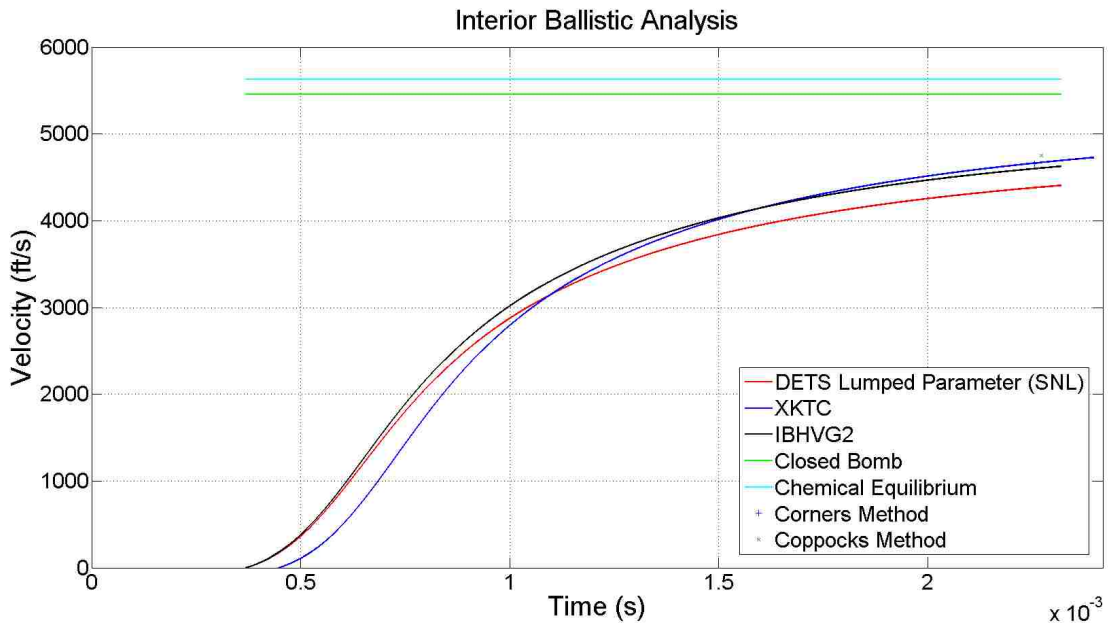


Figure 37. Velocity Curve .50 BMG (IMR 4350)

Model	OUTPUT PARAMETERS				$e_p$ (Piezometric Efficiency)	$e_b$ (Ballistic Efficiency)	Velocity Ratio	% Error
	Max Breech Pressure (MPa)	Max Breech Pressure (psi)	Muzzle Velocity (m/s)	Muzzle Velocity (ft/s)				
Chemical Equilibrium	362.96	52643.00	1714.42	5625.00	0.18472	1.056	1.28	28.0
Closed Bomb	348.78	50586.00	1661.99	5453.00	0.18065	0.992	1.24	24.1
Corners Method	293.44	42560.00	1419.46	4657.25	0.15663	0.724	1.06	6.0
Coppocks Model	277.52	40251.00	1448.71	4753.21	0.17251	0.754	1.08	8.2
Lumped Parameter	254.14	36860.50	1342.86	4405.91	0.16185	0.648	1.00	0.3
IBHVG2	266.85	38703.52	1410.00	4626.20	0.16994	0.714	1.05	5.3
XKTC	270.66	39256.43	1440.88	4727.54	0.17497	0.746	1.08	7.6
Emperical Results	236.15	34250.00	1339.15	4393.54				

Table 15. Results .50 BMG (IMR 4350)

### 3.3.6 SNL Powder Gun- 0.50 BMG IMR 4064

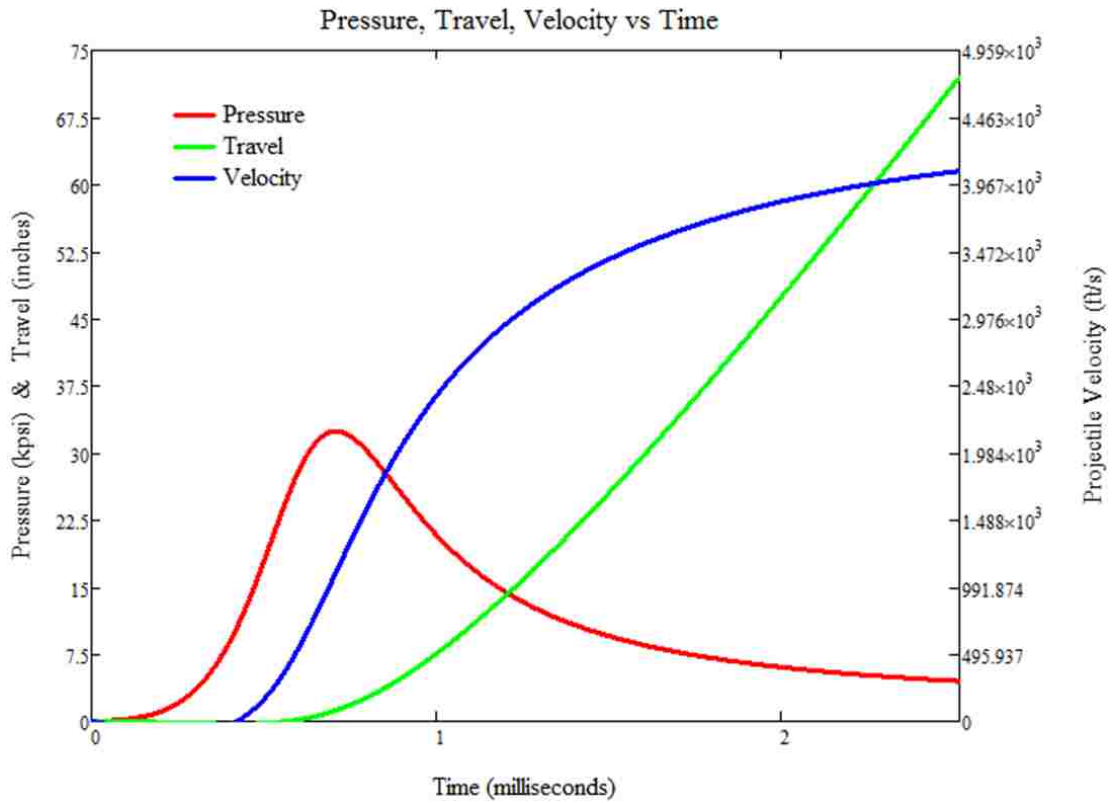


Figure 38. PTV Curve .50 BMG (IMR 4064)

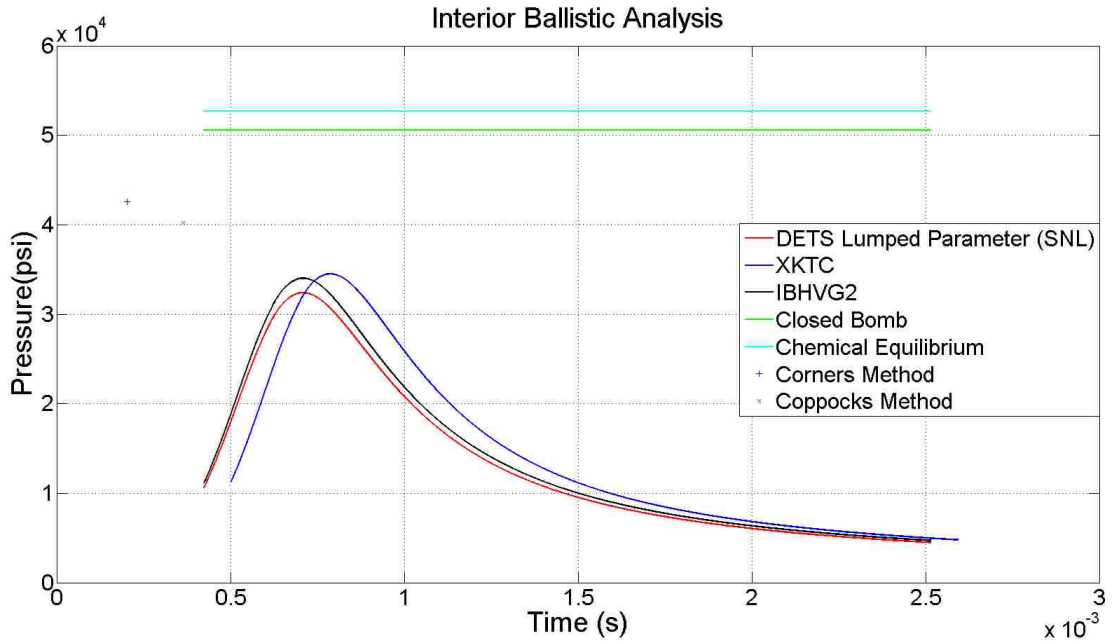


Figure 39. Pressure Curve .50 BMG (IMR 4064)

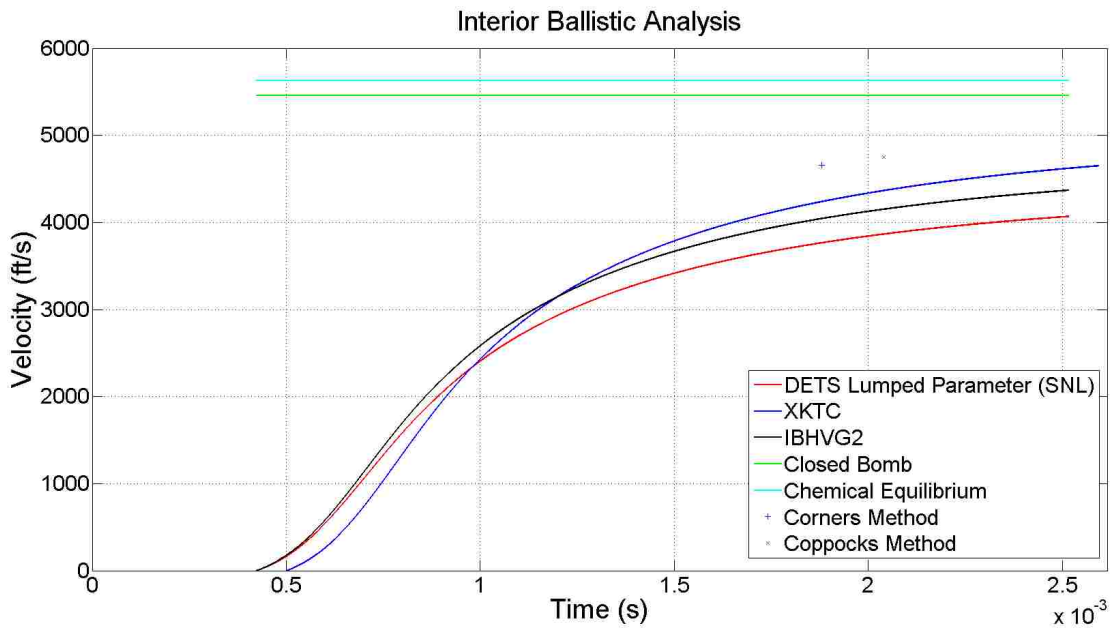


Figure 40. Velocity Curve .50 BMG (IMR 4064)

Model	OUTPUT PARAMETERS				$e_p$ (Piezometric Efficiency)	$e_b$ (Ballistic Efficiency)	Velocity Ratio	% Error
	Max Breech Pressure (MPa)	Max Breech Pressure (psi)	Muzzle Velocity (m/s)	Muzzle Velocity (ft/s)				
Chemical Equilibrium	362.96	52643.00	1714.42	5625.00	0.18472	1.056	36.4	
Closed Bomb	348.78	50586.00	1661.99	5453.00	0.18065	0.992	32.2	
Corners Method	293.44	42560.00	1419.46	4657.25	0.15663	0.724	12.9	
Coppocks Model	277.52	40251.00	1448.71	4753.21	0.17251	0.754	15.2	
Lumped Parameter	223.44	32406.80	1239.84	4067.91	0.15693	0.552	1.4	
IBHVG2	234.61	34027.14	1331.61	4369.00	0.17240	0.637	5.9	
XKTC	237.96	34513.24	1417.25	4650.00	0.19254	0.721	12.7	
Emperical Results	235.50	34156.00	1257.37	4125.24				

Table 16. Results .50 BMG (IMR 4064)

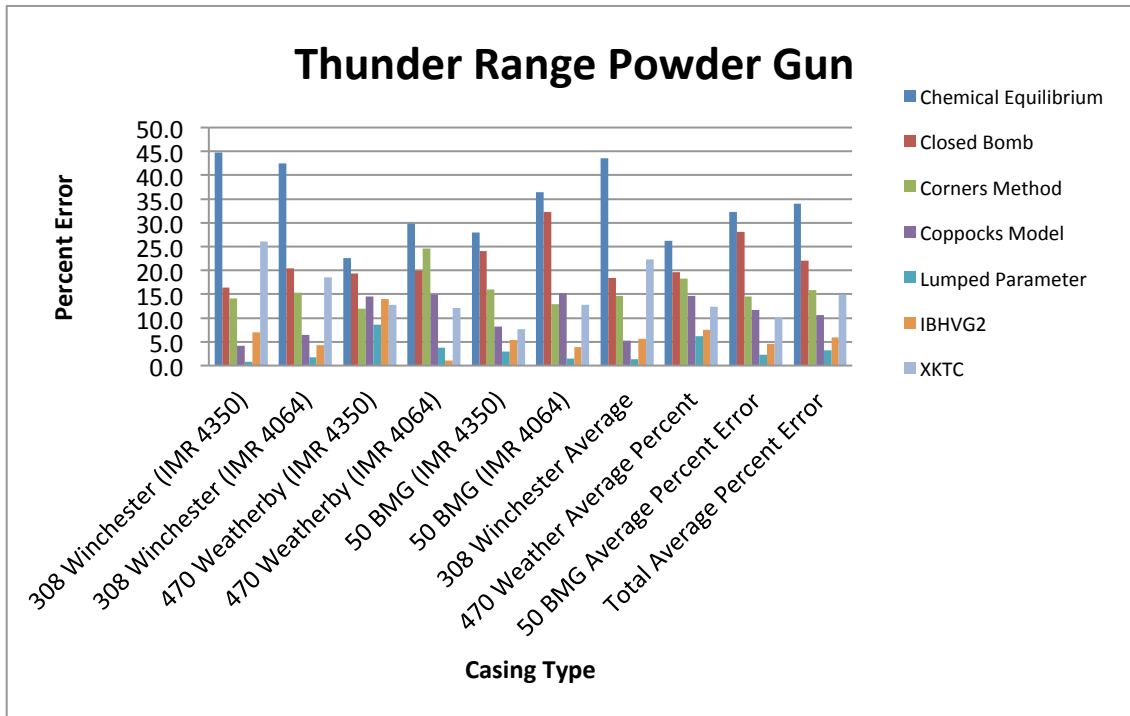


Figure 41. Thunder Range Powder Gun Percent Errors

### 3.4 Thunder Range Powder Gun Results

The results of this data are that the SNL lumped parameter model developed is comparable in percent error over all the different case volumes and burn rates with the IBHVG 2 model. The SNL Model falls below 5 percent error for all casing types besides the 470 Weatherby. The analytical models also predict well only going 1 or 2 percent above 15 percent error. This builds confidence in the lumped parameter model for predicting pressure and velocity profiles and predicting gun performance. This percent error plot also shows that the powder burn rate is captured accurately and able to model

the different powder burn rate characteristics. The difference between the powder burn rates only at most produces a 6 percent error range. The figure below shows a compilation of all the shots performed on the powder gun and many of the comparisons between the empirical data and the model data have been performed against this plot and also some analytical equations developed to predict performance characteristics of the powder gun. This shows that once enough empirical shots have been completed one can predict the performance with a minimum seventy three percent fit to the curve using the mass ratio which is the powder mass divided by the projectile mass as the independent variable to predict the dependent variable which is the velocity of the projectile.

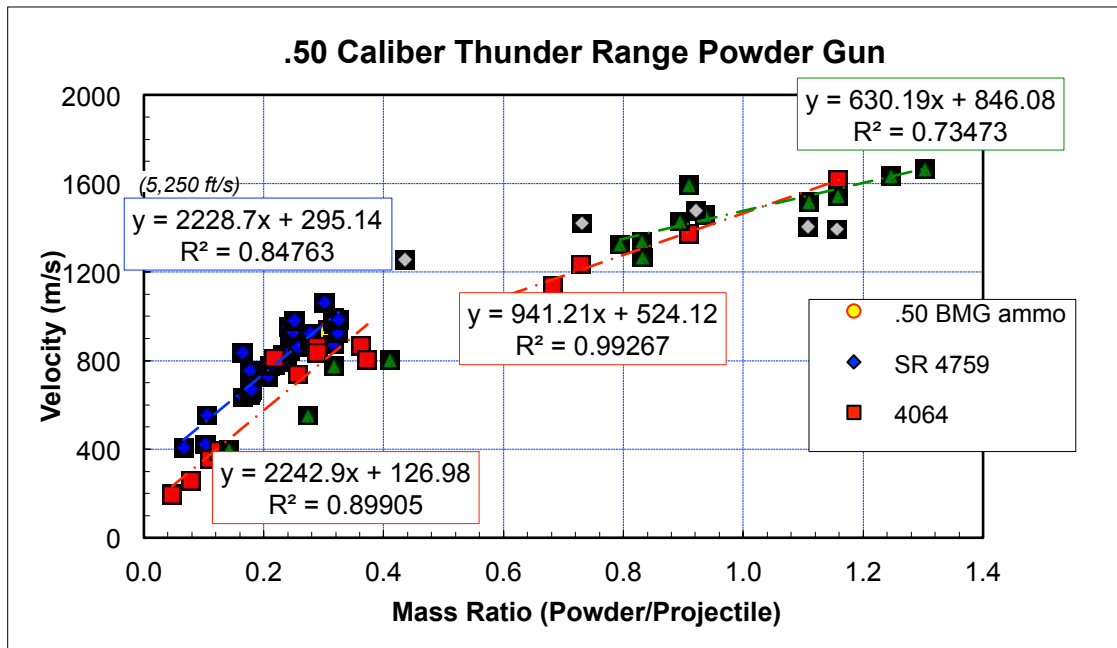


Figure 42. Thunder Range Empirical Results

### 3.5 50 mm Launcher

The last gun launcher is an experimental gun developed at Thunder Range for specific studies. This launcher was developed using the models from this study and was tested to check for model accuracy. The models shown are for the low velocity range to the high velocity range, which was the range the launcher was designed to produce. The first model shown is the low velocity model Figure 43. One thing to note is that the velocity curve is still increasing and not as flat as the preceding launchers studied and the reason for this is because if one looks at the length of the barrel for this launcher they will note it

is only 36 inches long which was a design requirement dictated by the customer. If the barrel length could be increased then a higher velocity could be achieved by the launcher because the projectile is still accelerating when it reaches the end of the muzzle.

**3.5.1- 50 mm Launcher Low Velocity Target**

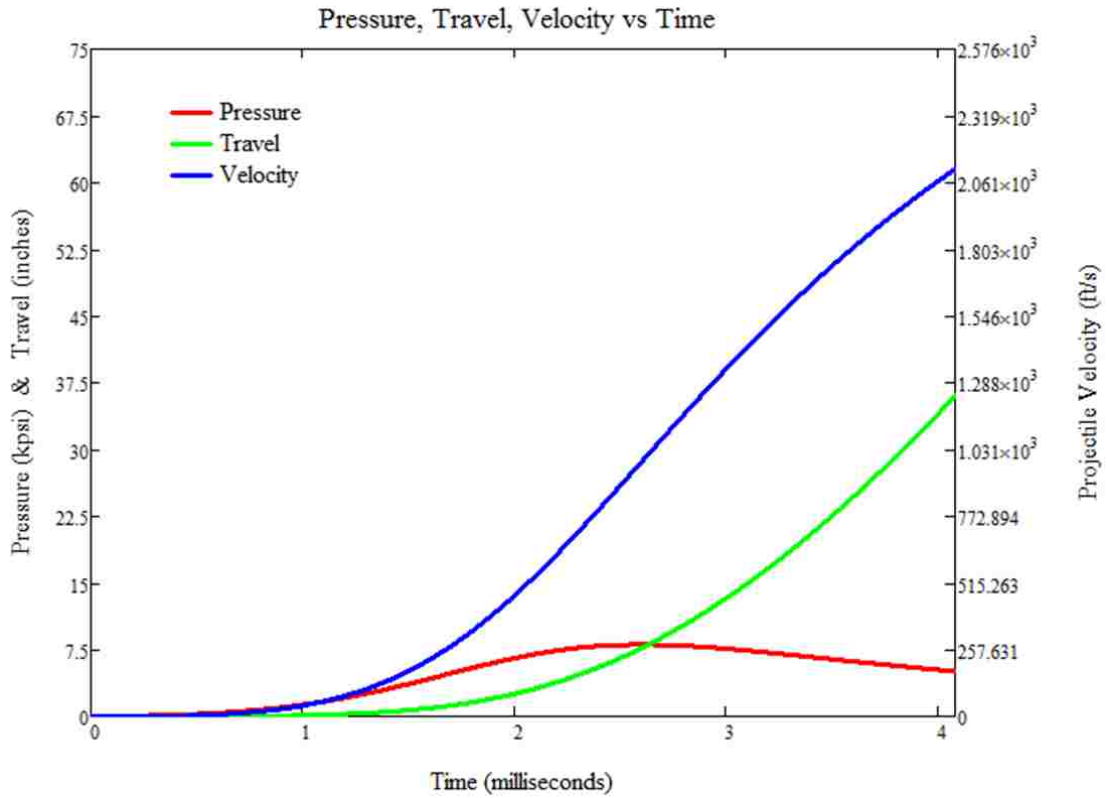


Figure 43. PTV Curve 50 mm (Low Velocity)

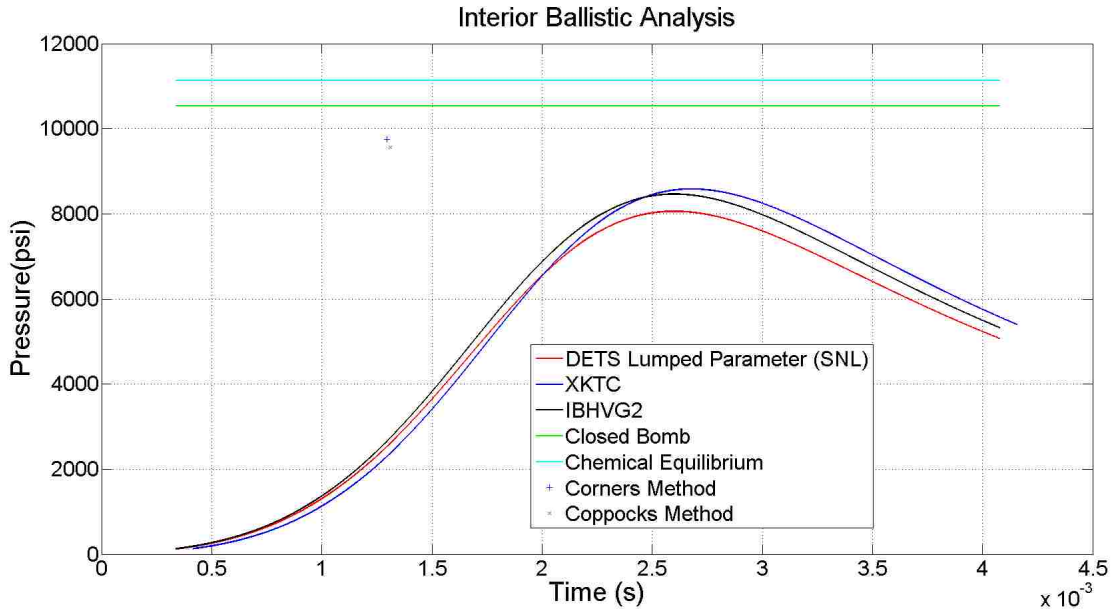


Figure 44. Pressure Curve 50 mm (Low Velocity)

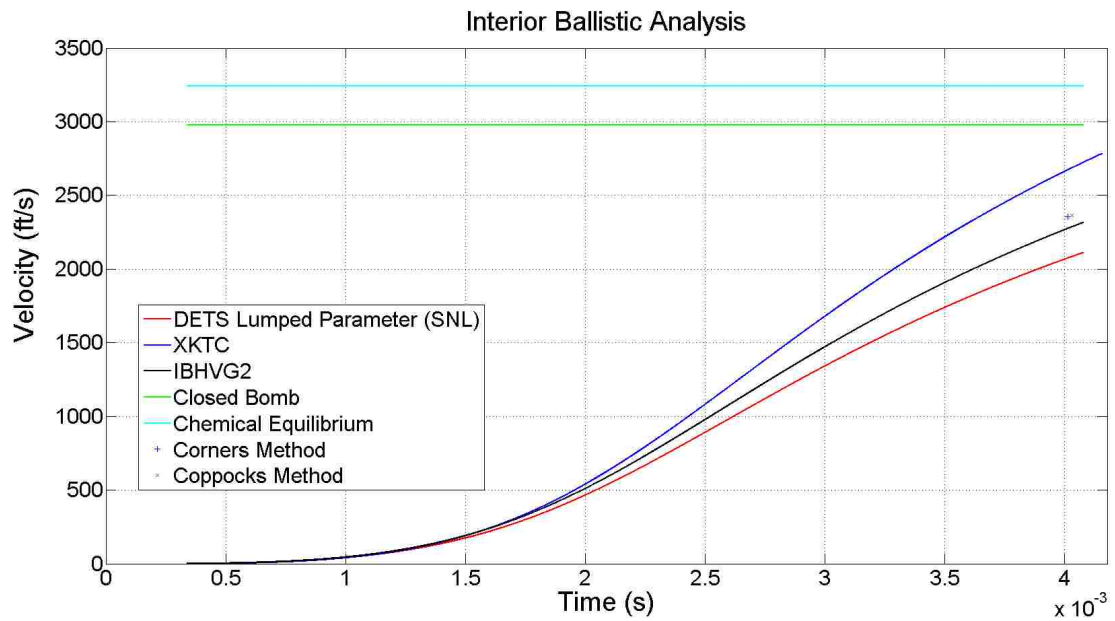


Figure 45. Velocity Curve 50 mm (Low Velocity)

### 3.5.2-50 mm High Velocity Target

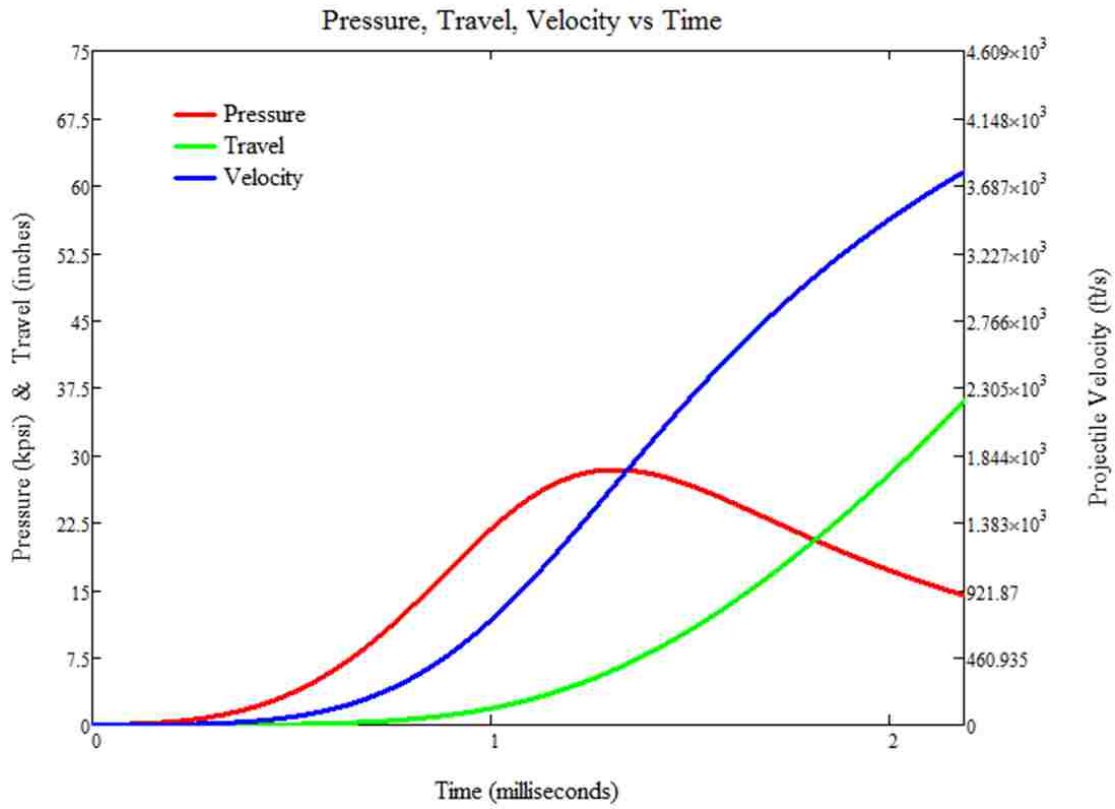


Figure 46. PTV Curve 50 mm High Velocity

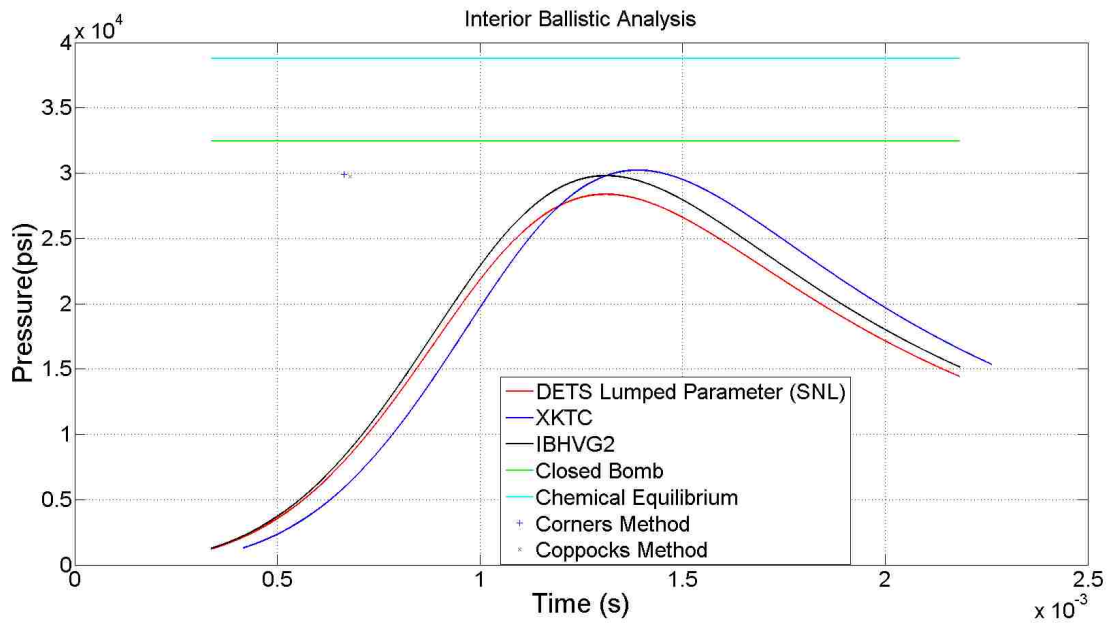


Figure 47. Pressure Curves 50 mm (High Velocity)

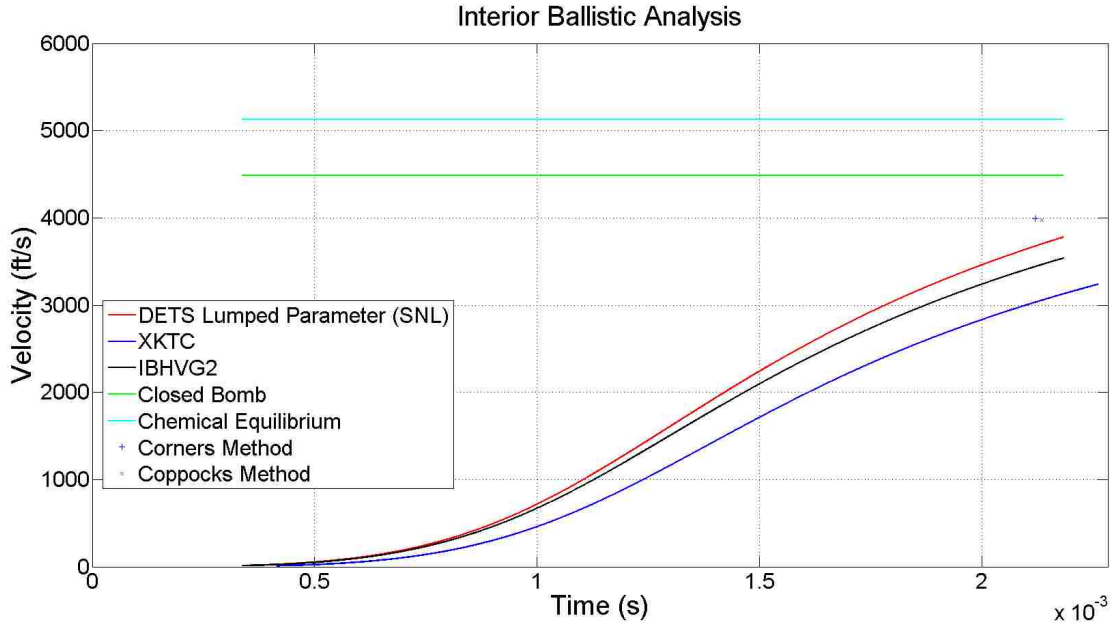


Figure 48. Velocity Curves 50 mm (High Velocity)

The high velocity model shows that the projectile is also still accelerating but at least is starting to flatten out. The reason this is the top velocity is because the breech pressure starts to become unsafe at powder loads exceeding this loading and the customer and Sandia needed to insure that a F.O.S of a minimum of 1.5 was maintained with a desired 2.0 F.O.S. The pressure curve was put into a finite element program and a von mises stress criteria was used to determine the F.O.S.

The modeling was used to develop a design that led to a field prototype in a relatively short amount of time and aligned with the results very well which can be seen in the low velocity results table below. The higher velocity has yet to be shot and there is no test data for the high velocity range as of yet.

Model	OUTPUT PARAMETERS				$e_p$ (Piezometric Efficiency)	$e_b$ (Ballistic Efficiency)	Velocity Ratio	% Error
	Max Breech Pressure (MPa)	Max Breech Pressure (psi)	Muzzle Velocity (m/s)	Muzzle Velocity (ft/s)				
Chemical Equilibrium	76.70	11125.00	987.50	3240.00	0.29000	0.350	1.48	48.1
Closed Bomb	72.68	10542.00	906.74	2975.00	0.25802	0.295	1.36	36.0
Corners Method	67.27	9756.00	718.07	2356.00	0.17486	0.185	1.08	7.7
Coppocks Model	65.93	9562.00	720.51	2364.00	0.17962	0.186	1.08	8.1
Lumped Parameter	55.57	8059.73	644.07	2113.20	0.17028	0.149	0.97	3.4
IBHVG2	58.35	8462.72	706.49	2318.00	0.19513	0.179	1.06	6.0
XKTC	59.18	8583.61	848.83	2785.00	0.27771	0.259	1.27	27.3
Emperical Results	55.59	8062.00	644.04	2187.00				

Table 17. 50 mm Low Velocity Results

## CHAPTER 4 DISCUSSION

### *4.1 Model Difficulties*

The compilation of the data from all the different codes proved to be the greatest challenge in the whole exercise. Some of the data files being outputted by the other lumped parameter codes did not have a time vector of same length as the SNL lumped parameter code so the time vector being used for the model comparison was the time vector of the longest length and then all other data plotted with the longest time vector. Therefore, some of the plots may be slightly shifted and the pressure profiles do not quite lay as close on top of each other as some of the plots suggest. Also some of the data was cut short after the pressure curve so some data from the lumped parameter was used to fill the tail end gaps for the longer time records.

### *4.2 Model Limitations*

There are limitations to analytical models that requires some of the coefficients to be fitted to certain guns and the model is improved if there is already a large database of empirical data available to fit coefficients, like the adiabatic heat loss or the kinetic friction coefficient. A large database of ballistic pressure curves or max peak breech pressure and muzzle velocity is preferable. Given the projectile velocity curve, then one can curve fit the program to existing data making it far more accurate and far more predictive.

## CHAPTER 5 CONCLUSIONS

### *5.1 Summary*

The SNL Lumped parameter model provides the user the ability to see the equations driving the results and provides accurate results when compared to three different empirical test scenarios.

The SNL lumped parameter model is able to predict equally or if not better than some of the commercial codes and is written as a Mathcad program that is good for user editing functionality and for diagnostic probing. Also by using Mathcad as the program there are a variety of open source Math programming tools with the solvers capable of

handling the seven ordinary differential equations that need to be solved so the program could be easily transferred to SMath Studio, or equivalent math program or any other programming language. Also by being able to see all the equations driving the model the code could be easily transferred to a Matlab® or Maple® program for plotting and solving the equations. A large Excel® file was created for the comparison of all the models that could be read into Matlab® and then be plotted to show a comparison of all the different codes. This program is also being used by SNL to develop other launcher systems and serving as a check program for other gun development tools.

The flexibility and editable nature of this program is what makes it attractive to the user. It can be tailored to the specific launcher system and come up with different projectile designs, chamber designs and allow the user to design a optimized launcher system by running multiple iterations in a timely manner. The results of the code are accurate for different gun types which was illustrated by using three launchers of completely different size using short barrels, different size projectiles and different powder types. As long as the input is accurate to the launcher geometry being fired this code will be successful at predicting the results and useful for impact studies or other applications.

## ***5.2 Lessons Learned***

The work presented in this thesis shows that a lumped parameter interior ballistic model can be useful for predicting projectile velocities and internal breech pressures and can be used as gun design tool to help optimize gun performance. This model has been used to aid in the development of at least one launcher. The accuracy and reliability of the code is acceptable for design work and because of the program being written in a program like MathCad can easily show the user what equations are being solved and the step by step process for doing an interior ballistic analysis. By solving the equations and writing this type of lumped parameter model one learns the ballistic cycle more in depth and gives a designer a better intuitive feeling for the ballistic cycle and what type of results to expect when doing a ballistic analysis allows them to be a better designer.

### ***5.3 Future Work***

The future work of this model would be to improve the program to improve its usability utilizing both a graphical user interface (GUI) but also allowing the program to be edited to change parameters and make improvements to the code. If the program has an open architecture it will allow the program to evolve and only become better. The other possible improvement to this type of program is to implement it into some type of FEA package or design package like Solidworks or ProE to allow the user to design a gun system while utilizing the pressure travel curves to help drive design and performance of the gun all in the same package.

## REFERENCES

- Brode, H. L., & Enstrom, J. E. (1970, September). A Numerical Method for Calculating Interior Ballistics. New York, New York, United States of America.
- Brode, H. L., & Enstrom, J. E. (1969). *Interior Ballistics and Gun Flash and Smoke*. New York: The Rand Corporation.
- Callen, H. B. (1985). *Thermodynamics and an Introduction to Thermostatistics* (2nd ed.). New York, New York, United States of America: John Wiley and Sons.
- Carlucci, D. E., & Jacobson, S. S. (2008). *Ballistics Theory and Design of Guns and Ammunition*. Boca Raton, Florida, United States of America: CRC Press.
- Chernyi, G. G., Losev, S. A., Macheret, S. O., & Potapkin, B. V. (2002). *Physical and Chemical Process in Gas Dynamics* (Vol. 196). (P. Zarchan, Ed.) Danvers, Massachusetts, United States of America: American Institute and Astronautics INC.
- Cooper, P. W., & Kurowski, S. R. (1996). *Introduction to the Technology of Explosives*. Hoboken, New Jersey, United States of America: Wiley-VCH.
- Corner, J. (1950). *Theory of the Interior Ballistics of Guns*. New York, New York, United States of America: John Wiley and Sons Inc.
- Davis, T. L. (1943). *The Chemistry of Powder and Explosives*. Norwell, Massachusetts, United States of America: National Fireworks INC.
- Ingalls, J. M. (1912). *Interior Ballistics* (3rd ed.). New York, New York, United States of America: John Wiley and Sons.
- Johnson, I. A. (2005). *The Nobel-Abel Equation of State: Thermodynamic Derivations for Ballistics Modeling*. Australian Government, Department of Defense. Sidney: Defense Science and Technology.
- Krier, H., Adams, M. J., Baer, P. G., Goldstein, S., Celmins, A. K., Serao, P., et al. (1979). *Interior Ballistics of Guns* (Vol. 66). (H. Krier, & M. Summerfield, Eds.) New York, New York, United States of America: American Institute of Aeronautics and Astronautics.
- Kuo, K. K. (2005). *Principles of Combustion* (2nd ed.). Hoboken, New Jersey, United States of America: John Wiley and Son Inc.
- Lewis, B., & Elbe, G. v. (1987). *Combustion, Flames and Explosions of Gases* (Third ed.). Orlando, Florida, United States of America: Academic Press.

Manelis, G. B., Nazin, G. M., Rubtsov, Y. I., & Strunin, V. A. (2003). *Thermal Decomposition and Combustion of Explosives and Propellants*. New York, New York, United States of America: Taylor and Francis.

Miura, H., & Matsuo, A. (2006). Numerical Simulation of Solid Propellant Combustion in a Gun Chamber. *42nd AIAA/ASME/SAE/ASEE Joint Propulsion Conference and Exhibit*. Sacramento : American Institute of Aeronautics and Astronautics.

Struble, R. (1996). *A Study of The Interior Ballistics Equations*.

Turns, S. R. (2006). *An Introduction to Combustion* (2nd ed.). Singapore: McGraw Hill.

Yang, V., Brill, T. B., & Ren, W. Z. (2000). *Solid Propellant Chemistry* (Vol. 185). (P. Zarchan, Ed.) Danvers, Massachusetts, United States of America: Progress in Astronautics and Aeronautics.

**(INTENTIONALLY LEFT BLANK)**

## APPENDIX A

### *Propellant Formulations*

# IMR

#### **IMPROVED MILITARY RIFLE (IMR)**

##### **FORMULATION:**

There are a number of IMR formulations. Please refer to Appendix B or C to determine which formulation is used in specific ammunition items.

##### IMR 4064:

Nitrocellulose 92.60  
Diphenylamine 1.00  
Graphite 0.40  
Dinitrotoluene 5.00  
Potassium Sulfate 1.00

##### IMR 4879:

Nitrocellulose 96.45  
Diphenylamine 1.00  
Graphite 0.40  
Dinitrotoluene 0.80  
Potassium Sulfate 1.00  
Silicon Powder 0.75

##### IMR 4895:

Nitrocellulose 91.18  
(nitrogen content 13.15%)  
Diphenylamine 0.87  
Graphite 0.40  
Dinitrotoluene 7.00  
Potassium Sulfate 0.55

##### **FORMULATION (CONTINUED)**

##### IMR 4903:

Nitrocellulose 91.47  
Diphenylamine 1.08  
Dinitrotoluene 6.50  
Potassium Sulfate 0.55  
Graphite Glaze 0.40 max. added

IMR 5010:

Nitrocellulose 89.92  
Diphenylamine 0.88  
Graphite 0.40  
Dinitrotoluene 8.25  
Potassium Sulfate 0.55

IMR 7013: (also known as M12)

Nitrocellulose 90.00  
Diphenylamine 0.87  
Tin 0.68  
Potassium Sulfate 0.55  
Dinitrotoluene 7.50

IMR 7383:

Nitrocellulose 83.67  
Diphenylamine 0.88  
Graphite 0.40  
Dinitrotoluene 11.50  
Dibutyl Phthalate 3.00  
Potassium Sulfate 0.55

**FORMULATION (CONTINUED)**

IMR 8097:

Nitrocellulose 95.68  
Diphenylamine 0.87  
Dinitrotoluene 2.50  
Potassium Sulfate 0.55  
Graphite Glaze 0.40

**SHAPE**

Single-perforated cylinder

**COLOR**

Graphite Coated: Shiny dark gray

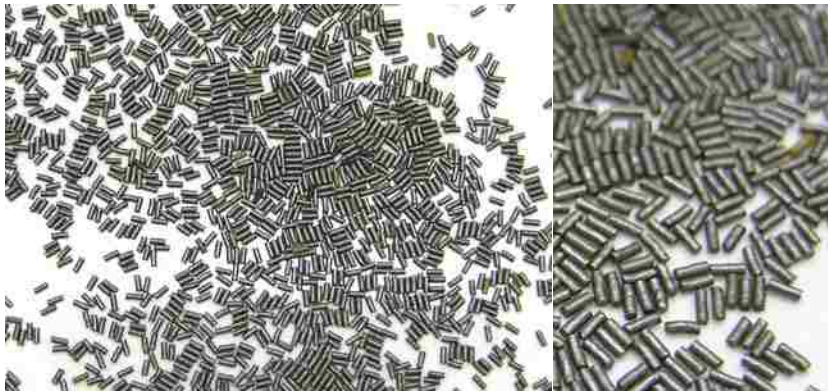
**DIMENSIONS**

Prop Model	Usage	Length (in)	Diameter (in)	Perf Diameter (in)	Inner (in)	Web Outer (in)	Average (in)	# of Perfs	Shape
IMR 4064	sp. app.	0.0450	0.0450	0.0110	-	-	0.0120	1	cylinder
IMR 4879	20MM	0.0909	0.0750	0.0150	-	-	0.0300	1	cylinder
IMR 4895	.30 CAL	0.0625	0.0490	0.0150	-	-	0.0180	1	cylinder
IMR 4903	20MM	0.0850	0.0500	0.0100	-	-	0.0210	1	cylinder
IMR 5010	.50 CAL	0.0909	0.0830	0.0210	-	-	0.0310	1	cylinder
IMR 7005	20MM	0.0909	0.0830	0.0210	-	-	0.0310	1	cylinder
IMR 7013	20MM	0.0909	0.0800	0.0150	n/a	n/a	n/a	1	cylinder
IMR 7383	.50 CAL	0.0850	0.0550	0.0240	-	-	0.0120	1	cylinder
IMR 8097	7.62MM	0.0450	0.0450	0.0110	-	-	0.0120	1	cylinder

**IMR PROPELLANT**

Note: Visually, a number of IMR formulations look identical. Each unique size is represented in the photos below. Both actual size and close-up photos are presented.

*IMR 4064, IMR 8097:*



*Actual size shown on left; close-up photo on right*

Penetrator Ballistics Calculations									
Propellant Properties									
POWDER TYPE: IMR SR 4759					POWDER TYPE: IMR 4831				
GEOMETRY: CYLINDER (1 PERFERATION)					GEOMETRY: CYLINDER				
MEASUREMENT	LENGTH	ID	OD		MEASUREMENT	LENGTH	ID	OD	
1	(in)	0.025	0.042		1	0.081	N/A	0.038	
2	0.055	0.022	0.045		2	0.08	N/A	0.037	
3	0.06	0.024	0.043		3	0.081	N/A	0.037	
4	0.056	0.023	0.044		4	0.08	N/A	0.038	
5	0.058	0.025	0.046		5	0.078	N/A	0.038	
AVERAGE	0.057	0.024	0.044		AVERAGE	0.080	N/A	0.038	
STD. DEV	0.002	0.001	0.001		STD. DEV	0.001	N/A	0.001	
POWDER TYPE: IMR 4350					POWDER TYPE: IMR 7828				
GEOMETRY: CYLINDER					GEOMETRY: CYLINDER				
MEASUREMENT	LENGTH	ID	OD		MEASUREMENT	LENGTH	ID	OD	
1	0.072	N/A	0.04		1	0.08	N/A	0.037	
2	0.082	N/A	0.037		2	0.085	N/A	0.038	
3	0.08	N/A	0.038		3	0.08	N/A	0.039	
4	0.081	N/A	0.038		4	0.08	N/A	0.038	
5	0.078	N/A	0.038		5	0.079	N/A	0.038	
AVERAGE	0.079	N/A	0.038		AVERAGE	0.081	N/A	0.038	
STD. DEV	0.004	N/A	0.001		STD. DEV	0.002	N/A	0.001	
POWDER TYPE: IMR 4064					POWDER TYPE: BLUEDOT				
GEOMETRY: CYLINDER					GEOMETRY: CYLINDER				
MEASUREMENT	LENGTH	ID	OD		MEASUREMENT	LENGTH	ID	OD	
1	0.085	N/A	0.032		1	0.008	N/A	0.055	
2	0.078	N/A	0.029		2	0.008	N/A	0.057	
3	0.084	N/A	0.031		3	0.009	N/A	0.055	
4	0.089	N/A	0.033		4	0.007	N/A	0.06	
5	0.085	N/A	0.032		5	0.008	N/A	0.056	
AVERAGE	0.084	N/A	0.031		AVERAGE	0.010	N/A	0.0620	
STD. DEV	0.004	N/A	0.002		STD. DEV	0.0007	N/A	0.002	
POWDER TYPE: BULLSEYE					POWDER TYPE: UNIQUE				
GEOMETRY: CYLINDER					GEOMETRY: CYLINDER				
MEASUREMENT	LENGTH	ID	OD		MEASUREMENT	LENGTH	ID	OD	
1	0.005	N/A	0.035		1	0.005	N/A	0.035	
2	0.006	N/A	0.033		2	0.006	N/A	0.033	
3	0.004	N/A	0.04		3	0.004	N/A	0.04	
4	0.004	N/A	0.041		4	0.004	N/A	0.041	
5	0.003	N/A	0.039		5	0.003	N/A	0.039	
AVERAGE	0.0030	N/A	0.0340		AVERAGE	0.0060	N/A	0.0620	
STD. DEV	0.0011	N/A	0.003		STD. DEV	0.0011	N/A	0.003	
Powder Type:					Impetus (ft-lb/lb)				
Bluedot					364500				
Bullseye					385000				
Unique					368000				

## APPENDIX B

### *Corners Method: Mathcad Numeric Modeling*

#### Corners Basic Analytical Interior Ballistics Model Appendix B

##### Projectile:

$$d_p \equiv 2 \text{ in}$$

$$w_1 \equiv 1.5 \text{ lbm}$$

$$L_p \equiv 5 \text{ in}$$

##### Propellant:

$$\rho \equiv 1.67 \frac{\text{gm}}{\text{cm}^3}$$

$$\text{gr} := \frac{\text{lb}}{7000}$$

$$m_c := 7000 \text{ gr}$$

$$D \equiv 0.034 \text{ in}$$

$$b \equiv 0.862 \frac{\text{cm}^3}{\text{gm}}$$

$$\theta \equiv \frac{D}{L_p}$$

$$R_u \equiv 1545 \frac{\text{ft} \cdot \text{lbf}}{\text{lbm} \cdot \text{mole} \cdot \text{R}}$$

$$n \equiv 0.037 \frac{\text{gm} \cdot \text{mole}}{\text{gm}}$$

$$T_0 \equiv 3740 \text{ K}$$

$$\gamma \equiv 1.209$$

$$\beta \equiv 0.000775 \frac{\text{in}}{\text{s} \cdot \text{psi}}$$

$$\lambda \equiv 385000 \frac{\text{ft} \cdot \text{lbf}}{\text{lbm}}$$

##### Gun:

$$V_c \equiv 60 \text{ in}^3$$

$$L_b \equiv 72 \text{ in}$$

$$A_w = \pi \left( \frac{d_p}{2} \right)^2$$

$$A = 3.142 \cdot \text{in}^2$$

**Solution:**

$$V_t := V_c - \frac{m_c}{\rho}$$

$$V_t = 43.425 \times 10^0 \cdot \text{in}^3$$

$$l_c := \frac{V_t}{A}$$

$$l_c = 13.823 \cdot \text{in}$$

**Central Ballistic Parameter**

$$M := \frac{A^2 \cdot D^2}{w_1 \cdot m_c \cdot \lambda \cdot \beta^2} \cdot \left[ \frac{\left( 1 + \frac{m_c}{3 \cdot w_1} \right)}{\left( 1 + \frac{m_c}{2 \cdot w_1} \right)^2} \right]$$

$$M = 0.728$$

**Pressure:**

$$f_m = \frac{M + \theta - 1}{M + 2 \cdot \theta}$$

$$f_m = -0.358$$

$$f_c := 0$$

$$R_L = \frac{\left( 1 + \frac{m_c}{2 \cdot w_1} \right)}{\left( 1 + \frac{m_c}{3 \cdot w_1} \right)}$$

$$R_L = 1.091$$

$$Q = \frac{\lambda \cdot m_c}{V_t} \cdot R_L$$

$$Q = 1.161 \times 10^3 \cdot \text{psi}$$

$$\phi = \frac{(M + \theta)(1 + \theta)^2}{(M + 2 \cdot \theta)^2}$$

$$\phi = 1.355$$

$$P_{bmax} := Q \cdot (1 - f_m) \cdot e^{-M \cdot (1 - f_m)}$$

$$P_{bmax} = 58.679 \times 10^3 \cdot \text{psi}$$

$$P_{bmx} = Q \cdot \frac{1}{M \cdot e}$$

$$P_{bmx} = 58.683 \times 10^3 \cdot \text{psi}$$

$$x_c := l_c \cdot e^M - l_c$$

$$x_c = 14.791 \cdot \text{in}$$

$$p_c := Q e^{-M}$$

$$p_c = 56.067 \times 10^3 \text{ psi}$$

$$p_{smax} := \frac{P_{bmax}}{\left(1 + \frac{m_c}{\gamma \cdot w_1}\right)}$$

$$p_{smax} = 4.401 \times 10^4 \text{ psi}$$

$$p_{sc} := \frac{p_c}{\left(1 + \frac{m_c}{2 \cdot w_1}\right)}$$

$$p_{sc} = 42.05 \times 10^3 \text{ psi}$$

$$v_{xc} := \frac{A \cdot D}{\beta \cdot \left(w_1 + \frac{m_c}{2}\right)}$$

$$v_{xc} = 2.217 \times 10^3 \frac{\text{ft}}{\text{s}}$$

$$v_m := \frac{A \cdot D \cdot (1 - f_m)}{\beta \cdot w_1 \cdot \left(1 + \frac{m_c}{2 \cdot w_1}\right)}$$

$$v_m = 3011.775 \frac{\text{ft}}{\text{s}}$$

$$\Phi_{\frac{w}{w_1}} := \frac{2}{1 - \gamma} \cdot \left[ \left( \frac{I_b + I_c}{x_c + I_c} \right)^{1 - \gamma} - 1 \right]$$

$$v_{mz} := \sqrt{\frac{m_c \cdot \lambda}{\left(w_1 + \frac{m_c}{3}\right)}} \cdot (M + \Phi)$$

$$v_{mz} = 4.264 \times 10^3 \frac{\text{ft}}{\text{s}}$$

$$P_1 = \frac{\lambda \cdot m_c \cdot R_{ba}}{A \cdot l_c} \left[ \frac{[(e + \gamma_1 - 2) \cdot M + 4 \cdot \theta]}{(1 + \theta)^2} - \eta \cdot F_{1ex} \right]^{-1} = 21.19 \times 10^3 \text{ psi}$$

if

$$\gamma_1 \cdot M = 2.243$$

is greater than

$$(1 - \theta) \left[ 1 + \left( b - \frac{1}{\delta} \right) \frac{P_1}{\lambda \cdot R_{ba}} \right] = 0.5$$

Peak pressure occurs before all burnt, if not, it occurs at all burnt

Distance at all burnt: Values at All Burnt Point (Subscript b)  
Values at Peak Pressure Point (Subscript m)

$$A_b = l_c \cdot (1 - \eta)$$

$$B_b = l_c \left( \frac{1 + \theta}{Z_b} \right)^{\frac{M}{\theta_1}} \left[ 1 - \frac{\gamma_1 \cdot \eta \cdot M \cdot (1 + \theta)^2}{(M + \theta_1)(M + 2 \cdot \theta_1)} \right]$$

$$C_b = \eta \cdot l_c \cdot Z_b \left[ \frac{(\gamma_1 - \theta) \cdot M - 2 \cdot \theta^2}{(M + \theta_1)(M + 2 \cdot \theta_1)} \right]$$

$$x_b = B_b + C_b - A_b = 48.676 \text{ in}$$

Pressure at all burnt:

$$P_b = \frac{m_c \cdot \lambda \cdot R_{ba} \cdot Z_b}{A \cdot [x_b + l_c \cdot (1 - \eta)]} = 7.69 \times 10^3 \text{ psi}$$

Fraction of propellant burnt a max pressure:

$$k := \frac{A \cdot l_c \cdot \eta \cdot P_1}{\lambda \cdot m_c \cdot R_{ba}} = 0.034$$

$$\gamma_p := \frac{\gamma_1}{1+k} = 1.256$$

$$\xi := \gamma_p - \gamma_1 + 1 = 0.958$$

$$f_m := 1 - \left( \frac{1+\theta}{\xi \cdot M + 2 \cdot \theta_1} \right) = 0.527$$

$$Z_m := \frac{(1+\theta) \cdot (\xi \cdot M + \theta_1)}{\xi \cdot M + 2 \cdot \theta_1} = 1.115$$

$$\phi_m := (1 - f_m) \cdot (1 + \theta \cdot f_m) = 0.602$$

Distance at maximum pressure:

$$A_m := l_c \cdot (1 - \eta \cdot \phi_m)$$

$$B_m := l_c \cdot (e \cdot M + 4 \cdot \theta_1) \cdot \left[ 1 - \frac{\gamma_1 \cdot \eta \cdot M \cdot (1 + \theta)^2}{(M + \theta_1) \cdot (M + 2 \cdot \theta_1)} \right]$$

$$C_m := \frac{\eta \cdot l_c \cdot (1 + \theta)^2 \cdot [\gamma_1 \cdot M \cdot (\xi \cdot M + 2 \cdot \theta_1) - 2 \cdot \theta \cdot (M + \theta_1)]}{(M + \theta_1) \cdot (M + 2 \cdot \theta_1)}$$

$$E_m := \frac{(\xi \cdot M + 2 \cdot \theta_1)^2}{(\xi \cdot M + \theta_1)}$$

$$x_m := \frac{B_m}{E_m} + \frac{C_m}{E_m} - A_m = 10.658 \text{ in} \quad \text{Distance at Peak Pressure}$$

Maximum Pressure:

$$P_m := \frac{m_c \cdot \lambda \cdot R_{ba} \cdot (1 + \theta)^2 \cdot (\xi \cdot M + \theta_1)}{A \cdot (\xi \cdot M + 2 \cdot \theta_1)^2 \cdot [x_m + l_c \cdot (1 - \eta \cdot \phi_m)]} = 14.875 \times 10^3 \text{ psi} \quad \text{Maximum Pressure}$$

Velocity at muzzle exit:

$$r := \frac{L_b + I_c(1 - \eta)}{s_b + I_c(1 - \eta)} = 1.385 \quad \text{Expansion Ratio From All Burnt}$$

$$\Phi := \frac{2}{(\gamma_1 - 1)} \cdot (1 - r^{1-\gamma_1}) = 0.621$$

$$v_{me} := \sqrt{\frac{\lambda \cdot m_c}{\left(w_1 + \frac{m_c}{3}\right)} \cdot (M + Z_b \cdot \Phi)} = 2543.098 \cdot \frac{\text{ft}}{\text{s}} \quad \text{Velocity at Muzzle}$$

## APPENDIX C

### *Coppocks Method: Mathcad Numeric Modeling*

#### Coppocks Advanced Analytical Interior Ballistic Model Appendix C

##### Projectile Parameters:

$$d_p \equiv 2\text{in} \quad \text{Projectile Diameter}$$

$$m_p \equiv 1.5\text{lbm} \quad \text{Projectile Mass}$$

$$l_s \equiv 5\text{in} \quad \text{Projectile Length}$$

$$V_p \equiv 0$$

$$w_1 \equiv 1.05 \cdot m_p \quad \text{Adjusted Projectile Weight (Recoil and Friction)}$$

##### Propellant Parameters:

$$\rho \equiv 0.61 \frac{\text{gm}}{\text{cm}^3} \quad \text{Solid Propellant Bulk Density}$$

$$\text{gr} \equiv \frac{\text{lb}}{7000} \quad \text{Definition of a Grain}$$

$$m_c \equiv 3000\text{gr} \quad \text{Propellant Charge Mass}$$

$$D \equiv 0.031\text{in} \quad \text{Web Linear Powder Burning Dimension}$$

$$\delta \equiv 1.67 \frac{\text{gm}}{\text{cm}^3} \quad \text{Solid Propellant Density}$$

$$b \equiv 0.862 \frac{\text{cm}^3}{\text{gm}} \quad \text{Propellant Covolume}$$

$$L_p \equiv .06\text{in} \quad \text{Powder Tube Length}$$

$$\theta \equiv \frac{D}{L_p} \quad \text{Shape Function} \quad \theta = 0.517$$

$$R_u \equiv 1545 \frac{\text{ft} \cdot \text{lb}_f}{\text{lbm} \cdot \text{mole} \cdot \text{R}} \quad \text{Specific Gas Constant}$$

$$n \equiv 0.037 \frac{\text{gm} \cdot \text{mole}}{\text{gm}}$$

$$T_0 \equiv 3379\text{K} \quad \text{Adiabatic Flame Temperature}$$

$$\gamma \equiv 1.222 \quad \text{Specific Heat Ratio}$$

$$\beta = 0.000775 \frac{\text{in}}{\text{s} \cdot \text{psi}} \quad \text{Burn Rate Coefficient}$$

$$\lambda = 368000 \frac{\text{ft} \cdot \text{lb} \cdot \text{f}}{\text{lb} \cdot \text{m}} \quad \text{Impetus Force Constant}$$

**Gun Parameters:**

$$V_c = 60 \text{ in}^3 \quad \text{Chamber Volume}$$

$$L_b = 72 \text{ in} \quad \text{Barrel Length}$$

$$A = \pi \left( \frac{d_p}{2} \right)^2 \quad \text{Bore Area} \quad A = 3.142 \text{ in}^2$$

$$l_{ec} = \frac{V_c}{A} = 19.099 \text{ in} \quad \text{Chamber Length Normalized to Barrel Length}$$

**Solution:**

$$R_{ba} = \frac{1 + \frac{m_c}{2 \cdot w_f}}{1 + \frac{m_c}{3 \cdot w_f}} = 1.042 \quad \text{Ratio of Breech Pressure to Average Pressure}$$

$$V_t = V_c + \frac{m_c}{\rho} \quad \text{Total Volume}$$

$$l_c = \frac{V_t}{A} = 12.908 \text{ in}$$

$$v_{est} = 3000 \frac{\text{ft}}{\text{s}} \quad \text{Estimated Projectile Velocity For Heat Loss Calculation}$$

$$d = \frac{d_p}{\text{in}} \quad \text{Unitless Variables for Thornhill Equation}$$

$$\Omega = 1.4 \quad \text{Hydrodynamic Barrel Roughness Factor}$$

## APPENDIX D

### *Lumped Parameter Model: Mathcad Numeric Modeling*

#### Propellant Input Parameters

Propellant Charge Mass	$m_c = 50 \text{ grain}$	$m_c = 3.24 \times 10^{-3} \text{ kg}$	$C_m := \frac{m_c}{\text{kg}}$
Solid Propellant Density	$P_\rho := 0.056 \frac{\text{lb}}{\text{in}^3}$	$P_\rho = 1.55 \times 10^3 \frac{\text{kg}}{\text{m}^3}$	$\rho_s := \frac{P_\rho}{\frac{\text{kg}}{\text{m}^3}}$
Covolume	$G_{\eta} := 28.70 \frac{\text{in}^3}{\text{lb}}$	$G_{\eta} = 1.037 \times 10^{-3} \frac{\text{m}^3}{\text{kg}}$	$\eta := \frac{G_{\eta}}{\frac{\text{m}^3}{\text{kg}}}$
Burning Rate Coefficient	$B_r := .0077 \frac{\text{in}}{\text{s}} \frac{1}{\left(\frac{\text{lb}}{\text{in}^2}\right)^{.920}}$	$B_r = 5.753 \times 10^{-8} \frac{\text{m}}{\text{s}} \frac{1}{\left(\frac{\text{N}}{\text{m}^2}\right)^{.920}}$	$B := \frac{B_r}{\frac{\text{m}}{\text{s}} \frac{1}{\left(\frac{\text{N}}{\text{m}^2}\right)^{.920}}}$
Propellant Specific Force Constant	$F_\lambda := 385000 \frac{\text{lb} \cdot \text{ft}}{\text{lb}}$	$F_\lambda = 1150790.8 \frac{\text{J}}{\text{kg}}$	$\lambda := \frac{F_\lambda}{\frac{\text{J}}{\text{kg}}}$
Propellant Grain Radius	$G_r = 0.017 \text{ in}$	$G_r = 4.318 \times 10^{-4} \text{ m}$	$R_g := \frac{G_r}{\text{m}}$
Propellant Grain Length	$G_l = 3 \times 10^{-3} \text{ in}$	$G_l = 7.62 \times 10^{-5} \text{ m}$	$L_g := \frac{G_l}{\text{m}}$
Propellant Grain Inner Radius		$G_i = 6.096 \times 10^{-4} \text{ m}$	$r_g := \frac{G_i}{\text{m}}$
Specific Heat Ratio	$\gamma := 1.209$		
Burn Rate Index	$n := .720$		

**Gun/Projectile Inputs:**

Projectile Mass	$m_p = 800 \text{ grain}$	$m_p = 0.052 \text{ kg}$	$W_s := \frac{m_p}{\text{kg}}$
Projectile Cross-Sectional Area	$S_a := .196 \text{ in}^2$	$S_a = 1.265 \times 10^{-4} \text{ m}^2$	$A_s := \frac{S_a}{\text{m}^2}$
Chamber Volume (no propellant)	$C_v := .687 \text{ in}^3$	$C_v = 1.126 \times 10^{-5} \text{ m}^3$	$V_{co} := \frac{C_v}{\text{m}^3}$
Barrel Length	$B_1 = 18 \text{ in}$	$B_1 = 0.457 \text{ m}$	$L_b := \frac{B_1}{\text{m}}$
Friction	$R_f = 1 \times 10^3 \text{ lbf}$	$R_f = 4448 \text{ N}$	$F_f := \frac{R_f}{\text{N}}$

**Constants:**

Gravity Constant	$g_a := 9.81$
Definition of Grain Mass Unit	$\text{grain} = \frac{1}{7000} \text{ lb}$
	$\delta_c := 1.5$

**Seven Ordinary Differential Equations for Lumped Parameter Internal Ballistics Analysis:**

Given

$$\frac{d}{dt} S_p(t) = V_p(t)$$

Projectile Travel

$$\frac{d}{dt} V_p(t) = \frac{A_s}{W_s} P_b(t)$$

$$\frac{d}{dt} V_p(t) = \frac{A_s P_b(t)}{W_s} - \frac{F_f}{W_s}$$

Projectile Acceleration

$$\frac{d}{dt} X(t) = B \cdot P_a(t)^n$$

Propellant Burning Rate Law

$$\frac{d}{dt} Z(t) = 3 \cdot \frac{(R_g - X(t))^2}{R_g^3} \frac{d}{dt} X(t)$$

Rate of change of mass fraction of propellant consumed, spherical propellant grains

$$\frac{d}{dt}Z(t) = \frac{2 \frac{d}{dt}X(t) (R_g - X(t))^2}{L_g R_g^2} + \frac{2 \frac{d}{dt}X(t) (L_g - 2X(t)) (R_g - X(t))}{L_g R_g^2}$$

Rate of change of mass fraction of propellant consumed, extruded tubular propellant grains

$$\frac{d}{dt}Z(t) = \frac{\left[ 2 \frac{d}{dt}X(t) (r_g + X(t)) + 2 \frac{d}{dt}X(t) (R_g - X(t)) \right] (L_g - 2X(t))}{L_g (R_g^2 - r_g^2)} - \frac{2 \frac{d}{dt}X(t) \left[ (r_g + X(t))^2 - (R_g - X(t))^2 \right]}{L_g (R_g^2 - r_g^2)}$$

Rate of change of propellant consumed propellant grains (

$$\frac{d}{dt}V_T(t) = A_s V_p(t) + \frac{C_m}{\rho_s} \frac{d}{dt}Z(t) - C_m \eta \frac{d}{dt}Z(t) \quad \text{Total Chamber Volume}$$

$$\frac{d}{dt}P_a(t) = \frac{\lambda C_m \frac{d}{dt}Z(t) - \frac{1}{6}(\gamma - 1)(1 + \beta) C_m \frac{d}{dt}Z(t) \cdot V_p(t)^2 - (\gamma - 1)(1 + \beta) \left( W_s + \frac{1}{3} C_m Z(t) \right) V_p(t) \frac{d}{dt}V_p(t)}{V_T(t)} - \frac{\lambda C_m Z(t) - \frac{1}{2}(\gamma - 1) C_m Z(t)}{V_T(t)}$$

$$\frac{d}{dt}P_b(t) = \frac{d}{dt}P_a(t) \left( 1 + \frac{1}{2} \frac{\gamma - 1}{\delta_c} \frac{V_p(t)^2}{g_a \gamma \lambda} \right)^{\frac{-\gamma}{\gamma - 1}} - P_a(t) \frac{\left( 1 + \frac{1}{2} \frac{\gamma - 1}{\delta_c} \frac{V_p(t)^2}{g_a \gamma \lambda} \right)^{\frac{-\gamma}{\gamma - 1}}}{\delta_c} \frac{V_p(t)}{g_a \lambda} \frac{d}{dt}V_p(t) \quad \text{Base Pressure Ac}$$

$$\begin{pmatrix} Z \\ P_a \\ P_b \\ V_T \\ X \\ V_p \\ S_p \end{pmatrix} = \text{Odesolve} \left[ \begin{pmatrix} Z \\ P_a \\ P_b \\ V_T \\ X \\ V_p \\ S_p \end{pmatrix}, t, 0.01 \right]$$

```

T_end := | j ← 0
         | tol ← 0.00000001
         | while S_p(j) ≤ L_b
         |   j ← j + tol
         | j

```

This while loop finds the time when the projectile exits the barrel

$$T_{\text{end}} = 0.00221514$$

$$\text{End}_{\text{time}} := T_{\text{end}}^s$$

$$\text{Time} := 0.00, 0.0000001 .. T_{\text{end}}$$

```

P_max := | j ← 0
         | tol ← 0.00000001
         | while P_a(j + tol) > P_a(j)
         |   j ← j + tol
         | P_a(j)

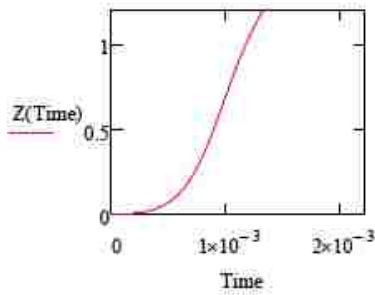
```

This while loop finds maximum pressure

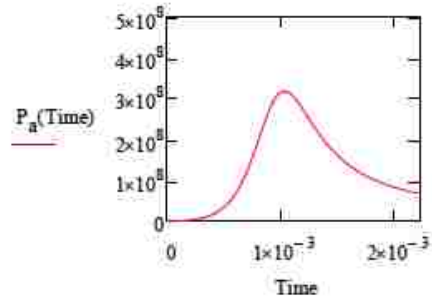
$$P_{\text{max}} = 3.182 \times 10^8$$

$$\text{Pressure}_{\text{max}} := P_{\text{max}} \cdot \text{Pa}$$

$$\text{Pressure}_{\text{max}} = 46152 \cdot \text{psi}$$



$$Z(T_{\text{end}}) = 1.74$$



$$P_a(T_{\text{end}}) = 6.782 \times 10^7 \frac{\text{N}}{\text{m}^2}$$

